Evolutionary Implications and Genetic Basis of Peroxide Survival in *Saccharomyces cerevisiae*

by

Stephanie Diezmann

University Program in Genetics and Genomics
Duke University

Date: _____

Approved:

_____
Fred S. Dietrich, PhD, Advisor

_____
James A. Alspaugh, MD

_____
Joseph Heitman, MD PhD

_____
John H. McCusker, PhD

_____
Thomas G. Mitchell, PhD

_____
Rytas J. Vilgalys, PhD

Dissertation submitted in partial fulfillment of the requirements for the degree of
Doctor of Philosophy in the University Program in Genetics and Genomics
in the Graduate School of Duke University
2009

Abstract

(Genetics)

Evolutionary Implications and Genetic Basis of Peroxide Survival in *Saccharomyces cerevisiae*

by

Stephanie Diezmann

University Program in Genetics and Genomics
Duke University

Date: _____

Approved:

_____
Fred S. Dietrich, PhD, Advisor

_____
James A. Alspaugh, MD

_____
Joseph Heitman, MD PhD

_____
John H. McCusker, PhD

_____
Thomas G. Mitchell, PhD

_____
Rytas J. Vilgalys, PhD

An abstract of a dissertation submitted in partial fulfillment of the requirements for the degree of Doctor of Philosophy in the University Program in Genetics and Genomics in the Graduate School of Duke University

2009

Abstract

Hydrogen peroxide is used by animals and plants to deter the growth of microbial invaders by inflicting DNA lesions, protein oxidation and lipid membrane modifications. Pathogens protect themselves with enzymes and scavenging proteins. This study investigated population genetic, biochemical and genetic aspects of peroxide survival in *Saccharomyces cerevisiae* to address its importance for yeast biology and fungal pathogenicity.

Population genetic analyses of DNA sequences from five loci from 103 strains encompassing the known ecological spectrum of *S. cerevisiae* show that it is a recombining species with three divergent subgroups, which are associated with soil, fruit, and vineyards. Clinical isolates cluster with fruit isolates but are significantly more resistant to peroxide. Clinical isolates are genetically diverse, indicating multiple origins of the pathogenic lifestyle and eliminating the possibility that peroxide resistance is due to shared ancestry rather than its importance for than its importance in colonizing the host.

Biochemical aspects of peroxide survival were studied in a resistant (high-survival) clinical isolate, a sensitive (low-survival) laboratory strain and their hybrid. Catalase activity and expression levels are indistinguishable among strains. Co-culture assays and growth curve records indicate that a secreted factor improves survival of the laboratory strain and that the phenotypic difference is most pronounced during exponential growth, excluding mechanisms of the General Stress Response effective

during stationary phase. Semi-quantitative expression profiles of stress response candidate genes do not differ, suggesting a novel resistance mechanism.

To elucidate the genetic basis of peroxide survival, the hybrid was sporulated and 200 F_1 segregants phenotyped and genotyped for oxidative stress candidate genes. Peroxide survival is a dominant quantitative trait and not linked to catalase, peroxidase or superoxide dismutase genes. 1,246 backcross segregants were phenotyped and 93 segregants selectively genotyped using microarrays. A 14-gene locus on chromosome XVI displayed marker-trait association. One gene, *RDS2*, encodes a zinc cluster protein acting as a regulator of drug sensitivity and contains a non-synonymous polymorphism whose exchange between the parental strains results a 15% decrease in survival in the clinical strain.

This work establishes a novel function for *RDS2* in oxidative stress response and demonstrates the effect a quantitative trait nucleotide has on a clinically relevant phenotype.

Für meine Mutter Gerlinde Diezmann, in Liebe und Dankbarkeit.

Contents

List of Tables

List of Figures

List of Abbreviations and Symbols

BC – backcross

BCE – before common era

BER – base excision repair

BSA – bulk segregant analysis

CER – common environmental response

cM – centi Morgan

DNA – deoxyribonucleic acid

ESR – environmental stress response

GSR – general stress response

H_2O_2 – hydrogen peroxide

HWE – Hardy-Weinberg Equilibrium

I_A – Index of Assocation

μg – microgram

μl – microliter

μM – micromolar

ml – milliliter

mm – millimeter

mM – millimolar

ms – millisecond

NaCl – sodium chloride

NER – nucleotide excision repair

ng – nanogram

OSR – oxidative stress response

π – nucleotide diversity

PBS – phosphate buffered saline

PCA – principal component analysis

PCR – polymerase chain reaction

QTG – quantitative trait gene

QTL – quantitative trait locus

QTN – quantitative trait nucleotide

RAPD – random amplification of polymorphic DNA

RFLP – restriction fragment length polymorphism

RHA – reciprocal hemizygosity analysis

ROS – reactive oxygen species

rpm – rotations per minute

SD – synthetic defined or standard deviation

SFP – single feature polymorphism

SEM – standard error of the mean

SNP – single nucleotide polymorphism

STRE – stress response element

SSA – single segregant analysis

TBA – tert-Butyl alcohol

TBHP – tert-Butyl hydroperoxide

U – unit

UPGMA – Unweighted Pair Group Method with Arithmetic Mean

YRE – *YAP1* recognition element

Acknowledgements

Fred, instilled in me the appreciation for the organism and inspired independent thinking. Thank you.

My thesis committee, Andy Alspaugh, Joseph Heitman, John McCusker, Tom Mitchell, and Rytas Vilgalys, was always ready with rigour, support, and encouragement. Thanks to you, I am on my way to become a scientist, which is what I wanted to be since grade seven.

Thank you Laura Kavanaugh, Jason Stajich, Charles Hall, and Andria Allen. I could not have asked for more supportive and patient lab mates. Thank y'all. A special thank you to Mark DeLong for being kind to computationally impaired graduate students.

Thanks to Joanne Kingsbury, Ludo Müller, and James Fraser, I know how to transform yeast cells, do microarray hybridizations and have a good time in Australia. Your help will always be appreciated.

I fell for Duke when I met the Duke Mycology lab, Austen Ganley, Rebecca Yahr, Tim James, Jeri Parrent, Daniel Henk, Jason Jackson, and Greg Bonito. You made mycology a wonderful experience all around, from advice on population genetic analyses at seven in the morning over running for busses in Sweden to home brew.

Thanks to the undefeatable Marchuk lab, especially Carol Gallione and Amy Akers, who gave my yeast a home in their shaker and were always ready to counter graduate student misery with fun and laughter. The vodoo doll definitely helped.

Suzanne Joneson, thank you for all the adventures along Ninth Street and helping with wild yeast hunting.

Gabriele Schönian and Carola Schweynoch from Charité University Hospital in Berlin encouraged me to pursue an academic career when I was a lab tech trainee and helped me along as an undergraduate. It's good to come home to you.

This work would not have been possible without the generosity of Cletus Kurtzman, John McCusker, Brad Nicholson, Anne Rouse, Meredith Blackwell, and Wiley Schell, who shared their *S. cerevisiae* strains with me.

For technical assistance in generating sequence data and cell sorting, I am deeply indebted to Lisa Bukovnik and her farm of sequencers and the Duke Comprehensive Cancer Center FACS facility.

Friends are a wonderful thing and an absolute necessity in graduate school. My girl friends from high school days Eva Bach, Ute Böttcher, Britta Fanck, Martina Ramin, Alex Schäfer, and Anna-Luise Stille held my hand when waters got rough. Silvia Engl, Sven Driesener and Jirko Kühnisch, thank you for listening and paddling.

I cannot even begin to express what my family's support meant to me over the years abroad. From mailing provisions of chocolate to endless hours of phone conversations, they were there.

Heath O'Brien, you gave frozen dinner and my life a new meaning. I could not have done it without you.

1

Hydrogen Peroxide Stress Response and Protection in the Model Eukaryote and Emerging Pathogen *Saccharomyces cerevisiae*

Oxygen radicals and molecular oxygen began to accumulate in earth's atmosphere after the origin of photosynthetic cyanobacteria some 3.5 billion years ago (280). Although atmospheric O_2 expedited the evolution of aerobic life, partially reduced O_2 is toxic, mutagenic and inflammable. Univalent reduction of molecular oxygen to water, leads to reactive oxygen species (ROS) such as superoxide radicals ($O_2\bullet$-), hydrogen peroxide (H_2O_2), and hydroxyl radicals (OH$\bullet$). The non-radical ROS H_2O_2 is a universal and versatile molecule that partakes in constructive and destructive aspects of life. H_2O_2 is effective as defense, degrading and signaling molecule. Animals and plants defend themselves with H_2O_2 from invasive pathogenic microbes. Wood-rotting fungi utilize H_2O_2 to break down lignin and cellulose, thereby returning carbon to the carbon cycle. Mutualistic plant-fungus relationships and the development of sexual structures in filamentous fungi depend on H_2O_2 as a signaling molecule. H_2O_2 can be detrimental when its presence disturbs the cellular redox

homeostasis, resulting in serious consequences for human life and health. Oxidative stress and cellular damage are implicated in a wide array of different conditions, including cancer (170), familial amyotrophic lateral sclerosis (267), Parkinsons disease (311), sickle cell anemia (282), and aging and programmed cell death (66). Due to the complexity of the eukaryotic oxidative stress response, these conditions are difficult to study in humans, requiring a tractable model system.

S. cerevisiae is an outstanding model system that facilitates the study of components of the multi-facetted eukaryotic oxidative stress response on a genetic, biochemical and systematic level. Cellular damage due to H_2O_2 is non-specific and includes DNA single base pair modifications and double strand breaks, protein carbonylation and disulfide bond formation and lipid peroxides (137). *S. cerevisiae* uses different avenues to respond to the oxidative challenge, depending on its severity. Low doses of H_2O_2 trigger adaptation by initiating expression of genes whose products act in detoxification and damage control (163). High H_2O_2 doses cause cell cycle arrest and an apoptosis-like cell death (99, 202). To prevent death by ROS, *S. cerevisiae* employs catalases, cytochrome-c peroxidase, and non-enzymatic ROS-scavenging molecules, such as glutathione, thioredoxin and vitamin C (129, 134, 156, 160, 181). The list of genes required for survival and repair has been extended by systematic efforts, including gene expression studies and systematic gene deletion mutants (40, 112, 145, 312).

Phylogenetic analyses have shown that *S. cerevisiae* is related to the ascomycetous opportunistic pathogens *Candida albicans*, *C. dubliniensis*, *C. glabrata*, *Aspergillus fumigatus*, and more distantly to the basidiomycetous opportunist *Cryptococcus neoformans* (83, 162). *C. albicans* is the most common causative agent of invasive fungal infections and causes a wide range of infections, reaching from thrush and vaginitis to life-threatening systemic infections in immunocompetent and immunocompromised (217, 345). The emerging pathogen *C. glabrata* is the second most common cause

of invasive candidiasis and the most common non-*Candida albicans Candida* species isolated from oral cavities of HIV-infected individuals (204, 250, 251). *C. dubliniensis* has only recently been identified and is primarily associated with oral infections in HIV-infected individuals and AIDS patients (61, 304). All together, *Candida* species rank fourth in nosocomial blood stream infections in the U.S. (337). Hyaline molds of the genus *Aspergillus* are one of the most common agent of opportunistic mycoses (251). *A. fumigatus* is the most common cause of invasive pulmonary disease in hematopoietic stem cell transplant recipients (207). The basidiomycetous yeast *C. neoformans* ranks third in causes of fatalities due to invasive mycoses (251). *C. neoformans* infections lead to meningoencephalitis in immunosuppressed patients (49). *S. cerevisiae* has traditionally been considered non-pathogenic but has been isolated in clinical settings in the recent past and is now considered an emerging pathogen (142, 290). It has been found on sterile and non-sterile body sites in immunocompetent and immunocompromised patients, as reviewed by McCusker (212). Although much less frequent, mucosal and invasive *S. cerevisiae* infections are indistinguishable from *C. albicans* infections (91, 293).

Fungal infections and associated mortality rates are on the rise due to increasing numbers of immunocompromised patients who lack critical components of the cellular immune response to fight microbial invaders of the blood stream (250). Immunocompetent individuals eliminate fungi and bacteria with the help of neutrophils and macrophages. Both phagocytic cell types significantly increase O_2 uptake and produce ROS upon ingesting foreign particles, such as microbes, a phenomenon recognized as respiratory burst (159, 276). The primary product of the oxidative burst is $O_2\bullet$-, which is generated by the NADPH oxidase and immediately converted into H_2O_2 (137).

This chapter focuses on the interactions of H_2O_2 with the eukaryotic cell. The chemistry of H_2O_2 is briefly introduced and its biochemistry, the ability to damage

organic molecules, is described. The biological effect of oxidative stress and damage on eukaryotic cells is illustrated on the example of *S. cerevisiae*, in combination with examples of how *S. cerevisiae* aides in the investigation of human conditions that result from oxidative stress. Aspects of the regulatory response and protective systems of *S. cerevisiae* and its pathogenic relatives are discussed, followed by a brief summary of systematic efforts to identify genes required for survival and repair concludes the review.

1.1 H_2O_2 is a potent oxidant

Hydrogen peroxide was discovered in 1818 by Louis Jacques Thénard (336). Peroxide's versatility as a decomposing, signaling and noxious molecule results from its chemistry as a weak acid with oxidizing and reducing activities. It originates during partial reduction of O_2 by light (photoexcitation), radiation, ferrous iron or enzymes. H_2O_2 is a permanent dipole and one of the smallest chiral molecules in nature (19). As a non-radical ROS it is more stable under physiological conditions than its radical relatives. Its half-life of 1 ms is 1000x longer than that of O_2•- (259). Due to this extended stability H_2O_2 can engage in the Fenton reaction producing the more toxic OH•, whose toxicity is only limited by the presence of transition metals and diffusion. The Fenton reaction (Fe^{2+} + H_2O_2 → intermediate oxidizing species → Fe^{3+} + OH• + OH-) describes the process (89). Fe^{2+}, that comprises ∼8% of the cells iron pool, is almost immediately oxidized to Fe^{3+} of which about 13 μM can be detected in *S. cerevisiae* cells (297). As described below, H_2O_2 damages biomolecules via the more potent OH•. Aerobic cells are constantly exposed to intracellular H_2O_2 originating from radiation-mediated H_2O dissociation or leaking from the respiratory chain when cytochrome-c oxidase releases partially reduced O_2. Indeed, mitochondria are a major source of endogenous oxidative stress as they consume 86% of the cell's O_2 (283).

When the redox homeostasis, the intricate balance between antioxidants and ROS is shifted towards ROS, cells experience oxidative stress. Excess ROS injuring biomolecules and the failure of repair or replacement systems cause oxidative damage (137).

As an uncharged small molecule, H_2O_2 can enter the cell by diffusing across the membrane. In *S. cerevisiae*, H_2O_2 cell membrane permeability decreases five-times between exponential and stationary phase, resulting in H_2O_2 resistance (295). Diffusion is not the only entrance mechanism. A recent study by Bienert et al. suggests that H_2O_2 enters via specific aquaporins, which are integrated membrane proteins, and that diffusion might be rather limited. Heterologous expression of 24 aquaporins from mammals and plants, including five human aquaporins, in *S. cerevisiae* confirmed that H_2O_2 is able to gain access through one human and two plant aquaporins (19).

1.2 H_2O_2 non-specifically damages DNA, proteins and lipids

As a consequence of an imbalanced redox homeostasis, cells can suffer heritable or lethal mutations, functionally impaired proteins, and destabilized membranes. Oxidative damage can have serious consequences as manifested in cancer, Parkinson's disease, and irreversibly sickled red blood cells (170, 282, 311). The following section gives an overview of oxidative damage in DNA, protein, lipids, the serious conditions they can cause in humans and how they are modeled and investigated in *S. cerevisiae*.

DNA damage. *S. cerevisiae*, together with *Escherichia coli*, has served as a model system to identify DNA damaging agents, damage patterns, and repair mechanisms. The DNA damaging properties of H_2O_2 were uncovered when H_2O_2-treated *S. cerevisiae* cells became respiration-deficient due to mutations in the mitochondrial genome (310). Oxidative damage is not restricted to mitochondrial DNA but affects all nucleic acid molecules in the cell. For example it has been estimated

that the human genome experiences 10^4 losses of purines in each cell every day (193). H_2O_2 exposure and the subsequent Fenton reaction lead to a wide variety of DNA injuries, including base and sugar modifications, single and double strand breaks, nucleotide dimerizations, and DNA-protein cross-linking of which the most common ones and their repair mechanisms are described here (137, 191). OH• oxidizes all four bases resulting in a variety of products. Oxidation of guanine causes 8-Oxo-7,8-dihydroguanin (8-oxoG), one of the most abundant and best-studied base modifications. Oxidative deamination of cytosine results in the formation of uracil and addition to guanine and thymine rings leads to ring opening and structural distortions causing the above-mentioned apurinic and apyrimidinic sites (26, 86). Oxidation of deoxyribose and ribose fragments the molecule and produces peroxyl radicals. Oxidative modification of proteins that are associated with DNA leads to cross-linking with DNA base-derived radicals prohibiting proper chromatin unfolding, DNA repair, transcription and replication (137).

The products of oxidative DNA base modifications are transitions, transversions and base mismatches. To prevent these mutations from being passed on to the next generation or from producing erroneous RNAs, cells have developed repair mechanisms that remove oxidized bases and remedy single and double strand breaks. DNA lesions have been classified as lethal or mutagenic (321). Lethal lesions distort structure and prevent DNA polymerases from progressing. Mutagenic lesions allow DNA polymerase read through and are passed on to the next generation. For example, 8-oxoG is mutagenic as it introduces a transversion. Thymine glycol and its complementary adenine are lethal because they are extrahelical and distort DNA structure. *S. cerevisiae* removes modified DNA bases primarily by base excision repair (BER), sometimes synergistically with nucleotide excision repair (NER) (114). The components of BER, the DNA N-glycosylases/AP lyases Ntg1, Ntg2 can repair a broad spectrum of base modifications (343). The glycosylase Ogg1 removes oxidized

purines and the apurinic endonuclease Apn1 repairs oxidized cytosine (253, 316). The enzymes responsible for DNA repair are evolutionary conserved, emphasizing the applicability of yeast as a model eukaryote (8). For a detailed review on the chemistry of oxidative DNA damage and repair enzymes see Bjelland and Seeberg (22).

DNA damage and its consequences on genomic instability have been studied in *S. cerevisiae*, demonstrating that yeast cells without BER and NER experience DNA lesions and exhibit a cancer like phenotype expressing itself in aberrant morphology, DNA content and growth (94). Degtyareva et al. found that elevated levels of DNA damage, increase the frequency of chromosomal alterations and led to karyotypic instability (78, 94). This reflects, at least in part, the scenario of oxidative damage to mammalian DNA. ROS accelerate mutation rates and promote neoplastic transformations. Mice that lacked the glycosylase to repair 8-oxoG were five-times more likely to develop intestinal tumors than wild type animals (274).

Protein oxidation. H_2O_2 and OH• damage proteins resulting in enzyme inactivation and structural disturbances. H_2O_2 inactivates enzymes in two different ways. Oxidation of cysteine and methionine sulfhydryl groups, which often reside in active sites, causes disulfide cross-links and inactivation as demonstrated on the yeast alcohol dehydrogenase (70, 135, 332). H_2O_2 attacking Fe/S clusters inactivates dehydratase and aconitase (101). *S. cerevisiae* prevents inactivation of Fe/S cluster containing enzymes with the mitochondrial glutathione Grx5 and heat shock protein 60 (35, 266).

As a Fenton reagent, H_2O_2 disrupts protein structure. Exposure to OH• results in covalently bound protein aggregates (75). OH• modifies amino acids, particularly tryptophan, tyrosine, histidine and cysteine leading to alterations in primary structure (77). Once the primary structure is impaired, continued oxidative carbonylation leads to distortions of the secondary and tertiary structure and ag-

gregate formation due to progressive cross-linking (76). Yeast proteins that are being carbonylated in response to H_2O_2 include glyceraldehyde-3-phosphate dehydrogenase, Cu,Zn-superoxide dismutase, phosphoglycerate mutase and cyclophilin 1 (67). *S. cerevisiae* removes irreversibly damaged proteins via the proteasome and the lysosomes/vacuole. The 20S proteasome is critical for survival during stationary phase.(52). Oxidative stress triggers expression of genes that encode 20S proteasome subunits, emphasizing the proteasome's role for regulation of oxidized protein levels (187). Fast removal of oxidized proteins is important for recovery from oxidative stress and vacuolar function is a core property of cells exposed to a wide variety of oxidative stresses (312). Accordingly, genes required for vacuolar proteolysis respond with increased expression to oxidative stress (206).

Protein oxidation has serious consequences for human health; it is involved in Parkinson's disease (PD) and sickle cell anemia (282, 306). The PD protein DJ-1 exerts its neuroprotective function by undergoing self oxidation to eliminate H_2O_2 that would otherwise trigger apoptosis (306). However, co-expressing DJ-1 with synuclein alleles in yeast did not change synuclein toxicity (319). A sickle cell crisis is caused by the oxidation of two conserved cysteine residues of β-actin in the red blood cells of homozygous sickle cell patients. The resulting disulfide brigde prohibits actin depolymerization and locks the cell in the irreversibly sickled state (282). The physiological role of these two actin cysteine residues in oxidative stress sensing and response has been investigated in *S. cerevisiae* (96). *S. cerevisiae* has furthermore aided in the development of a reliable mass spectrometric method that enables identification and characterization of oxidative protein damage (221).

Lipid peroxidation. The oxidative deterioration of polyunsaturated lipids damages biological membranes (137). In general, lipid peroxidation increases membrane viscosity, alters thermotropic phase behaviour, decreases electrical resistance and enables phopholipid exchange between monolayers (263). For mitochondrial mem-

branes, Tappel and Zalkin showed as early as 1958 that mitochondria deteriorate and mitochondrial enzymes get inactivated upon oxidation (307). Phospholipids are oxidized in an iron salt-dependent fashion, indicating that OH• is the causative agent (136). ROS attack on polyunsaturated lipids is initiated by hydrogen abstraction, subsequent oxygenation and formation of peroxyl radicals (109). The resulting lipid peroxides are reduced by phospholipid hydroperoxide glutathione peroxidase. *S. cerevisiae* expresses three peroxidases in response to oxidative stress (12). Those act in concert with phospholipase A2 that cleaves lipid peroxides from membranes (51, 317). Phospholipases are considered virulence factors in *C. albicans*, *A. fumigatus* and *C. neoformans* because they promote host invasion by allowing fungal pathogens to adhere to the host's membranes (116).

1.3 Consequences of H_2O_2-induced damage

Responses to oxidative stress and the resulting damage are complex and differ depending on which cell component has been damaged. Studies on *S. cerevisiae* have elucidated the consequences of oxidative damage to the eukaryotic cell. Nuclear DNA damage results in cell cycle arrest. By halting the cell cycle, cells gain time for repair. The critically injured mitochondrial genome is lost from the cell, a lethal situation for mammalian cells that can be studied in petite *S. cerevisiae* strains, which survive without a mitochondrial genome. ROS accumulation and damage in mitochondria promote aging and life span and severe damage leads to programmed cell death.

Cell cycle arrest and mitochondrial genome instability. The outcomes of nuclear and mitochondrial DNA damage differ in *S. cerevisiae*. H_2O_2 damages of nuclear DNA cause cell cycle arrest in a *RAD9*-dependent manner (99). *RAD9* affects the transcription of genes related to DNA metabolism and repair and triggers cell cycle arrest in G1, S and G2. Deletion of *RAD9* leaves cells highly sensitive to H_2O_2 but with normal glutathione metabolism, STRE-mediated gene expression

and adaptive response. Severe oxidative mtDNA damage leads to the loss of the mitochondrial genome in *S. cerevisiae*. Mutants that lacked mitochondrial base excision repair and superoxide dismutase (*SOD2*) lost their entire genome in response to accumulating ROS. Under certain conditions, *S. cerevisiae* survives without a mitochondrial genome and this case presents the opportunity to study a situation that is always lethal in mammalian cells (85).

Aging and apoptosis. Aerobic cells are constantly exposed to free radicals and this internal radiation is thought to be responsible for aging and potentially cancer (139). *S. cerevisiae* ages in two distinct ways, replicative and chronological. Replicative aging is measured by the number of daughter cells generated by each mother cell and chronological aging is determined by the length of cell viability in stationary phase (66). This implies that although each individual cell senesces and dies, the population is immortal, promoting *S. cerevisiae* as a model for aging research. Aging in yeast is accompanied by a host of changes in cell morphology and biochemistry. Cell size, bud scar number and vacuole size increase in old cells while protein synthesis, the ability to mate and ribosome activity decrease. In yeast only the mother cell ages. Daughter cells start out with the potential of a new whole life span. *S. cerevisiae* life span is affected by genes governing signal transduction, transcriptional silencing, DNA recombination and ROS (165). Mother cells lacking catalases that were exposed to $O_2\bullet$- or kept in an oxygen-rich atmosphere exhibited a significantly shorter life span. The decrease in life span was reversed when the radical scavenger glutathione was added, supporting the relevance of ROS for cellular aging (235).

Apoptosis is a form of programmed cell death and important for the maintenance of multi-cellular organisms, organ development and the removal of potentially cancerous cells. Mammalian cells undergoing apoptosis exhibit a series of biochemical alterations that lead to morphological changes, including membrane blebbing,

cell shrinkage, chromatin condensation, DNA fragmentation and the occurrence of membrane-bound apoptotic bodies (100). An apoptosis-like phenotype in response to ROS has been described for *S. cerevisiae*. The *cdc48* mutant strain displays a phenotype resembling mammalian apoptosis markers, such as membrane inversions, DNA fragmentation, chromatin condensation and fragmentation (201). Although *S. cerevisiae* lacks some mammalian apoptosis genes, such as Bcl-2s, it is a versatile model system to study programmed cell death. It lends itself to study the influence of ROS accumulation on apoptosis and the mitochondrial aspect of ROS augmentation. The yeast two-hybrid system can be exploited to investigate physical interactions of known mammalian apoptosis gene products and to identify new interactions. *S. cerevisiae* is amenable to heterologous and co-expression experiments of apoptotic markers to address phenotypic questions (100).

Apoptosis is induced by low external doses of H_2O_2 and depletion of the intracellular glutathione pool. *S. cerevisiae* cells initiate apoptosis upon oxidation of two conserved cysteine residues in the actin cytoskeleton (96). ROS play an active role in apoptosis initiation and are not merely a product of apoptosis because the apoptotic phenotype is suppressed in cells treated with radical scavengers or grown in an anaerobic environment (202). Old yeast cells accumulate ROS in their mitochondria and display markers of apoptosis, such as chromatin fragmentation, multiple nuclei per cell and plasma membrane inversions. Young cells did not accumulate ROS in their mitochondria, had compact single nuclei, no DNA breaks and only very infrequently stained positive for plasma membrane inversions (186).

ROS evoke apoptosis in concert with two *S. cerevisiae* genes that resemble mammalian apoptosis genes. YOR97W (*YCA1*), encodes a caspase-like protein with structural homology to human caspases, is processed like a caspase and cleaves caspase substrates. *YCA1* overexpression together with oxidative stress evokes apoptosis and *YCA1* disruption abolishes H_2O_2 or age-induced apoptosis in yeast (203).

More recently a second gene (*RHO5*) was identified that resembles mammalian Rac GTPases, which are involved in apoptosis. Rac GTPases activate NADPH oxidases, thereby generating $O_2\bullet$- and triggering cell death. Yeast Rho5 GTPase contributes to ROS accumulation and promotes apoptosis. As a consequence of oxidative stress, Rho5 physically interacts *in vitro* and *in vivo* with Trr1 (thioredoxin reductase). Inhibition of Trr1 leads to an increase in intracellular H_2O_2 levels that in turn trigger apoptosis (285).

The pre-synaptic α-synuclein, one of the central proteins in the etiology of Parkinson's disease, is a modulator of oxidative damage. Certain mutant alleles cause a pathological phenotype in mitochondria and induce apoptosis resulting in neurodegeneration, as reviewed by Thomas and Flint (311). The relationship between mutant alleles of α-synuclein and ROS accumulation has been investigated in the *S. cerevisiae* PD model revealing that α-synuclein-induced ROS accumulation is caspase-dependent (102).

1.4 Oxidative stress response and adaptation

Cells are constantly exposed to the toxic by-products of oxygen reduction. It is critical to understand how eukaryotic cells sense and respond to imbalances in the redox homeostasis. A particularly dramatic example of cells suffering oxidative stress is the neurodegenerative disorder amyotrophic lateral sclerosis (ALS). Missense mutations in the Cu,Zn superoxide dismutase, a O_2- detoxifying enzyme, are tightly linked to familial cases of ALS (267). *S. cerevisiae* is a leading model organism to study oxidative stress response (OSR) phenomena, such as ALS (237). Beyond that, studying the OSR in *S. cerevisiae* may also lead to conclusions about the OSR in its pathogenic relatives of the genus *Aspergillus* and *C. albicans*, in which classic genetic studies were impossible until the recent discovery of a sexual cycle in *A. fumigatus* (239) or are still limited due to a parasexual cycle in *C. albicans* (104).

Adaptation to H_2O_2 and cross-adaptation to other environmental stressors. The OSR in *S. cerevisiae* and its pathogenic kin is characterized by the organisms ability to adapt to low doses of H_2O_2, resulting in resistance to otherwise lethal doses. Adaptation to H_2O_2 is transient and, as an added benefit, leads to cross-protection from other environmental stresses (cross-adaptation). The OSR is coordinated by the transcription factors Yap1 (yeast AP-1-like) and Skn7 (suppressor of kre null) that modulate expression of ROS-detoxifying genes.

Exposure of respiring *S. cerevisiae* cells to sub-lethal doses of H_2O_2 leads to resistance to otherwise lethal doses (163). *C. albicans* (164), *C. dubliniensis* (314), and *C. glabrata* (71) exhibit adaptation as well but the degree of adaptation, as measured in survival at higher doses, varies widely between species. *S. cerevisiae* adapts significantly less well than *C. dubliniensis* and *C. albicans*. Almost all adapted *C. albicans* cells survived a dose twenty-times higher than the lethal dose for *S. cerevisiae*. The differing degrees of adaptation are reflected in differences in catalase enzyme activity induction. *C. albicans* catalase is induced 21-fold and in the other species at least 2-fold (164). Other ROS-detoxifying enzymes induced include peroxidase, glucose-6-phosphate dehydrogenase, superoxide dismutase, glutathione peroxidase, and quinone reductase. A direct comparison between *C. glabrata*, *C. albicans* and *S. cerevisiae* confirmed the low adaptive response observed in *S. cerevisiae* (*C. glabrata* $>$ *C. albicans* $>>$ *S. cerevisiae*). Clinical isolates of *C. glabrata* and *C. albicans* adapted less well than the laboratory strains, whereas clinical *S. cerevisiae* strains adapted better to H_2O_2 than the laboratory strain (71).

To determine whether adaptation to H_2O_2 yields resistance to superoxide and vice versa, yeasts were exposed to the the $O_2\bullet$- generating compounds menadione and methyl viologen. *C. albicans*, *C. dubliniensis* displayed cross-adaptation but *S. cerevisiae* pre-treated with H_2O_2 is sensitive to menadione. Further investigations into the cross-adaptive OSR in *S. cerevisiae* revealed that temperature and osmo-

larity lead to H_2O_2 adaptation but exposure to sub-lethal doses of H_2O_2 did not improve survival of heat stress and high osmolarity (63, 197).

In an effort to identify the underlying cell biology of H_2O_2 adaptation, duration and level of protein synthesis were quantified in *S. cerevisiae*. Adaptation is transient, repeatable, and associated with protein synthesis. Pre-treated cells synthesized at least 21 new proteins and adaptation was obliterated with the addition of cycloheximide (74). A more comprehensive investigation of protein synthesis demonstrated that *S. cerevisiae* synthesized 115 new proteins in response to low doses of H_2O_2 (122). Most proteins that scavenge ROS, such as the cytosolic catalase (Ctt1) and glucose-6-phosphate dehydrogenase (G6PDH), returned to baseline after about one hour (122). The adaptive power of G6PDH and Ctt1 has been verified genetically. Mutants deleted for catalases and G6PDH do not adapt (160, 199). To distinguish whether adaptation in *S. cerevisiae* is due to tolerance or prevention of protein oxidation, the presence of oxidized phenylalanine residues was determined and an increase in damaged proteins detected (252). Yet, with increasing doses of H_2O_2 the rate of protein damage declined, indicating that yeast tolerate damaged proteins when exposed to adaptive doses of H_2O_2 (252). Recently a second mechanism underlying adaptation was described. Exposure to sub-lethal doses causes membrane permeability for H_2O_2 to decline by a factor of two, blocking H_2O_2 from entering the cell (28). In summary, adaptation to H_2O_2 in *S. cerevisiae* is temporary and repeatable. Adaptation is associated with the synthesis of ROS detoxifying enzymes, an increased tolerance towards damaged proteins, and changes in membrane permeability. The H_2O_2 adaptive response in *S. cerevisiae* suggests the presence of a specific OSR program.

H_2O_2 oxidizes and activates the transcription factor Yap1. OSR and adaptation are associated with time-dependent protein synthesis. One of the factors that regulate transcription in response to H_2O_2 is Yap1, a basic region-leucine zipper

transcription factor that was identified and purified based on its ability to recognize the mammalian activator protein-1 (AP-1) recognition element (ARE). Similarities to human AP-1 and yeast Gcn4 suggest that Yap1 is a member of the jun-family of transcription factors that regulate stress response (140, 228). The *yap1* mutant is five-times more sensitive to H_2O_2 than the wild type. Yet, wild type and mutant strain have comparable levels of catalase activity, indicating that Yap1 does not regulate catalase gene expression (278). To identify the mechanism through which Yap1 acts, the *yap1* mutant and a strain containing *YAP1* on a multi-copy plasmid were compared for levels of ROS-detoxifying enzymes. The deletion mutant showed decreased levels of glutathione reductase (*GLR1*), Cu,Zn superoxide dismutase (*SOD1*), and G6PDH (*ZWF1*). The multi-copy plasmid strain had elevated levels of these gene products. G6PDH and Cu,Zn SOD contain ARE binding motifs in their promoter regions, suggesting that Yap1 acts as a positive modulator of transcription (279). 2D gel electrophoresis patterns reveal that a total of 32 genes, half of which contain a *YAP1* recognition element (YRE), are under Yap1 control (187), including *TRX2* (thioredoxin) (177), *GSH1* (γ - glutamylcysteine synthetase) (340), *GLR1* (130), and *GPX2* (glutathione peroxidase) (157) (Table 1.1). Transcription of some of those genes (*GSH1*, *GLR1*, *GPX2*) is further adjusted by YRE number and YRE sequence. A more recent investigation of H_2O_2 modulated expression profiles revealed that the number of Yap1 regulated *S. cerevisiae* genes is closer to 70 (40).

The mechanism of Yap1 gene activation in response to hydroperoxides has been carefully examined in the case of *TRX2*. Yap1 activates transcription under oxidative stress and binds to the YER when cells were treated with H_2O_2 (177). To identify the part of Yap1 that is necessary for transcriptional activation, a reporter gene screen was employed. A *yap1* strain was transformed with chimeras of Yap1 domains fused to heterologous domains from other transcription factors and Yap1 alleles containing different internal deletions and deletions of the C- or N- termi-

nus. Surprisingly, different parts of the molecule responded to O_2•- and H_2O_2 (325). Concurrently, Yap1 DNA-binding activity, cellular localization and the influence of the conserved cysteine-rich carboxy terminus (c-CRD) on Yap1 functionality were investigated. H_2O_2 affects Yap1 cellular localization. In the presence of H_2O_2, Yap1 moves from the cytoplasm into the nucleus. This process requires three conserved cysteine residues in the c-CRD (178, 324). O_2•- exposure still activated Yap1 that lacked the cysteine residues essential for activation by H_2O_2 (79). Differential regulation of Yap1 by H_2O_2 and O_2•- allows *S. cerevisiae* cells to tailor their oxidative stress response depending on the impending challenge, which is beneficial because O_2•- predominantly shift the cellular glutathione pool towards the oxidized state but H_2O_2 nonspecifically damages macromolecules (172).

H_2O_2 oxidizes cysteine residues in the N- and C-terminus of Yap1 causing its nuclear accumulation and activation (79). Oxidized Yap1 is locked in its active form in the nucleus because the reversible intra-molecular disulphide bond masks the nuclear export signal that no longer can interact with the conserved nuclear exporter Crm1/Xpo1 (176). H_2O_2 mediated regulation of Yap1 localization is carried out by the Yap1-binding protein 1 (Ybp1) and the glutathione peroxidase-like enzyme (Gpx3), which transfers electrons from H_2O_2 onto Yap1 cysteine residues (80). Once oxidative stress has passed, thioredoxin reduces Yap1 and Gpx3, thereby turning off the pathway (80). In conclusion, H_2O_2 influences gene expression in *S. cerevisiae* by oxidizing specific amino acid residues in the transcription factor Yap1. The differential activation by H_2O_2 and O_2•- is in keeping with the unique adaptive response described above.

Yap1 in *C. albicans*, *C. glabrata* and *A. fumigatus*. The OSR of pathogenic fungi is of particular interest, given that H_2O_2 produced by phagocytic cells represents the first line of defense against dissemination in the blood stream. After the Yap1-dependent transcriptional intricacies of the OSR were investigated in *S. cere-*

visiae, Yap1 homologs were identified in *C. albicans* (Cap1), *C. glabrata* (CgAP1) and *A. fumigatus* (Afyap1) (179) that exhibit sequence similarity in the bZip domain and the n- and c-CRDs of *S. cerevisiae YAP1*. Deletion mutants are sensitive to H_2O_2 and as expected, homologs complement a *S. cerevisiae yap1* mutant. Their gene products relocate to the nucleus upon oxidative stress. Cap1 and Afyap1 initiate transcription of a similar set of genes to those regulated in *S. cerevisiae* and Cap1 confers fluconazole resistance in *S. cerevisiae* and *C. albicans* (179).

Oxidative stress signaling via a phosphorelay system. The other key regulator of the OSR is the transcription factor Skn7, which acts as the response regulator in a phosphorelay signal transduction system. Phosphorelays are extended versions of bacterial two-component signaling systems that sense and respond to environmental conditions. Phosphorelays differ from two-component systems by using additional regulator and phosphotransferase domains, which allows them to regulate more complex pathways such as cell cycle control in bacteria, heterocyst formation in cyanobacteria, sporulation timing in *Myxococcus* and hyphal formation in *C. albicans* as summarized by Hoch (146).

Components of the oxidative stress sensing phosphorelay system in *S. cerevisiae* include a sensor kinase, a phosphotransferase and a response regulator. The sensor kinase Sln1 has strong sequence similarities to the transmitter and receiver domain of bacterial systems and contains two hydrophobic transmembrane segments in the N-terminus (240). The phosphotransferase Ypd1 transmits the phosphoryl group under oxidative stress to the response regulator Skn7 (192). Accordingly, the *skn7* mutant is sensitive to H_2O_2 (174). The Skn7 response regulator region alone is sufficient for transcriptional activation. An aspartic acid residue on position 427 of Skn7 is responsible for gene activation (174). When D427 was replaced with alanine or arginine, transcriptional activation was abolished. Replacement with another acidic amino acid, hardly changed transcriptional activation.

Genetic studies revealed that *SKN7* and *YAP1* are in the same epistasis group and likely act in the same pathway. They co-activate expression of H_2O_2-detoxifying genes by interacting with the promoter regions of those genes. For example Skn7 binds between the two YREs of *TRX2* (174, 223). Other examples of co-activation include thioredoxin reductase (*TRR1*) (223), peroxiredoxin (*TSA1*) (187), thioredoxin peroxidase (*TPX1*) (46), and alkyl hydroperoxide reductase (*AHP1*) (188). To date, 15 genes of the 32 gene Yap-regulon have been shown to require Skn7 for co-activation as well (187). In addtion to Yap1-interactions Skn7 can also bind to heat shock elements and in concert with heat shock factor Hsf1 activates heat shock proteins in response to oxidative stress (255).

Deletions or disruptions of *SKN7* in *C. albicans* (286), *C. glabrata* (71), *A. fumigatus* (184), and *C. neoformans* (339) lead to increased sensitivity to oxidative stress. *C. albicans* and *A. fumigatus skn7* mutants exhibited reduced resistance to H_2O_2 and tert-Butyl hydroperoxide (TBHP). *C. neoformans* showed reduced growth in TBHP and *C. glabrata* demonstrated reduced survival in H_2O_2. Attenuated virulence was observed in *C. albicans* and *C. neoformans* but no significant difference could be detected between the *A. fumigatus skn7* mutant and the wild type. Interestingly, Skn7 influences morphology of *C. albicans* and flocculence in *C. neoformans*. These studies show that Skn7 is directly involved in the OSR in human fungal pathogens and. Since phosphorelay systems are virtually absent from mammalian cells, they provide an excellent drug target (48, 146).

1.5 General and environmental stress response

Stress response profiles in *S. cerevisiae*. In addition to responding with adaptation to H_2O_2 stress through Yap1- and/or Skn7-dependent transcription of ROS-detoxifying genes, yeasts mount a general stress response (GSR) when exposed to multiple or severe stresses, such as oxidative stress, heat shock, and high osmolar-

ity (270). To capture the breadth of the transcriptional response, the expression profiles of cells exposed to various environmental conditions, including H_2O_2, have been recorded using microarrays (40, 112). The signature of general or global stress response is characterized by genes that respond to all environmental changes in a stereotypical way and named environmental stress response (ESR (112)) or common environmental response (CER (40)). A total of 900 genes (ESR) and 499 genes (CER) participate, functioning in carbohydrate metabolism, protein folding, and energy conservation. The ESR furthermore includes protein kinases and genes involved in glutathione and thiol metabolism. 180 ESR and 136 CER are governed by transcription factors Msn2 and Msn4 (Msn2/4).

***S. cerevisiae* transcription factors Msn2 and Msn4 and their homologs in *C. albicans* and *C. glabrata*.** The Cys_2His_2 zinc finger transcription factors Msn2 and Msn4 were identified in a multi-copy suppressor screen for growth under glucose limiting conditions. Msn2 and Msn4 share 41% identity and are functionally redundant, hence Msn2/4 (93). Msn2/4 bind to stress response elements (STREs) and activate expression of genes that confer resistance to oxidative stress, carbon starvation, heat shock, and severe osmotic conditions. Deletion of both factors abolishes stress-induced activation via STREs (208). Msn2/4 control the expression of a wide array of genes, including genes that encode antioxidants and chaperones, and function in carbon metabolism and protein degradation (141). The gene products are responsible for the removal of damaged proteins and toxic oxygen species and promote accumulation of protective trehalose.

Like Yap1, Msn2/4 accumulate in the nucleus under stress. Nuclear localization is rapid and reversible and negatively controlled by proteine kinase A and cAMP (128). Deletion mutants are sensitive to high doses of H_2O_2 and the double mutant resembles the *yap1* mutant. The *yap1 msn2 msn4* mutant is H_2O_2 sensitive and unable to adapt to H_2O_2. These results were corroborated by proteome analysis. Of

the 71 genes of the H_2O_2 regulon 27 are under the control of Msn2/4 and 7 of those are under Yap1 control as well (122). This emphasizes the importance of Msn2/4 for the general stress response as opposed to the Yap1-driven adaptive response or survival in low doses of H_2O_2. Msn2/4 appear to be important for oxidative damage control rather than detoxification like Yap1 and Skn7.

Orthologs of *MSN2* and *MSN4* were identified in the *C. glabrata* and *C. albicans* genome (71, 92). Surprisingly, *C. albicans* does not seem to have a GSR (92). The *C. albicans msn2/4* double mutant did not respond with phenotypic alterations or transcriptional activation to oxidative stress (92). Potential explanations for the absence of a GSR in *C. albicans* could be evolutionary divergence of stress signaling and response and ecological adaptation.

1.6 Systematic efforts to identify H_2O_2 stress response genes in *S. cerevisiae*

The completion of the *S. cerevisiae* genome sequence opened the door for the development of systematic applications, such as the EUROpean Saccharomyces Cerevisiae ARchive For Functional Analysis (EUROSCARF) that permits the study of biological effects of single gene deletions (123, 335). Haploid strains with non-essential gene deletions and diploid strains hemizygous for essential genes are available in microtitre plates that allow high-throughput queries using robotic work-stations (264). The annotated genome sequence allows computer-based motif searches for genomic features, such as transcription factor binding sites, promoter regions, and transcription start sites. Search algorithms can mine the genome sequence faster than any human ever could, providing lists of motifs that can than be further investigated. EUROSCARF, microarrays and computational tools have been utilized to get a whole genome view on the OSR, identify new OSR genes, disentangle the web of interactions and discover new gene functions.

OSR and GSR gene function discovery using EUROSCARF. Systematic deletion mutants were utilized to identify genes required for survival in H_2O_2. Based on the assumption that a sensitive deletion strain lacks a gene whose product is necessary for survival in H_2O_2, two studies compared mutants for sensitivity to H_2O_2 and other ROS. Higgins et al. (2002) included 600 diploid deletion mutants, with mainly unknown gene functions, and Thorpe et al. (2004) screened the complete set of viable mutants (n=4,546) (145, 312). Both studies found that mutants that are sensitive to H_2O_2 are rarely sensitive to any of the other oxidants tested, corroborating the findings from adaptation studies that suggest that H_2O_2 triggers a specific response in yeast. The proportions of sensitive mutants are comparable between studies. Higgins et al. find ∼9% and Thorpe et al. identify ∼14% mutants that are sensitive to H_2O_2 alone. The H_2O_2 sensitive mutant set from the Thorpe et al. study was enriched for genes with mitochondrial function. This study also extended the scope by screening for H_2O_2-resistant deletion mutants. Five mutants were resistant and included members of the THO complex that functions in transcriptional elongation and genome stability.

Another systematic approach to identify genes involved in response to oxidative stress is microarray-based transcriptional profiling. This technology relies on the assumption that cells experiencing a certain stress alter the expression of genes that are important for stress response. Transcriptional profiles of *S. cerevisiae* after H_2O_2 treatment have been recorded (40, 112). Recurring findings of the same set of genes in independent studies provides additional validation for the importance of these genes in a particular response pathway and corroborates results from single gene studies. With respect to a global transcriptional stress response in *S. cerevisiae* two independent studies characterized the response as transient and described a correlation between the numbers of genes induced and fold change in expression levels (40, 112). The ESR and CER differ in the set of genes responding to sub-

lethal doses of H_2O_2. Gasch et al. identified genes that are required for oxidative and reductive reactions inside the cell and confirmed Yap1-dependent OSR regulation (112). Causton et al. established that genes acting in small molecule transport and RNA metabolism but not H_2O_2 detoxification or redox homeostasis responded with differential regulation (40).

Comparing the results of the systematic deletion mutants and expression studies reveals that the overlap of genes found in both approaches is rather limited. To address this discrepancy, Birrell et al. combined H_2O_2 sensitivity assays of systematic gene deletion mutants with expression profiling to test for a correlation between sensitivity in deletion mutants and gene. The authors measured survival after exposure to DNA damaging agents, including H_2O_2, and recorded gene expression profiles in diploid non-essential gene deletion mutants (n=4,627). More than 900 genes induced transcription more than 2-fold but only 11 of those belonged to H_2O_2 sensitive mutants, a result that can be expected by chance alone (20).

The systematic gene identification and gene function discovery efforts have advanced the *S. cerevisiae* OSR field by confirming the cell's rather particular response to H_2O_2, the central role of Yap1, and the importance of mitochondria for H_2O_2 stress response and survival. The discordance between findings in deletion mutants and expression data needs to be further investigated. These large-scale approaches are valuable tools to generate novel research hypotheses that can then be verified and single-gene contributions determined.

1.7 Protection provided by enzymatic and non-enzymatic antioxidants

To protect themselves from the toxic effects of H_2O_2 and other ROS and to maintain redox homeostasis, cells have evolved antioxidant molecules that delay, prevent or remove oxidative damage (137). Antioxidants can be enzymes, such as catalases

and peroxidases, or non-enzymatic molecules, like the ROS scavenging peptides glutathione and thioredoxin, and vitamins C and E.

Catalases reduce H_2O_2. The heme-containing catalases facilitate the reaction $H_2O_2 + H_2O_2 \rightarrow 2H_2O + O_2$. The mechanism of action has been studied in great detail in *S. cerevisiae*, which has two catalases. Both catalases are encoded in the nucleus but locate to different cellular compartments. Catalase T (*CTT1*) is cytosolic (296) and catalase A (*CTA*) peroxisomal (60, 148). Expression of *CTT1* and *CTA1* is repressed in the presence of glucose, oxygen and heme (149). The promoter of *CTT1* contains a STRE that is sufficient to induce transcription in response to various stresses, such as H_2O_2, osmotic stress, heat-shock and nutrient starvation. The factor that binds to the STRE remains, as of yet, elusive (205). *CTA1*, whose expression is initiated by fatty acids, is of lesser importance for redox homeostasis (289).

Catalase expression and activity is tightly linked to the presence of glucose in the growth medium. Nutrient starvation is a negative regulator of *CTT1* expression acting via cAMP and the RAS pathway (21). Only when glucose is depleted, at the beginning of the stationary phase, does *S. cerevisiae* express *CTT1*. Hence, stationary phase cells are more H_2O_2 resistant than exponentially growing cells (231, 310). Stationary growth in *S. cerevisiae* is characterized as physiological state that is the result of carbon and nutrient starvation and represents a stress-intense environment (327). Consequently, stationary *S. cerevisiae* cells have been found to be resistant to a variety of stressors including heat, osmolarity, and oxidants such as H_2O_2 and $O_2\bullet$-. In order to identify the underlying mechanism of H_2O_2 resistance, stationary cells were compared to cells growing in synthetic defined media under carbon starvation. Both treatments result in resistant cells, indicating that similar defense mechanisms, namely the catalases, might be responsible (163). *S. cerevisiae* mutants without functioning catalases are indistinguishable from wild type in rich media and oxida-

tive stress during exponential growth but adaptation to H_2O_2 was impaired in single mutants and almost nonexistent in the double mutant strain, which survived only low doses of H_2O_2 during stationary phase (160). In addition to removing H_2O_2 catalytically from the cell, catalases appear to protect G6PDH from inactivation (199).

The importance of catalases for virulence has been investigated in *C. albicans*, *C. glabrata*, *A. fumigatus*, and *C. neoformans* and catalases seem to be largely negligible for virulence. The number of catalase genes and cellular enzyme localizations differ between species. *C. albicans* and *C. glabrata* have one catalase gene (*CAT1*/orf19.6229, *CTA1*) that shares 68% sequence similarity, and 85% respectively, with *S. cerevisiae CTA1* (71, 231). Four catalase genes have been found in the *C. neoformans* genome. Phylogenetic analyses of catalase gene sequences from multiple species suggest that two of the *C. neoformans* catalases are spore-specific (*CAT1*, *CAT3*), one is peroxisomal (*CAT2*) and one cytosolic (*CAT4*) (119). Of the three catalases in *A. fumigatus*, *CAT1* and *CAT2* are expressed in mycelium and *CATA* is only found in the conidia (37, 241).

Virulence of catalase mutants was assessed in the appropriate animal models and surprisingly no difference could be found between mutants and wild type. Disruption of all four catalase genes in *C. neoformans* did not reduce virulence (119). The *C. albicans* homozygous disruption strain killed only 60% of the mice compared to 100% for the wild type (341). Disruption of *CAT1* in *A. fumigatus* had no effect on survival in H_2O_2, neutrophils and in a murine inhalation model (37). Yet, disruption of *CAT1* and *CAT2* lead to slightly increased sensitivity to H_2O_2 but wild type behavior in a PMN assay and in the rat model (241). Disruption of *CATA* in *A. fumigatus* lead to increased sensitivity to H_2O_2 but the strain behaved like wild type when tested in a murine alveolar macrophage killing assay and in the rat aspergillosis model (241). A *C. glabrata cta1* deletion mutant was sensitive to H_2O_2 both in logarithmic and

stationary phase. However, the same strain tested for virulence did not differ from the wild type (71).

Cytochrome-c peroxidase reduces H_2O_2 with reducing equivalents from cytochrome c. Based on the observation that a petite *S. cerevisiae* strain was sensitive to H_2O_2 and incapable of mounting an adaptive response, mitochondria were considered to be important for H_2O_2 detoxification (137). Mitochondria are home of the cytochrome-c peroxidase and cytochrome c that form a physical complex in the intermembrane space. Cytochrome c delivers the two reducing equivalents necessary for cytochrome-c peroxidase to execute two-electron oxidations, thereby reducing H_2O_2 to H_2O and regaining redox homeostasis (72, 137, 246). *S. cerevisiae* cytochrome-c peroxidase is encoded by a nuclear gene (*CCP1*); the gene product functions in the mitochondria and is imported by an intricate process that has only recently been elucidated (126, 308). *CCP1* is not essential but required for survival in the presence of H_2O_2 (181). Cells respond to oxidative stress with increased expression of *CCP1* in order to buffer the stress. In addition to its reducing power, cytochrome-c peroxidase has signaling activity that is specific to oxidative stress. Ccp1 activates the phosphorelay response regulator Skn7 that triggers expression of other detoxifying genes, such as thioredoxin (45).

Like the catalases, cytochrome-c peroxidase was thought to protect fungal pathogen from the toxic effects of phagocyte-derived ROS. Indeed in *C. neoformans* cytochrome-c peroxidase provides protection from oxidative stress in an *in vitro* assay, offering an explanation why catalase deletion mutants were not harmed by ROS. However, the *ccp1* mutant is as virulent in the murine cryptococcosis model as the wild type (118), suggesting that protection by antioxidants might just not be important for *C. neoformans* virulence.

Cytochrome-c peroxidase directly affects redox homeostasis by removing H_2O_2 and indirectly by signaling oxidative stress. As with the catalases, cytochrome-c

peroxidase does not seem to be relevant for fungal virulence.

The glutathione, thioredoxin/glutaredoxin ROS-scavenging system. Glutathione (GSH) is ubiquitous in eukaryotes, except for some primitive anaerobes such as *Entamoeba histolytica* (95). Due to its high abundance in cyanobacteria and purple photosynthetic bacteria, it is thought to be evolutionarily old. Its origin probably coincided with the emergence of aerobic conditions on earth and eukaryotes acquired it, like chloroplasts and mitochondria, via endosymbionts (248).

GSH is the most abundant thiol in the yeast cell and, depending on growth conditions, can make up to 1% of the cells dry weight. This tripeptide is composed of cysteine, glutamate and lysine that are connected with each other in two ligase reactions (Table 1.1). The sulphydril group of cysteine defines the biological role of GSH as a reactant with oxidative agents. Oxidized GSH can form disulfide bonds with another GSH (GSSG), with oxidized proteins (GS-S-Cys) or with coenzyme A (GS-S-CoA). GSSG is reduced by glutathione peroxidase (Gpx3), utilizing NADPH (247). Although Gpx3 was originally identified as glutathione peroxidase, it was later shown to additionally be involved in the nuclear localization of the OSR transcription factor Yap1 (80).

To determine if GSH or catalases are more important during H_2O_2 stress in *S. cerevisiae*, single and combination mutants of *GSH1*, *GLR1*, *CTT1*, and *CTA1* were tested for survival in H_2O_2. Strains without *GSH1* and *GLR1* were sensitive but the catalase mutants behaved like wild type. Only catalase double-mutants that also lacked *GSH1* or *GLR1* were sensitive. Hence, glutathione appears to be the primary defense against H_2O_2 and not the catalases, as they were both dispensable (134).

GSH acts in concert with thioredoxins (Trx) and glutaredoxins (Grx) to maintain redox homeostasis. Trx and Grx are structurally similar, heat stable oxidoreductases (Table 1.1) with a conserved cysteine residues in their active sites that aid in electron transfer electrons. Trx and Grx are regulated by Yap1 but the thioredoxin

system additionally requires Skn7 for induction of thioredoxin (*TRX2*) and thioredoxin reductase (*TRR1*). Thioredoxin peroxidase (Tsa1) transfers electrons from H_2O_2 to Trx, which is reduced by Trr1 (Table 1.1). Cells lacking Tsa1 are sensitive to oxidative stress exerted by H_2O_2 and TBHP (129).

S. cerevisiae is viable under normal growth conditions with just one functional copy of *GRX1/2* or *TRX1/2* but both are required for survival during oxidative stress (88). The recurrent theme of differential responses to $O_2\bullet$- and H_2O_2 is reflected in this antioxidant system too. The *grx1* mutant is sensitive to $O_2\bullet$- and the *grx2* mutant to H_2O_2 (Table 1.1) (198). *TRX1* and *TRX2* are up-regulated in response to peroxides. Trx2 is required during stationary phase for peroxide resistance but not during logarithmic growth (110). In addition to the repair of oxidatively damaged proteins, Trx and Grx are involved in additional cellular processes, including protein folding, reduction of dehydroascorbate, and sulphur metabolism.

To keep the glutathione and thioredoxin /glutaredoxin pools reduced, cells require an agent to reduce oxidized GSSG, thioredoxin and glutaredoxin. The reducing power is provided by NADPH, which is generated by the pentose phosphate pathway. G6PDH, encoded by *ZWF1*, converts glucose 6-phosphate to 6-phosphoglucono-δ-lactone whilst reducing two molecules of $NADP^+$ to NADPH. The reductases then use NADPH to reduce the thiols (137). The importance of G6PDH in the cell's redox metabolism is illustrated by the H_2O_2 susceptibility phenotype of G6PDH-deficient cells (161). The central role of G6PDH in this non-enzymatic antioxidant system was confirmed in a comparative study of mutant strains depleted for NADPH generating enzymes G6PDH (*ZWF1*) and isocitrate dehydrogenase (*IDP2*) and peroxidases (*CCP1*, *CTT1*). *zwf1* mutants, lacking G6PDH, were unable to grow on glucose in the presence of H_2O_2, whereas disruption of *IDP2* or *CCP1* had no effect. Only the double mutant showed impaired growth in H_2O_2. A *zwf1/ccp1* mutant did not grow at all in H_2O_2. Based on these experiments, the importance of gene products in

defense of exogenous H_2O_2 can be expressed as follows: *ZWF1* > *CCP1* = *CTT1* > *IDP2*. These data confirm the significance of G6PDH for the cells redox homeostasis. In the absence of *CCP1* and *CTT1*, *ZWF1* and *IDP2* still generate sufficient antioxidant potential. *CCP1* and *CTT1* seem to be required for growth on acetate and then only when either one of the NADPH generating enzymes is missing as well (220).

Fungal genome sequences were searched for homologous sequences to dithiol GRX (*S. cerevisiae GRX1/2*), monothiol GRX (*GRX5*) and monothiol with a TRX-GRX domain (*GRX3/4*). Homologs of all three GRX classes were found in *C. albicans*, *A. fumigatus*, *C. neoformans* and other fungi. GRX and TRX-GRX monothiols were discovered in the *C. glabrata* genome. Cellular localizations have been determined in silico and experimentally (144). In addition to the enzymes described here, different thioredoxin peroxidase isoforms are present in diverse cell compartments in *S. cerevisiae* (129).

Low molecular weight antioxidants. Small molecules that have ROS scavenging properties but no thiol group include vitamins and the disaccharide trehalose. Vitamins are organic compounds that are classified by their biological function and vitamin C, E, and A have been shown to scavenge ROS. Vitamin C is an important co-factor for enzymes in animals and plants. Vitamin E prevents lipid peroxidation and vitamin A interacts with oxidizing radicals aiding in electron delocalization. In vitro assays suggest antioxidant effects for these molecules but physiological relevance remains to be established. Most animals, but not primates, and plants are capable of synthesizing vitamin C, also known as ascorbate (137). Fungi produce the five-carbon analog D-erythroascorbic acid (D-glycerol-2-pentenono-1,4-lactone, EASC) that differs from ascorbate in the structure of its side chain but has similar antioxidant properties (13, 89, 155, 196, 236). Despite its antioxidant characteristics, cells do not increase synthesis of EASC in response to H_2O_2 or TBHP and

the intracellular EASC level does not seem to affect the adaptive response to H_2O_2 in *S. cerevisiae* (137). However, *S. cerevisiae* and *C. albicans* mutants lacking the enzyme that catalyzes the final step in EASC synthesis (*AOL1*) are sensitive to H_2O_2 (154, 156). Unlike the enzymatic defense mechanisms that do not seem to be required for fungal virulence, EASC synthesis is involved in virulence. *C. albicans aol1* mutants are less virulent and show decreased hyphal formation (154). Although most of the research on fungi and ROS scavenging vitamins has focused on vitamin C, experimental data show that vitamin E protects *S. cerevisiae* cells from oxidative DNA damage as well (256).

Trehalose is present in a diverse array of life forms such as insects, invertebrates and plants, but not animals. In *S. cerevisiae* and *C. albicans*, trehalose accumulates during heat shock and stationary growth. In high concentrations, it has free radical scavenging properties and protects proteins from carbonylation (137). A *S. cerevisiae* mutant that was unable to synthesize trehalose was sensitive to H_2O_2 and accumulated carbonylated proteins shortly after exposure to H_2O_2 (17). Both effects were remedied by the addition of trehalose to the growth media. The immediate accumulation of damaged proteins in the mutant indicates that trehalose acts as a radical scavenger rather than in the removal of damaged and mis-folded proteins. Trehalose has also been shown to protect *S. cerevisiae* membranes from oxidative injury (143). This non-enzymatic detoxification mechanism is furthermore implicated in fungal virulence. A trehalose-deficient *C. albicans* mutant displayed reduced survival in H_2O_2 (127).

Antioxidants utilized by pathogenic fungi. An effective non-enzymatic antioxidant used by pathogenic fungi is the biopolymer melanin, which is deposited in the fungal cell wall where it acts as ROS scavenger (138). Melanin functions as radical sink for superoxide and peroxyl radicals that reduce melanin quinones and oxidize hydroquinones (137). Most studies of melanin synthesis and action have focused on

the human pathogens *C. neoformans* and the dematiaceous hyphomycete *Exophiala dermatitidis*. *C. neoformans* melanin-negative strains were not typically found in clinical settings and displayed attenuated virulence in mice (182, 183). As summarized by Hamilton and Holdom, melanin-deficient *C. neoformans* mutants were more sensitive to oxidative stress than the wild type and died from high molecular weight DNA damage (138). Furthermore, melanin production in the infectious conidida of *A. fumigatus* but not in the vegetative hyphae, suggest a role for melanin protection from ROS in fungal virulence and oxidative stress protection (344).

Laccase is an oxidoreductase performing one-electron oxidations. The enzyme has been shown to protect *C. neoformans* from being killed by macrophages. It is thought to convey resistance by oxidizing phagosomal Fe^{2+} to Fe^{3+} and thereby removing it from the Fenton reagent that leads to the production of toxic OH• (195).

The sugar alcohol mannitol has been shown to contribute to survival of *C. neoformans* cells inside neutrophils. A strain producing less manitol was significantly less likely to survive phagocytosis than the wild type. The neutrophil ingesting the mutant showed a higher production of ROS species distal to H_2O_2, indicating that mannitol acts as ROS scavenger (47).

Eukaryotic cells have developed a wide repertoire to protect themselves from the toxic aftermath of H_2O_2 and other ROS. Enzymes, such as catalases and peroxidases and small molecules play important roles in surviving the daily-life attacks of H_2O_2. Although they seem like a natural choice, enzyme-based ROS defense mechanisms do not appear to be crucial for survival of fungal pathogens in H_2O_2 or for fungal virulence. Enzymes are very powerful yet high maintenance cell components. For proper function they require specific physico-chemical parameters like temperature and pH. In a fungal pathogen that is fighting the host defense these might be compromised and small molecules emerge as the better because more stable choice.

1.8 Summary

Ever since the 1960's, when the deleterious effects of H_2O_2 manifested itself in the origin of petite *S. cerevisiae* mutants, the baker's yeast has been used to study the eukaryotic oxidative stress response. H_2O_2 damage of DNA, protein and lipids results in structural distortion, functional impairment, DNA base modifications, and membrane instability. In *S. cerevisiae*, H_2O_2 elicits a unique adaptive response. Exposure to sub-lethal doses results in resistance to otherwise lethal amounts of H_2O_2. Only priming with H_2O_2 leads to improved survival in H_2O_2. Conditioning with heat, salt and other ROS resulted in adaptation to higher concentrations of H_2O_2 but not vice versa. *S. cerevisiae* cells protect themselves from oxidative damage by employing a suite of enzymatic and non-enzymatic antioxidants, including catalases and the glutathione and glutaredoxin/thioredoxin system. If these fail, cells suffer oxidative stress resulting in mitochondrial genome loss, cell cycle arrest, aging and apoptosis, all of which have been investigated in *S. cerevisiae*. The petite-positive yeast facilitates studies on scenarios that are lethal in obligately respiring mammalian cells. The transcriptional response is regulated by Yap1, Skn7 and Msn2/4. Yap1 and Skn7 initiate transcription of ROS scavenging genes, while Msn2/4 regulate transcription of damage control genes. These signaling and response pathways appear to be evolutionary conserved, providing insight into ROS related diseases. Understanding the genetic bases of the oxidative stress response has been advanced by large-scale systematic analysis using systematic deletion mutants and microarrays.

While *C. neoformans* and *A. fumigatus* (239) undergo recombination, the most common pathogenic fungi of the genus *Candida* lack meiosis, precluding them from classical genetic analysis. Biochemical assays, cell molecular biological manipulations, and the use of *S. cerevisiae* as a surrogate system have provided information on their oxidative stress response. Pathogens adapt to low doses of H_2O_2, like *S.*

cerevisiae, and have homologs of the transcription factors that regulate stress response. Investigations in *C. albicans* showed that Cap1 and Skn7 do not contribute to virulence. *C. albicans* lacking the GSR indicates potential divergence of signaling pathways. To fend off the toxic oxygen species exuded by phagocytic cells, fungal pathogens employ an arsenal of enzymatic and non-enzymatic ROS scavenging molecules but only the latter are required for virulence. Melanin, trehalose, mannitol, and vitamin C are necessary for virulence but the enzymes catalase and peroxidase are not. Enzymes require well-defined conditions that might not exist in a fungus exposed to antagonistic host conditions. Studies of the effect of H_2O_2 on *S. cerevisiae* have enriched our knowledge of the eukaryotic oxidative stress response, provided insight into ROS related human diseases, and furthered our understanding of fungal pathogenicity.

Table 1.1: Listed are genes, gene products and their function of components of the thiol glutathione/glutaredoxin system in *S. cerevisiae*. The mutant phenotype category is confined to H_2O_2 and oxidative stress-related phenotypes.

Gene	Protein	Function	Mutant phenotype	Reference
Glutathione - thiol group containing tripeptide electron donor				
GSH1	γ-glutamylcysteine synthetase	GSH biosynthesis (Glu + Cys)	hypersensitive to H_2O_2, TBHP	(132)
GSH2	glutathione synthetase	GSH biosynthesis (γ-GluCys + Gly)	unaffected by H_2O_2, TBHP	(133)
GPX1	glutathione peroxidase	H_2O_2 + 2GSH $\rightarrow$ GSSG + H_2O		(157)
GPX2	glutathione peroxidase	H_2O_2 + 2GSH $\rightarrow$ GSSG + H_2O		(157)
GPX3	glutathione peroxidase	H_2O_2 + 2GSH $\rightarrow$ GSSG + H_2O	H_2O_2 and TBHP sensitive	(157)
GLR1	glutathione reductase	GSSG + NADPH + H^+ $\rightarrow$ 2GSH + $NADP^+$		(64, 229)
GTT1	ER-associated glutathione S-transferase	conjugates xenobiotics to GSH for transport to vacuole	no increased sensitivity to ROS	(55)
GTT2	glutathione S-transferase	conjugates xenobiotics to GSH for transport to vacuole	no increased sensitivity to ROS	(55)
Glutaredoxins - GSH-dependent disulfide oxidoreductases				
GRX1	dithiol glutaredoxin	reduction of protein disulfides	$O_2\bullet$- sensitive	(62, 198)
GRX2	cytoplasmic dithiol glutaredoxin	reduction of protein disulfides	H_2O_2 sensitive	(62, 198)
GRX3	monothiol glutaredoxin	reduction of protein disulfides	H_2O_2 moderately sensitive	(266)
GRX4	monothiol glutaredoxin	reduction of protein disulfides	H_2O_2 moderately sensitive	(266)
GRX5	mitochondrial monothiol glutaredoxin	reduction of protein disulfides	H_2O_2 sensitive	(266)

Continued on next page

Gene	Protein	Function	Mutant phenotype	Reference
Thioredoxin - polypeptide with 2 thiol group				
TRX1	cytoplasmic thioredoxin	reduction of protein disulfides	unaffected by H_2O_2	(110)
TRX2	cytoplasmic thioredoxin	reduction of protein disulfides	H_2O_2 hypersensitive	(110)
TRX3	mitochondrial thioredoxin	reduction of protein disulfides	unaffected by H_2O_2	(245)
TSA1	cytoplasmic thioredoxin peroxidase	Trx-dependent reduction of protein disulfides	$O_2\bullet$-, H_2O_2, TBHP sensitive	(43)
TSA2	cytoplasmic thioredoxin peroxidase	Trx-dependent reduction of protein disulfides	organic peroxide sensitive	(167)

2

Saccharomyces cerevisiae: Population Divergence and Resistance to Oxidative Stress in Clinical, Domesticated and Wild Isolates

2.1 Introduction

S. cerevisiae has long been associated with humans as the fermentative agent in the production of bread, beer, and wine. Archeological evidence for the production of fermented beverages in China dates to 7,000 before common era (BCE), and molecular evidence demonstrating *S. cerevisiae* was the fermentative agent has been found in wine jars from ancient Egypt dating to 3,150 BCE (41, 216). The close relationship between humans and yeast is further reflected in molecular signatures recovered from African artifacts that contained palm wine and from European wine and beer vessels that can be traced to Mesopotamia (97, 189). Due to its close association with humankind, it has been speculated that yeast may have been the first domesticated organism (318). Yet, the ecology of *S. cerevisiae* embraces a wider range than domesticated strains found in the vineyard and the brewery. Wild strains have been isolated from mushroom fruiting bodies as well as oak tree-associated soils

and fluxes (38, 39, 121, 233, 234, 292). Wild isolates of *S. cerevisiae* are furthermore a major cause of spoilage of mango fruit and peach puree, and it has recently been identified in surveys of the fungal diversity in beetle guts (1, 180, 258).

This breadth in ecological diversity, encompassing domesticated and wild isolates, has spurred interest in *S. cerevisiae* life history and population genetics. Yet, studying population biology in an organism so tightly associated with humans is challenging due to sampling bias, limited sampling sizes, human influence, and non-random sampling (233, 290, 318). Consequently, questions concerning population structure and genetic diversity in *S. cerevisiae* have mainly been addressed using strains from grape berries, vineyards and other industrial applications. Fay and Benavides analyzed approximately 7 kb of coding and non-coding DNA sequences in 81 strains from vineyards, sake fermentation and fermentation of palm wine, millet and apple juice, diverse fruit sources, including lychee, fig, and mushrooms, oak-associated strains from New Jersey, and patients in the U.S. and Europe. This extensive analysis resulted in the recognition of domesticated, i.e. human-associated, and wild populations in *S. cerevisiae* (97). Aa et al. examined 6.6 kb of coding and non-coding sequences from 27 strains including soil and oak-associated isolates from Pennsylvania, vineyard strains from two locations in Italy and strains from rotten figs from California (1). The authors found signatures of distinct population structure, moderate levels of recombination and demonstrated that the oak isolates form a monophyletic group. Most recently, a study conducted by Kvitek, Will and Gasch combined investigations into genetic diversity with stress response and identified a distinct sake fermentation clade but no discrete clades for clinical or oak-associated isolates. Interestingly, strains isolated from similar environments share comparable stress response expression profiling patterns and oak isolates appear to have been selected for growth in this particular niche (180). In summary, previous studies indicated that ecology rather than geography coincided with population structure and

that clinical isolates are only distantly related to isolates used in fermentation.

In addition to investigations into the origin and consequences of domestication, *S. cerevisiae*'s rise as an opportunistic pathogen has stimulated studies into its virulence (142, 290). Since the late 1950s, there have been increasing case reports of *S. cerevisiae* infections (56). *S. cerevisiae* and its commercially available preparations known as *S. boulardii*, that are used to treat antibiotic-related diarrhea, have been shown to cause a wide variety of infections, ranging from cutaneous infections and vaginitis to systemic infections of the bloodstream and vital organs (11, 14, 42, 53, 54, 91, 171, 210, 211, 215, 291, 293, 309, 331). These infections are similar to those caused by *Candida albicans*, the most common human fungal pathogen (217, 293, 345). Because of its evolutionary kinship with *C. albicans* and its status as a genetic model system, *S. cerevisiae*, the benevolent baker's yeast, has acquired enhanced scientific value as a model pathogen in the study of virulence-related traits (83, 212).

Microbial virulence-related traits promote host invasion, colonization and virulence. One of these is the ability to survive oxidative stress.The generation of radical oxygen species (ROS) is an integral component of mammalian host defenses and has been shown to be associated with virulence in various bacteria (2, 159, 257, 260, 276). Other virulence traits that have been studied in *S. cerevisiae* include growth at high temperature (213), the formation of multiple colony phenotypes (57), pseudohyphal growth (214), and origin of petite mutants, which lack mitochondria (322). These studies showed that clinical isolates differed phenotypically from laboratory and wine strains, but could not exclude the possibility that the observed association between clinical origin and a virulence trait is due to shared ancestry rather than host adaptation. If clinical isolates share a common ancestor, the evolution of virulence (or a virulence trait) could be attributed to an isolated event(s) that imparted selective advantage to one or more progenitor, pathogenic strains. However, if clinical iso-

lates exhibit multiple evolutionary histories, pathogenicity would more likely reflect an adaptive advantage conferred by the acquisition of multiple virulence traits in different strains.

Despite progress in understanding the population structure of domesticated and wild *S. cerevisiae*, little is known about the emergence of this versatile yeast as a pathogen and the role of selection and/or adaptation in this evolutionary process. This study aims to (i) test for genetic differentiation between strains of a broad range of origins, (ii) investigate the evolutionary origin of clinical isolates, and (iii) identify an association between a virulence-related trait and pathogenicity. The targeted virulence trait is survival of oxidative stress. To investigate population structure and evolution of pathogenicity an ecologically diverse sample of 103 *S. cerevisiae* isolates, comprising seven populations, was analyzed. Clinical isolates with confirmed virulence were obtained from the California Institute for Medical Research in Stanford and Duke University Medical Center in Durham, NC (213). The domesticated, fermentation-associated, isolates consisted of brewery strains from Europe, and vineyard isolates collected from small commercial vineyards in North Carolina and Australia (AU) (268, 292). The wild strains consisted of fruit isolates, collected from tropical monocultures and fermenting fruits from different locales around the world, soil isolates from an arboretum in Pennsylvania (PA) and parks in North Carolina (NC) and insect guts from Louisiana. Commercial *S. boulardii* strains from France, Italy and Germany, complete the sampling (211, 303).

The results confirm previous findings and generated several novel conclusions. (i) At least three divergent groups representing different evolutionary trajectories were detected in *S. cerevisiae*, expanding the previous findings. (ii) Clinical isolates are genetically similar to the isolates from fruit, which supports the hypothesis that monoculture or fermenting fruits may serve as a natural reservoir for the evolution of clinical isolates. (iii) Strains from the clinic and Pennsylvania soil tolerate oxidative

stress better than any other group. However, the clinical isolates are genetically diverse and the soil isolates are clonal, which strongly suggests that resistance to H_2O_2 is an adaptive property of the clinical strains.

2.2 Materials and Methods

2.2.1 Yeast strains, culturing and DNA extraction

S. cerevisiae strains were isolated from the clinic (N=15), soil in Pennsylvania (PA, N=10), soil in North Carolina (NC, N=14), vineyards in NC (N=10) and Australia (AU, N=14), various fruits (N=18), brewery (N=16), commercial *S. boulardii* preparations (N=4), and the insect gut (N=2) (Table 2.1). All strains were permanently stored at -80^{o}C in 15% glycerol or cultivated on rich media plates (YPD, 1% (w/v) yeast extract, 2% (w/v) peptone, 2% (w/v) dextrose, 2% (w/v) agar)(34). DNA was extracted using the CTAB buffer method (108). Soil NC samples were collected as part of this study using a previously established enrichment protocol and ITS sequencing for identification (292, 329).

2.2.2 DNA sequencing and sequence analysis

Genomic DNAs were diluted 1:100 and 2 μl added to a 25 μl reaction from TaKaRa Ex Taq kit (Takara Bio Inc.) with a final primer concentration of 0.6 μM (Table 2.2). The PCR regime consisted of 5 minutes initial denaturation at 95^{o}C, followed by 35 cycles of 30 seconds at 95^{o}C, 30 seconds at the appropriate annealing temperature (T_A) (Table 2.2), and 45 seconds at 72^{o}C, concluding with 10 minutes extension at 72^{o}C. PCR products were purified using the Montge-SEQ$_{96}$Cleanup Kit (Millipore) or the ExoSAP protocol and their concentration determined electrophoretically (326). Between 500 and 1000 ng PCR product were sequenced with BigDye chemistry version 3 according to the instructions supplied by Applied Biosystems. Chromatograms were assembled and analyzed in Sequencher 4.8 (Gene Codes Corp.) and sequences

edited in MacClade 4.06 (Sinauer Associates, Inc.). ITS sequence data were BLAST searched against GenBank using the nr database and the blastn algorithm (7).

The haplotype phase of nuclear loci in strains with more than one heterozygous site per locus was determined using PHASE 2.1.1. (300, 301). Loci that received low confidence probabilities were cloned using the pCR2.1 TOPO TA Cloning Kit (Invitrogen) and sequenced as described above. Two haplotypes per strain were further analyzed. PCA, HWE, AMOVA, F_{st}, π, I_A were calculated in GenAlEx 6, DnaSP 4.50.3, and MultiLocus 1.3 (3, 244, 269). Strains with missing data points were excluded from these analyses and statistical significance values were calculated in 999 permutations (F_{st}), and 10,000 (I_A). Due to limited sampling size *S. boulardii* and beetle gut isolates were not included in HWE, F_{st}, π and I_A calculations. An UPGMA tree based on pair-wise genetic distances between isolates included in PCA was build in PHYLIP 3.68 (98). Haplotype networks were inferred from *MLS1*, *ACT1*, *ADP1*, *PHD1* and *RPB1* in PAUP* 4.0b10 applying the parsimony criterion, conducting heuristic searches, and using tree-bisection-reconnection (TBR) as branch swapping algorithm.

2.2.3 Survival during oxidative stress

Two-day old cultures from YPD plates were inoculated into liquid synthetic defined media (SD, 2% (w/v) glucose, 37.8mM $(NH_4)_2SO_4$, 1.7g/l yeast nitrogen base (YNB) without amino acids and ammonium sulfate), incubated at 30^{o}C while shaking (250rpm), transferred once, and grown over night. Cells were washed twice with 0.9% (w/v) NaCl solution and resuspended in 1x phosphate buffered saline (PBS). After adjusting the cell number to $2x10^3$ cells/ml, 20 mM tert-Butyl hydroperoxide (TBHP, Sigma) were added and treated and control samples incubated for one hour at 30^{o}C, while shaking. 100 μl cell suspensions from both samples were spread on YPD plates with six 4 mm glass balls, incubated for 48 hours at 30^{o}C and colonies

counted. Survival was calculated as the ratio of treated over untreated cells. Each strain was tested three times and results were clustered by origin and plotted in box-and-whisker plots. A one-way ANOVA with Bonferroni correction was carried out to assess differences in variation for all groups with a sampling size of N$\geq$ 10.

2.2.4 Fluorescence-Activated Cell Sorting (FACS)

The ploidy of each *S. cerevisiae* strain was assessed using a previously published procedure with two modifications (34). Exponentially growing cells were used and the final cell number was adjusted to 5x10^7 cells/ml. The successful completion of the staining procedure was verified microscopically and cells were stored in the dark at 4^{o}C until ready for FACS analysis. On average 9,860 gated events were measured per strain.

2.3 Results

2.3.1 All strains are diploid isolates of S. cerevisiae

All isolates in this study belong to the species *S. cerevisiae*, as confirmed by ITS sequencing and all strains were determined by FACS analysis to be diploid (data not shown). To ensure correct estimates of population genetic parameters, haplotype phase within each locus was determined. For the majority of isolates the correct locus haplotype phase could be determined by visual analysis of sequence alignments. For 22 strains the correct phase of one or more loci was identified using PHASE 2.1.1. (300, 301). For ten of those, haplotype phase assignments were verified by cloning and sequencing. Consequently, co-dominant marker assignments and two haplotypes per strain were used in the subsequent analyses (Table 2.1). For calculations of population genetic parameters, strains sharing the same origin were grouped into populations. Seven populations were recognized including clinic, fruit, brewery, NC and AU vineyard, NC and PA soil (Table 2.3).

2.3.2 Within S. cerevisiae three genetically divergent groups are recognized

Principal component analysis (PCA), a transformation method that reduces multidimensional data sets to lower dimensions, was employed to detect putative structure among 87 isolates for which complete sequence data for five loci could be obtained (Table 2.1). Visual inspection of PCA results, revealed three major groups of 20, 26, and 31 isolates, each were identified and designated A, B, and C (Figure 2.1). The clustering was supported by UPGMA analysis (Unweighted Pair Group Method Arithmetic) of a genetic distance matrix derived from strains included in PCA (Figure 2.2).

The composition of groups A, B, and C differs. The majority of clinical isolates (80%) and about half of the fruit (53%) and brewery (42%) isolates are clustered in group A. All soil isolates from Pennsylvania and North Carolina and one clinical isolate comprise group B. All of the isolates from the Australian vineyards, about two-third of the those from the North Carolina vineyards (67%), almost half the brewery isolates (42%), one-fourth of the fruit isolates (24%), one clinical isolate, and *S. boulardii* form group C. Note that two fruit isolates in group C stem from grapes, two fruit isolates from Holly and a papaya. Interestingly, all group C vineyard isolates have been collected from *Vitis vinifera* in Australia or North Carolina. The two vineyard NC isolates that are outside the major clusters were isolated from *V. rotundifolia* grapes, the Muscadine grapes that are native to the southeastern United States. Seven of the nine isolates collected in Adelaide (AU) are identical.

As measure of genetic differentiation, pairwise F_{st} values were calculated for groups A, B, and C. F_{st} values showed significant genetic differentiation between the three groups and analysis of molecular variance (AMOVA) indicated that 33% of the observed variance occurs within these groups and 67% between them. The index of association (I_A), measuring the extent of linkage equilibrium, was significantly

different from zero for groups A and C but not for B.

2.3.3 Levels of recombination, genetic diversity and linkage differ among S. cerevisiae populations

Seven populations encompassed a total of 82 strains for which complete sequence data were obtained. Five population genetics parameters concerning genetic differentiation (F_{st}), recombination, linkage equilibrium (I_A), nucleotide diversity (π), and deviation from Hardy-Weinberg equilibrium (HWE) were calculated (Figure 2.1, Table 2.3). Genetic differentiation varied between populations from different origins (Figure 2.1). Clinical and fruit isolates were not significantly different from each other, but the clinical isolates were distinct from all other isolates. Fruit isolates differed from all except NC vineyard isolates. There was a large degree of genetic differentiation between AU vineyard and NC and PA soils (0.822, 0.845), and soil samples from NC and PA exhibited extensive genetic differentiation from each other (0.831). NC and AU Vineyard populations differed less from each other (0.282). The brewery population was most different from the soil populations (0.445, 0.551) and less different from vineyard and clinical populations (0.239, 0.101, 0.124).

Linkage equilibrium and the minimum number of recombination events calculated for each population differ between populations (Table 2.3). The I_A was significant for the NC vineyard, brewery and fruit populations. Each of the clinic, fruit and brewery populations could be explained by a minimum of five recombination events. The soil isolates showed no evidence of recombination and the vineyard isolates of only a single recombination event among these five loci. I_A and recombination results were reflected in the differences in nucleotide diversity between populations. Fruit, brewery, clinical, and NC vineyard populations exhibit high relative nucleotide diversity. Low π values were calculated for isolates from NC and PA soils and the AU vineyard population. π values are to a large degree in concordance with observed

heterozygosity (Table 2.1). Between 33% and 88% of fruit, brewery, clinical and NC vineyard strains are heterozygous at one ore more loci. Indeed, four brewery isolates are heterozygous at every locus tested. NC and PA soil isolates are completely homozygous and 28% of AU vineyard isolates were heterozygous for at least one locus.

All populations were tested for deviations from HWE at each locus. A population that deviates from HWE does so because of non-random mating, mutation, and selection and other factors that affect population structure. Only the fruit population differs significantly at all loci from HWE (Table 2.3). The clinical population differs at three loci, NC soil, NC and AU vineyard, and brewery populations deviate at least at one locus. HWE calculations could not be conducted on the PA soil population.

2.3.4 Clinical and domesticated isolates of S. cerevisiae exhibit haplotype diversity, soil isolates do not

Haplotype networks were inferred from the DNA sequence data of five nuclear coding loci, totaling 2,527 bp (Figure 2.3, Table 2.1). Although haplotype diversity varied between loci, from 18 for *PHD1* to 7 for *ACT1* and *ADP1*, a common pattern was identified. Each network is characterized by the presence of one to three dominant haplotypes. Those accumulated mutations and gave rise to six to nineteen minor haplotypes in different networks, some of which have not been sampled in this study and are marked accordingly (Figure 2.3).

The haplotype diversity between populations differs widely, and three groups with different levels of diversity can be discerned. The soil populations are the least diverse. With two exceptions, all strains from NC and PA soils are represented by one of the dominant haplotypes in each network. In *ADP1*, NC soil isolates are represented by two haplotypes, and in *PHD1*, NC and PA soil isolates have different haplotypes. Both vineyard populations exhibit an intermediate amount of haplotype

diversity - between two and four types per network. The clinical, brewery and fruit populations demonstrate the greatest diversity, in concordance with the population genetic parameters described above. They are represented by three to eleven different types in each network. Haplotypes from isolates of the same population do not cluster; for example, at the *MLS1* locus, clinical isolates originate from all three common haplotypes, not just one (Figure 2.3).

2.3.5 Clinical and PA soil isolates of S. cerevisiae are highly resistant to oxidative stress

All isolates were tested for survival of oxidative stress exerted by tert-Butyl hydroperoxide, a stable organic analog of H_2O_2. Clinical isolates, PA soil isolates, and strains from insect guts exhibited the highest mean survival rates (Figure 2.4A, Table 2.1). NC soil, both vineyard populations and the *S. boulardii* isolates show decreased survival and intermediate levels of variation. Brewery and fruit populations display survival rates ranging from very low to very high. Analysis of variance (ANOVA) confirmed significant differences in oxidative stress between groups of N$\geq$10 ($P < 0.0001$). Clinical isolates differ significantly ($P < 0.001$) from all groups but PA soil (Figure 2.4B). PA soil isolates differ significantly ($P < 0.001$) from the vineyard and the brewery isolates and only slightly ($P < 0.05$) from the NC soil and fruit isolates. The remaining pair-wise comparisons were either not or only marginally significant ($P < 0.05$).

2.4 Discussion

Although *S. cerevisiae* is a species of inter-fertile isolates (249, 292, 299), PCA delineated three genetically distinct groups with different strain compositions. Group A, comprises isolates from genetically diverse and recombining populations collected in the clinic, the brewery and fruits. Group B includes the clonal but distinct PA

and NC soil populations, in addition to a beetle gut strain. Group C unites the distinct yet homogeneous NC and AU vineyard isolates with genetically diverse brewery strains. These results are similar to the findings from the Fay and Benavides and Aa et al. studies where they reported that human association has shaped *S. cerevisiae* life history and led to domesticated isolates distinct from wild soil isolates (1, 97). This study identified a third group that is dominated by clinical isolates and genetically different from domesticated and wild lineages. These three life history trajectories of *S. cerevisiae* are characterized by different levels of recombination and genetic differentiation that could explain their origin and maintenance.

The clinical isolates are genetically similar to the strains from fruit but not the brewery strains, which suggests that clinical strains may have evolved from wild fruit isolates (group A). Since pathogenicity requires the ability to grow at 37^{o}C, it is teleologically reasonable to hypothesize that this trait is more likely to be acquired by yeasts growing on fruit, which attain high temperatures during decomposition, than brewery vats, which are maintained at low temperatures. This hypothesis is supported by the results from heat death point studies, which showed that *S. cerevisiae* isolates from spoiled peach pure and grape juice were heat resistant (9, 111).

Low levels of recombination and genetic diversity among soil populations (PCA group B) suggest a predominantly clonal life style that contributes to differentiation from clinical and domesticated groups and maintenance of a wild lineage that also exhibits geographic structure because all of its isolates were collected in the eastern United States. Interestingly, the soil isolates share four of five haplotypes with beetle gut isolates, suggesting that insects acquire *S. cerevisiae* while foraging on the ground. In concordance with the Fay and Benavides results, ecology, rather than geography, appears to dominate evolution and origin of domestication in the vineyard and the brewery (group C) (97). Although yeast isolates from NC and AU

vineyards, collected from wine grapes, are genetically differentiated, they were recognized as most similar to each other and different from the Muscadine grape isolates in PCA. The importance of ecology is further emphasized by the observed distribution of brewery strains in PCA groups A and C, which suggests that brewery strains in wine-growing regions originated from grapes, and in areas lacking viniculture, the domesticated brewery yeasts were derived from wild fruit isolates.

The clinical and PA soil populations exhibited the highest mean resistance to ROS. Therefore ROS resistance in the clinical isolates arose either independently or was contributed by the soil isolates. The genetic diversity among the clinical isolates suggests multiple origins of the genetic material required for ROS resistance in these strains. Regardless, fungal resistance to ROS offers protection from oxidative host defenses and is undoubtedly an advantageous pathobiological property. Consistent with this conclusion, the probiotic strains of *S. boulardii* were not as resistant to ROS as the clinical strains. Indeed, strains of *S. boulardii* were less virulent compared to a clinical (YJM145) and a laboratory (Y55) strain (211). The *S. boulardii* isolates used here were cultured from commercial products sold in France, Italy and Germany. Their close association with vineyard strains suggests that some *S. boulardii* may have originated from vineyard strains.

This investigation presents an exciting and provocative demonstration of the complex life history of *S. cerevisiae* beyond its prosaic service as a scientific tool in the laboratory or an agent of fermentation. As a species, *S. cerevisiae* entered two new life history trajectories while continuing its life in the soil and on decomposing fruit. It became domesticated in fermentation and brewing, and it became a human pathogen. With the accumulation of ecological and population genetic data, this versatile microbe becomes an invaluable model for evolutionary biology and population genetics. The current report offers a new paradigm for studying pathogenesis by identifying correlation(s) among the virulence traits of isolates and the ecology of

their ancestral reservoirs. These correlations will identify the genotypes associated with pathogenic strains or the potential for pathogenicity and elucidate the evolution of pathogenicity.

Table 2.1: Survival in TBHP ± one standard deviation (SD) and haplotypes for *S. cerevisiae* strains included in this investigation. Isolates are grouped by sources as indicated. For each isolate the average survival in 20 mM TBHP with one standard deviation and two haplotypes per locus are represented.

Strain ID	Source	Survival ± SD	*MLS1*	*ACT1*	*ADP1*	*PHD1*	*RPB1*
Clinic (N=15)							
YJM145	Lung (309)	0.83 ± 0.124	6/6	1/1	1/1	1/1	1/1
MMRL124[1]	Human flank, DUMC[2]	0.64 ± 0.284	3/5	1/3	1/1	5/5	3/3
MMRL125	Human stool, DUMC	0.8 ± 0.135	2/3	1/1	1/1	1/3	3/3
MMRL1620	Luzon, The Philippines (33)	0.74 ± 0.163	1/3	1/7	4/4	1/5	1/1
MMRL2497	Peritoneal dialysate, NC State lab	0.76 ± 0.151	3/5	1/3	1/1	5/15	3/3
YJM273	(213)	0.78 ± 0.09	1/6	1/1	1/6	1/12	1/3
YJM308	Paracentesis fluid [66]	0.79 ± 0.178	2/4	1/3	1/1	1/1	3/3
YJM309	Blood (58)	0.77 ± 0.016	3/6	1/1	1/1	2/2	3/3
YJM310	(213)	0.81 ± 0.081	4/4	1/2	1/1	2/2	3/3
YJM311	Bile tube (58)	0.89 ± 0.031	1/3	1/1	1/4	8/19	1/3
YJM419	(213)	0.93 ± 0.07	3/3	3/3	1/1	5/5	3/3
YJM434		0.74 ± 0.049	2/2	2/3	1/4	2/2	1/1
YJM436	Mouth (58)	0.79 ± 0.121	3/3	1/1	1/1	1/1	3/3
YJM440	Blood (58)	0.9 ± 0.019	1/3	2/2	1/2	1/2	2/3
YJM454		0.77 ± 0.136	7/7	1/1	1/1	3/3	2/2
PA Soil (N=10) (292)							
YPS128	*Q. alba*, soil	0.76 ± 0.016	1/1	1/1	1/1	1/1	2/2
YPS129	*Q. alba*, flux	0.88 ± 0.104	1/1	1/1	1/1	1/1	2/2
YPS133	*Q. alba*, soil	0.31 ± 0.381	1/1	1/1	1/1	1/1	2/2

Continued on next page

[1] Medical Mycological Research Laboratory

[2] Duke University Medical Center

Strain ID	Source	Survival ± SD	*MLS1*	*ACT1*	*ADP1*	*PHD1*	*RPB1*
YPS134	*Q. velutina*, soil	0.89 ± 0.047	1/1	1/1	1/1	1/1	2/2
YPS139	*Quercus* spp., soil	0.8 ± 0.178	1/1	1/1	1/1	1/1	2/2
YPS141	*Q. velutina*, soil	0.78 ± 0.107	1/1	1/1	1/1	1/1	ND[3]
YPS142	*Q. rubra*, bark	0.69 ± 0.159	1/1	1/1	1/1	1/1	ND
YPS143	*Q. rubra*, soil	0.82 ± 0.128	1/1	1/1	1/1	1/1	ND
YPS154	*Q. velutina*, bark	0.74 ± 0.061	1/1	1/1	1/1	1/1	ND
YPS163	*Q. rubra*, soil	0.87 ± 0.128	1/1	1/1	1/1	1/1	ND
NC Soil (N=14) (this study)							
O1	*Liriodendron tulipifera*, soil, OS	0.59 ± 0.209	1/1	1/1	1/1	3/3	2/2
O2	*Q. prinus*, soil, OS	0.64 ± 0.232	1/1	1/1	1/1	3/3	2/2
O3	*Gaultheria* spp., soil, OS	0.6 ± 0.094	1/1	1/1	1/1	3/3	2/2
O4	*Q. prinus*, soil, OS	0.71 ± 0.155	1/1	1/1	1/1	3/3	2/2
O6	*Acer* spp., soil OS	0.75 ± 0.068	1/1	1/1	1/1	3/3	2/2
O7	*Q. prinus*, soil, OS	0.61 ± 0.082	1/1	1/1	1/1	3/3	2/2
O8	*Q. prinus*, soil, OS	0.45 ± 0.07	1/1	1/1	1/1	3/3	2/2
O9	*Q. prinus*, soil, OS	0.59 ± 0.05	1/1	1/1	1/1	3/3	2/2
SM1	*Q. alba*, soil, SM	0.46 ± 0.07	1/1	1/1	3/3	3/3	2/2
SM2	*Q. alba*, soil, SM	0.58 ± 0.084	1/1	1/1	3/3	3/3	2/2
SM12	*Acer* spp., soil SM	0.59 ± 0.145	1/1	1/1	1/1	3/3	2/2
SM17	*Q. alba*, soil, SM	0.5 ± 0.072	1/1	1/1	1/1	3/3	2/2
SM66	*Q. alba*, soil, SM	0.39 ± 0.159	1/1	1/1	1/1	3/3	2/2
SM69	*Q. prinus*, soil, SM	0.43 ± 0.063	1/1	1/1	1/1	3/3	2/2

Continued on next page

[3] no data

Strain ID	Source	Survival ± SD	*MLS1*	*ACT1*	*ADP1*	*PHD1*	*RPB1*
NC Vineyard (N=10) (268)							
ARN019A	*Vitis vinifera* Chardonnay	0.37 ± 0.083	2/2	1/3	1/4	2/2	1/1
ARN020A	*Vitis vinifera* Cabernet	0.37 ± 0.113	2/2	1/3	1/4	2/2	1/1
ARN022A	*Vitis vinifera* Syrah	0.55 ± 0.269	2/2	1/3	1/4	2/2	1/1
ARN056A	*Vitis vinifera* Riesling	0.7 ± 0.09	2/2	3/3	1/5	1/2	2/4
ARN179A	*Vitis vinifera* Sangiovese	0.3 ± 0.086	1/1	ND	1/1	3/3	ND
ARN202A	*Vitis vinifera* Syrah	0.38 ± 0.211	1/1	ND	1/1	3/3	ND
ARN231A	*Vitis vinifera* Carlos	0.64 ± 0.191	3/3	1/1	2/2	11/11	2/2
ARN239A	*Vitis vinifera* Carlos	0.25 ± 0.08	1/1	ND	1/1	3/3	ND
ARN244A	*Vitis vinifera* Carlos	0.37 ± 0.244	3/3	1/1	1/1	3/3	ND
ARN245A	*Vitis vinifera* Carlos	0.69 ± 0.188	3/3	1/1	2/2	11/11	2/2
AU Vineyard (N=14) (268)							
ARC112A	*Vitis vinifera* Shiraz, Coonawarra	0.78 ± 0.012	2/2	3/3	1/1	2/2	ND
ARA194B	*Vitis vinifera* white, Adelaide	0.26 ± 0.083	2/2	2/3	1/1	8/8	1/1
ARS216A	*Vitis vinifera*, red, Sydney	0.96 ± 0.038	2/2	1/3	1/1	2/2	1/4
ARS250B	*Vitis vinifera*, red, Sydney	0.91 ± 0.038	2/2	1/2	1/4	2/2	1/1
ARS277B	*Vitis vinifera*, red, Sydney	0.3 ± 0.132	2/2	3/3	1/1	2/2	1/1
ARA297A	*Vitis vinifera* Riesling, Adelaide	0.48 ± 0.115	2/2	1/1	1/1	2/2	1/1
ARA299A	*Vitis vinifera* Shiraz, Adelaide	0.55 ± 0.165	2/2	1/1	1/1	2/2	1/1
ARA306A	*Vitis vinifera* Shiraz, Adelaide	0.46 ± 0.076	2/2	1/1	1/1	2/2	1/1
ARA315A	*Vitis vinifera* Shiraz, Adelaide	0.39 ± 0.178	2/2	1/1	1/1	2/2	1/1
ARA316A	*Vitis vinifera* Shiraz, Adelaide	0.43 ± 0.131	2/2	1/1	1/1	2/2	1/1
ARC364A	*Vitis vinifera* Shiraz, Coonawarra	0.03 ± 0.024	2/2	2/2	1/1	2/2	1/1
ARA412A	*Vitis vinifera* Shiraz, Adelaide	0.6 ± 0.157	2/2	1/1	1/1	2/2	1/1
ARA324A	*Vitis vinifera* Shiraz, Adelaide	0.47 ± 0.084	2/2	1/1	1/1	2/2	1/1
ARA496A	*Vitis vinifera* Shiraz, Adelaide	0.29 ± 0.202	2/2	1/3	1/1	2/2	1/1

Continued on next page

Strain ID	Source	Survival ± SD	*MLS1*	*ACT1*	*ADP1*	*PHD1*	*RPB1*
Brewery (N=16)							
WY2124	Bohemian Lager	0.01 ± 0.007	ND	2/2	1/6	4/4	ND
WY3787	Trappist	0.66 ± 0.135	2/2	1/4	1/5	1/12	1/1
WY1026	British Cask Ale	0.45 ± 0.099	2/9	1/2	2/9	4/10	3/7
WLP838	German Lager	0.04 ± 0.029	ND	2/2	1/6	4/4	ND
WLP029	German Ale	0.03 ± 0.034	ND	2/2	1/1	4/4	ND
WY3347	Eau de Vie	0.69 ± 0.203	2/2	1/1	1/1	2/5	1/1
WY1388	Belgian Strong Ale	0.37 ± 0.068	2/9	2/2	1/5	2/2	3/3
WLP033	English Ale	0.22 ± 0.171	1/9	1/2	6/9	4/10	6/7
WLP775	English Cider	0.86 ± 0.131	2/2	2/3	1/1	2/2	1/1
WLP036	Dsseldorfer Alt	0.43 ± 0.071	9/14	1/2	1/9	5/8	1/3
WLP570	Belgian Golden Ale	0.24 ± 0.052	2/9	1/2	1/5	2/2	1/3
WLP007	Dry English Ale	0.02 ± 0.004	1/2	1/2	2/6	4/16	1/6
WLP099	High gravity	0.74 ± 0.141	2/2	1/4	1/5	4/16	1/1
WY3632	Mead	0.59 ± 0.178	2/2	1/4	1/5	1/10	1/1
WLP565	Belgian Saison I	0.61 ± 0.261	9/9	1/1	1/1	ND	5/5
WY3184	Mead	0.56 ± 0.3	1/9	1/2	6/6	4/10	3/7
Fruit (N=18)							
NRRL Y-35	*Ilex aquifolium*	0.04 ± 0.044	2/2	3/3	1/1	2/2	1/1
NRRL Y-963	Sour figs	1 ± 0	3/3	1/1	1/1	2/2	2/2
NRRL Y-382	Grain	0.37 ± 0.079	5/9	1/1	1/2	1/17	3/9
NRRL Y-1537	Grapes	0.27 ± 0.081	2/2	1/1	1/1	2/2	1/1
NRRL Y-7568	Rotten papaya	0.87 ± 0.059	2/2	1/1	1/1	2/2	1/1
NRRL YB-210	Spoiled banana	0.6 ± 0.315	3/15	2/3	1/1	5/5	1/2
NRRL YB-4081	Ripe guava	0.43 ± 0.164	3/3	1/1	1/1	1/1	2/2
NRRL YB-4082	Ripe papaya	0.39 ± 0.194	5/5	1/1	1/1	1/1	3/3
NRRL YB-432	Pineapple peal, Cuba	0.26 ± 0.082	3/3	2/2	1/2	5/8	1/3

Continued on next page

Strain ID	Source	Survival ± SD	*MLS1*	*ACT1*	*ADP1*	*PHD1*	*RPB1*
NRRL YB-908	Wild cherry tree gum	0.69 ± 0.201	11/11	5/5	1/1	13/13	8/8
NRRL Y-5511	Coconut pod drippings	0.51 ± 0.079	2/2	1/1	1/1	2/2	ND
NRRL Y-5997	Ragi	0.84 ± 0.119	1/1	1/1	6/6	7/7	3/3
NRRL Y-7662	Pozol, Mexico	0.85 ± 0.193	3/13	1/1	1/6	6/6	3/3
NRRL Y-11857	Sugar refinery	0.9 ± 0.098	1/3	1/1	2/2	2/2	3/3
NRRL Y-11878	Cane juice, Jamaica	0.87 ± 0.064	1/2	1/1	1/1	2/18	2/3
NRRL Y-12769	Malayan fermented tapioca	0.56 ± 0.108	12/12	6/6	6/6	9/9	3/3
S344	diploid S288c, Rotten fig (224)	0.15 ± 0.062	3/3	1/1	1/1	12/12	3/3
RM11	Fermenting grape must, Italy (225)	0.62 ± 0.106	8/8	3/3	1/1	2/2	1/1
S. boulardii (N=4) (211)							
Ysb1	Perenterol forte, this study	0.57 ± 0.285	2/2	2/2	1/1	2/2	1/1
YJM1004	Commercial (211)	0.18 ± 0.133	2/2	2/2	1/1	2/2	1/1
YJM1005	Commercial (211)	0.68 ± 0.094	2/2	2/2	1/1	2/2	1/1
YJM1006	Commercial (211)	0.52 ± 0.138	2/2	2/2	1/1	2/2	1/1
Insect gut (N=2) (303)							
IY 03-5-26-5-1-1	*Chauliodes rastricornis* (female), Livingston Parish, LA	0.71 ± 0.035	ND	1/1	3/3	3/3	ND
IY 03-5-30-1-1-1	*C. rastricornis* (male), Livingston Parish, LA	0.86 ± 0.033	3/3	1/1	3/3	3/3	2/2
Total Haplotypes			198	200	206	204	176

Table 2.2: Shown are the sequences and appropriate annealing temperatures (T_A) of primers used to amplify partial nuclear coding loci for population genetic analyses and the ITS for species identification.

Locus	Primer	Sequences (3' → 5')	T_A (^{o}C)	Reference
RPB1	A_f	GARTGYCCDGGDCAYTTYGC		
	C_r	CCNGCDATNTCRTTRTCCATRTA	50	(209)
MLS1	MLS1F	TATGRCYGATTTTGAAGATT		
	MLS1R	TARTCCCAWCKWCCRCARTT	50	this study
ACT1	ACT1	TACCCAATTGAACACGGTAT		
	ACT2	TCTGAATCTTTCGTTACCAAT	58	(83)
ADP1	ADP1F	AATAAGTGGTATCGTGAAG		
	ADP1R	CTGACACTTTTTTGGCATTT	50	this study
PHD1	PHD1F	TCCCAGCCTATAACTTTGTGG		
	PHD1Fv2	CATGTTCCTGAAATGAGGCT		
	PHD1R	AGGAATCCAAACACCCTTGA	50	this study
ITS	ITS1	TCCGTAGGTGAACCTGCGG		
	ITS4	TCCTCCGCTTATTGATATGC	53	(108)

Table 2.3: Nucleotide diversity (π), minimum number of recombination events, index of association (I_A), and Hardy-Weinberg Equilibrium (HWE) for seven defined populations.

Population	# of Strains	π x 10^4 (SD[1])	Minimum # of Recombination Events[2]	I_A	HWE[3]
Clinic	15	2.26 (0.18)	5	0.22[NS4]	*PHD1***[5], *MLS1**[6], *RPB1***
PA Soil	5	0.00 (0.00)	0	na[7]	
NC Soil	14	0.3 (0.11)	0	na	*ADP1****
NC Vineyard	6	2.18 (0.26)	1	3.05***[8]	*MLS1**
AU Vineyard	13	0.41 (0.11)	1	0.17[NS]	*PHD1****
Brewery	12	2.64 (0.16)	5	0.67*	*PHD1**
Fruit	17	2.82 (0.25)	5	0.32*	*PHD1****, *ACT1****, *ADP1***, *MLS1****, *RPB1****
Total	82	2.43 (0.09)	6	0.81***	

[1] one standard deviation

[2] four gamete test

[3] deviation from HWE calculated for each locus in each population

[4] not significant

[5] $P < 0.01$

[6] $P < 0.05$

[7] not applicable

[8] $P < 0.0001$ (I_A), $P < 0.001$ (HWE)

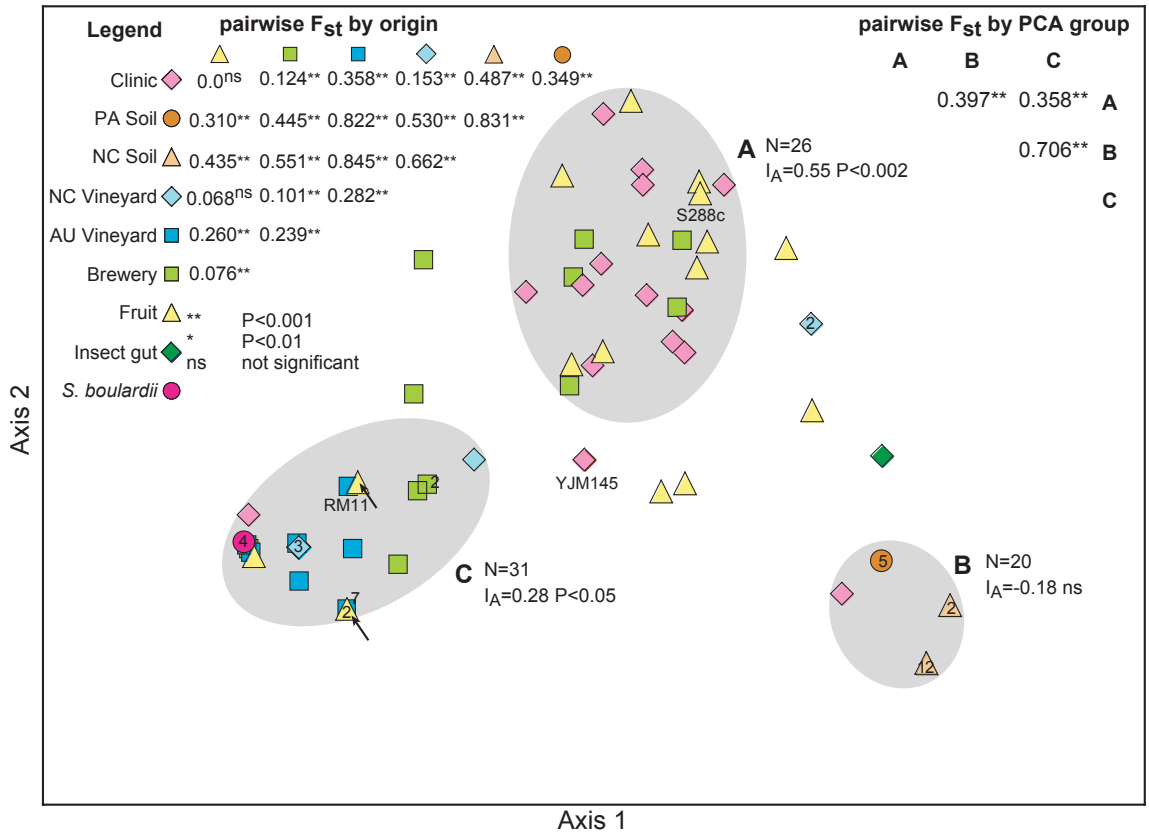

FIGURE 2.1: PCA recognized three major groups (A, B, and C) in a combined analysis of complete sequence data for strains (N=87) from all ecological backgrounds. The size (N) and index of assocation (I_A) of each group is given next to the group name. Strain origins are coded with symbols and colors (see legend to the left). The arrows inside group C point to fruit isolates that have been isolated from grapes but are not part of the Australian or North Carolinian sampling. Strains of particular interest due to their history as lab strains (RM11, S288c) or importance as a model fungal pathogen (YJM145) have their names attached. Numbers inside symbols indicate how many strains share this genotype. Pairwise F_{st} values and significance levels for comparisons by origin (left) and PCA group (right) are indicated.

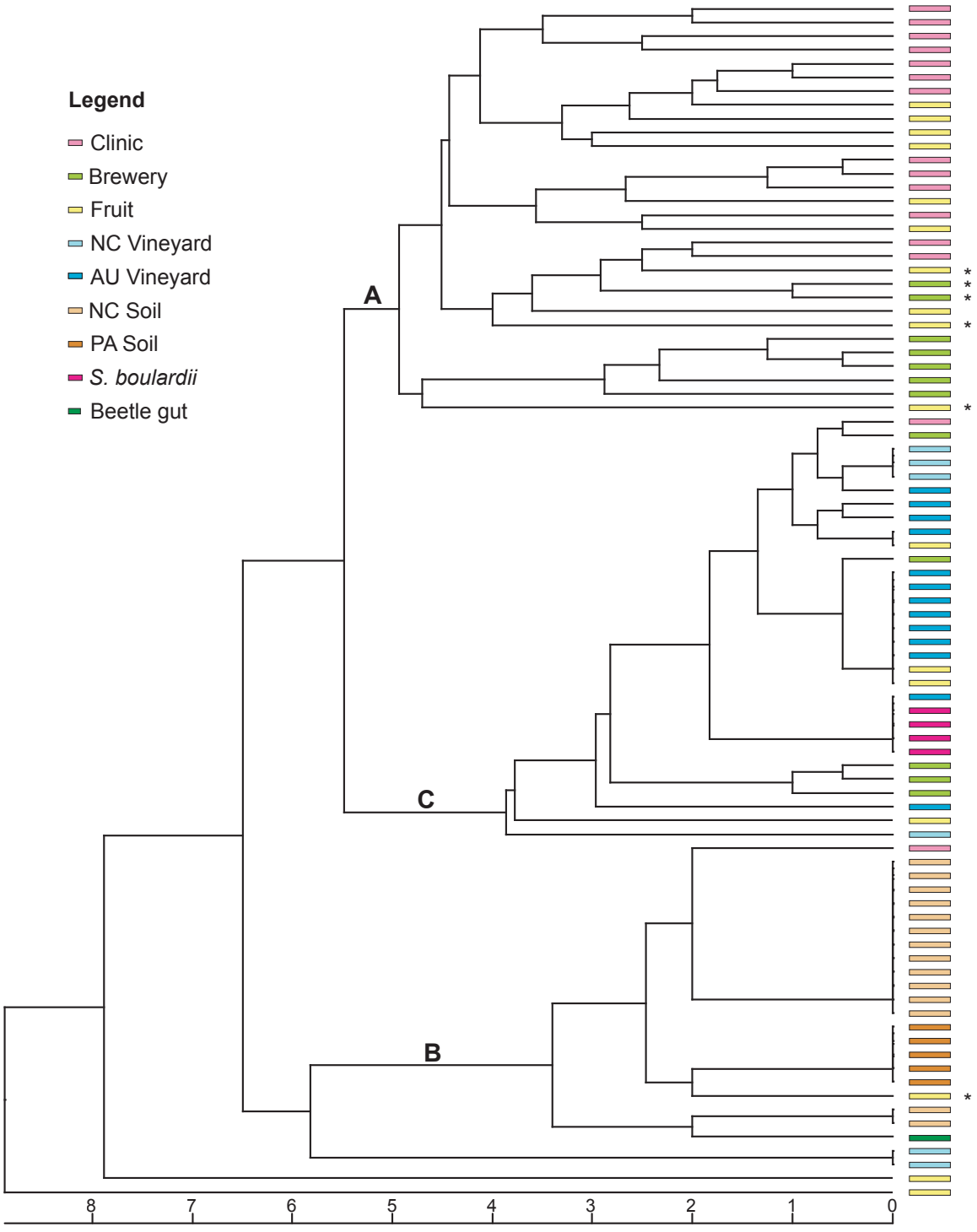

FIGURE 2.2**:** The UPGMA tree was generated from a pair-wise genetic distance matrix based on haplotype data of the 87 strains that were included in PCA. The strains are color-coded by origin (see legend) and groups recognized visually in PCA indicated at internodes in the tree. Strains marked with * denote isolates that are not included in PCA groups A, B or C. The numbered bar below the tree indicates total genetic distance observed in the data set.

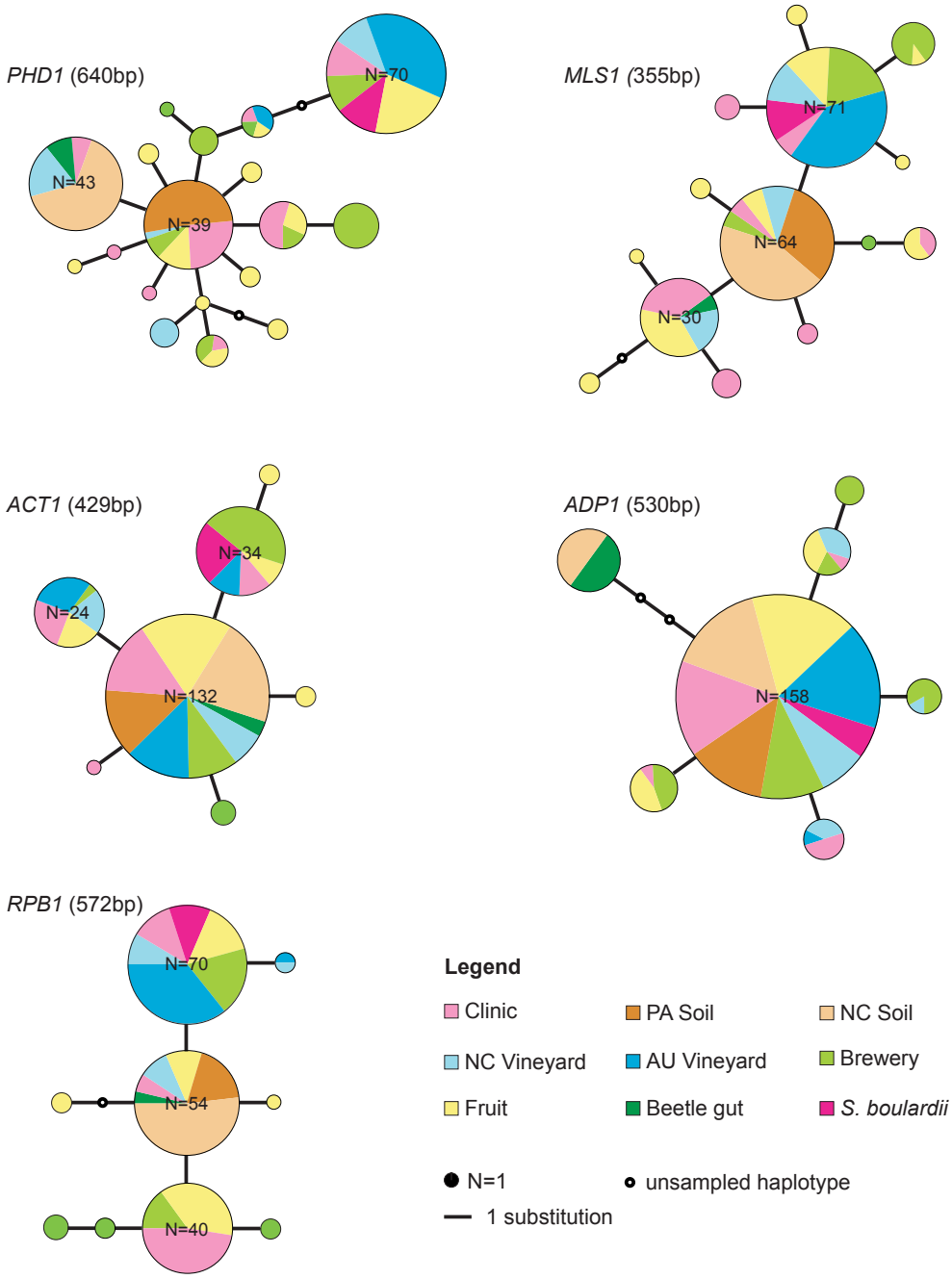

FIGURE 2.3: Two haplotypes per strain were analyzed for five nuclear coding loci. Lengths of analyzed sequence data and number of sampled haplotypes are given for each locus. The size of each pie represents the number of identical haplotypes and the proportions indicate how many of those share a particular origin. If N≥20, the number of haplotypes is indicated in the pie. The length of the connecting lines translates into nucleotide substitutions distinguishing one haplotype from another. Haplotypes collected from the clinic, the brewery and fruit sources are randomly distributed in each network, whereas soil isolates share one or two haplotypes. No correlation between strain origin and haplotype could be detected and no haplotype that unifies all strains from one origin.

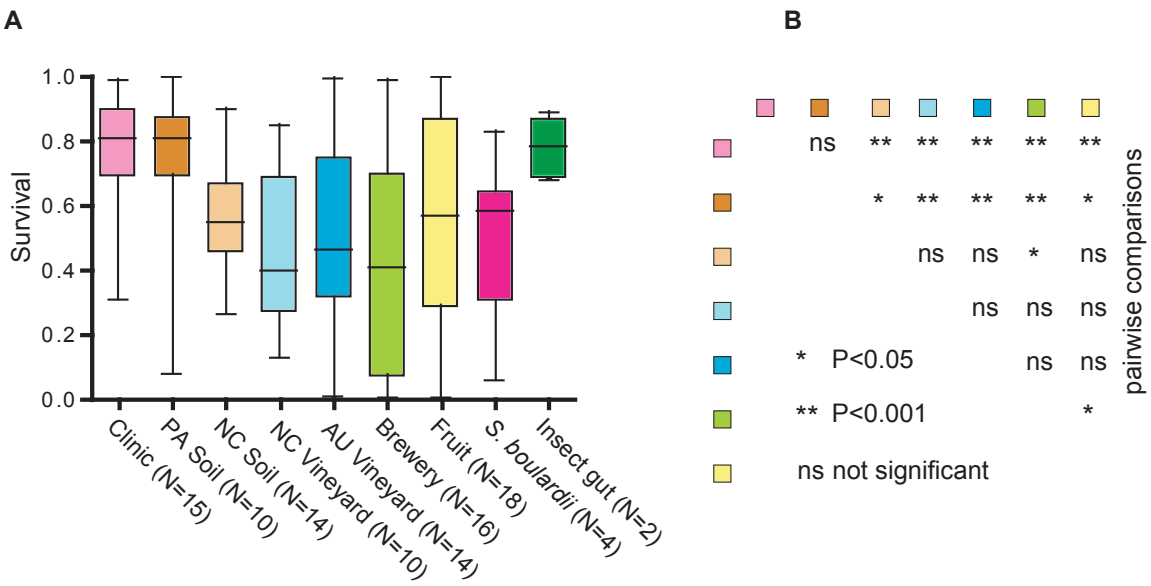

FIGURE 2.4**:** (A) Box and whiskers plot for survival in 20 mM TBHP as tested in the CFU assay. Strains are clustered and color-coded by origin (Table 2.1). For each group of strains the colored box entails the size of the 25th and 75th percentile. The horizontal line dividing the box is the median (50th percentile) and the whiskers represent the most extreme outliers with highest or lowest survival. (B) The multiple pair-wise comparisons of all groups of N≥10 indicate that clinical isolates and strains from the soil in PA differ significantly from strains from other demographic groups. The legend denotes significance values obtained in ANOVA.

3

Biochemical Characterization of Peroxide Survival in a Clinical and Laboratory *S. cerevisiae* Strain

3.1 Introduction

Upon phagocytosis of foreign particles or microbes, white blood cells produce copious amounts of reactive oxygen species, including superoxide radical and hydrogen peroxide (159, 276). The importance of the respiratory burst is reflected in patients that lack this mechanism and subsequently suffer from potentially fatal infections, in a condition known as chronic granulomatous disease (124). ROS oxidatively damage and/or destroy microbial pathogens and thereby deter them from invasion and colonization. Studies on gram-negative and gram-positive bacteria established a correlation between oxidative stress response and virulence (2, 257, 260, 261). In pathogenic fungi, such as *C. neoformans*, the situation appears to be more complex. Oxidative defense mechanisms contribute to virulence but do not seem to be required (69, 138). *S. cerevisiae* plays a double role in studying oxidative stress response, as eukaryotic model system and emerging opportunistic pathogen.

A correlation between the clinical origin of *S. cerevisiae* isolates and peroxide

survival has been described in the previous chapter. Here, biochemical aspects of the phenotypic difference between a laboratory strain and a clinical isolate are investigated. The peroxide sensitive strain S344 (low-survival) is a derivative of the heterothallic laboratory strain S288c, whose progenitor strain EM93 had been isolated from a rotting fig in California (224). S344 is diploid, homothallic, due to replacement of mutant ho with wild type HO, and resistant to Geneticin (G418) (166, 218, 320). The resistant strain YJK1272 (high-survival) has been derived from the clinical isolate YJM128, which had been isolated from the lung of an AIDS patient (309). YJK1272 is diploid, homothallic and resistant to hygromycin B (125). The drug resistance markers, embedded in MX4 cassettes, have been integrated into the genome by replacing the *GAL2* locus. Both markers are neutral with respect to peroxide survival as no phenotypic variation could be detected between strains of the same background that are resistant to G418 and Hygromycin B. The phenotypic difference is reproducible regardless of the nature of the drug marker. These strains have been obtained from the McCusker Lab Collection.

Investigations into the oxidative stress response often use the organic peroxide tert-Butyl hydroperoxide (TBHP, $(CH_3)_3COOH$) instead, or in addition, to H_2O_2. TBHP is commonly employed for its higher thermodynamic stability or if questions regarding the metabolism of organic peroxides are under scrutiny. Both molecules are characterized by the peroxide functional group (ROOR) that spontaneously dissociates and leads to the formation of free radicals (RO•) (homolysis),which cause oxidative stress in living systems. The standard enthalpy change for homolysis of H_2O_2 has been reported as 210.4 ± 0.5 kJ mol^{-1} (271) and for TBHP 193 ± 2 kJ mol^{-1} (284) explaining the higher thermal stability of TBHP. Since both molecules also differ in size, yeast cells were shown to employ catalases to detoxify H_2O_2 and the glutathione system to remove the larger TBHP (131, 160). Consequently, the *grx1 grx2* double mutant is sensitive to TBHP but not to H_2O_2 (198). For the study

of microbial pathogenicity it is relevant to establish if the organism's response to the product of the respiratory burst, H_2O_2, differs from that to the organic, yet more applicable, TBHP.

As described in detail in the introductory chapter, yeast cells respond to low or adaptive doses of H_2O_2 with the oxidative stress response (OSR) and to severe oxidative stress (in combination with other stressors) with the general stress response (GSR). Molecules that are intimately involved in detoxification, redox balance and damage removal are the cytochrome-c peroxidase (*CCP1*), thioredoxin (*TRX2*), and the catalases catalases (*CTA1*, *CTT1*) (126, 134, 160, 205). Gene expression of these and other stress response genes is regulated by the transcription factors Yap1 and Msn2/4 (40, 112, 177, 270, 277). In addition to OSR and GSR, *S. cerevisiae* responds to heat and other stressors with up-regulation of the molecular chaperone heat shock protein 90 (Hsp90). Hsp90 is encoded by two isoforms, one of which responds to stress with increased expression (*HSP82*) (25). Hsp90 re-folds proteins that have experienced heat-stress and subsequently suffered structural changes (232). Like heat, H_2O_2 damages proteins causing structural deformation and inactivation (see Chapter 1).

The low-survival strain S344, the high-survival strain YJK1272, and their hybrid YJS, have been compared for biochemical aspects of survival in peroxide. Four sets of experiments were conducted, targeting the (i) cells response to different peroxides, (ii) the importance of growth stage on survival, (iii) catalase activity, and (iv) expression of stress response candidate genes. This investigation implicates a potentially novel factor or mechanism that is restricted to actively growing cells and differs from known resistance mechanisms such as the catalases, peroxidase and transcription factors that have been shown to regulate stress responses.

3.2 Materials and Methods

3.2.1 Mating S344 with YJK1272 to generate YJS

The hybrid (YJS) was generated by crossing the low-survival strain S344 (HO/HO MATa/MATα *gal2*Δ::kanMX4/*gal2*Δ::kanMX4) with the high-survival strain YJK 1272 (HO/HO MATa/MATα *gal2*Δ::hphMX4/*gal2*Δ::hphMX4). Prior to mating, both parental strains were sporulated for 3 days in liquid 0.5% (w/v) potassium acetate (KAc) at 25^{o}C (S344) or 30^{o}C (YJK1272) on a roller drum (59). 5 μl of each spore solution were mixed and spotted separately as controls on a YPD plate. After 24 hours incubation at 30^{o}C the matings and controls were replica plated onto selective media (YPD with 300 μg/ml Hygromycin B or 200 μg/ml Geneticin) and incubated for 2 days at 30^{o}C. Following confirmation of successful mating, mating products were streaked for single colonies on selective YPD plates and eight of these sporulated for 3 days at 30^{o}C on regular KAc plates (0.22% (w/v) yeast extract, 0.05% (w/v) dextrose, 2% (w/v) potassium acetate, 2% (w/v) agar) (McCusker Laboratory General Instructions for Yeast Plates). A small amount of spores was removed from the KAc plate, dissolved in 100 μl sterile water and 20 μl of this spore solution digested with 20 μl 1:100 dilution of β-glucoronidase (Roche) for 30 minutes at room temperature. Following digestion, 100 μl sterile water were added and the reaction incubated for 2 hours at room temperature. Ten tetrads per isolate were dissected on YPD plates, incubated for 48 hours at 30^{o}C and replicate plated onto YPD plates containing either Hygromycin B or G418 to test for drug resistance segregation patterns. One single colony that gave rise to viable spores with 2:2 segregation of drug resistances was designated YJS.

3.2.2 Dose response profiles, killing rate, and conditioned media and co-culture assays

All survival measures were done using the colony forming unit (CFU) assay as described in Chapter 2. For peroxide dose response profiles, S344, YJK1272 and YJS were exposed to TBHP and H_2O_2 concentrations ranging from 0 – 30 mM and to equal concentrations of tert-Butyl alcohol (TBA) to control for effects of the tert-Butyl group. The rate of TBHP-mediated killing was assessed by recording a killing curve for S344, YJK1272 and YJS. Cells were exposed to 16 mM TBHP and samples collected and tested for survival every ten minutes.

The possible action of secreted factors was explored by employing conditioned media and a co-culture assays. To condition the media, $2x10^3$ cells/ml of S344 and of YJK1272 were incubated for one hour in 2 ml 1xPBS in the presence of 20 mM TBHP as described above. After sterile-filtration with a 0.2 μM size syringe filter, the conditioned PBS solution was freshly inoculated with $2x10^3$ cells/ml from the other strain, incubated for one hour at 30^{o}C and processed for CFU count. For the co-culture assay $2x10^3$ cells/ml of S344 and YJK1272 were co-inoculated in 2 ml 1xPBS and incubated at 30^{o}C while shaking for one hour in the presence of 20 mM TBHP. 100 μl of treated and untreated samples were spread onto YPD plates containing Hygromycin B (300 μg/ml) or G418 (200 μg/ml) and processed as described above.

3.2.3 Growth in SD media and survival

Growth of S344, YJK1272 and YJS was monitored for 24 hours and a growth curve was recorded. Cells from overnight cultures were freshly inoculated in SD media to a starting optical density (OD) of $\sim$0.1 at λ=600nm. ODs were measured every hour for 0 – 20 hours and hours 23 and 24. Parallel to recording growth, samples were subjected to the CFU assay (20 mM TBHP) and peroxide survival was determined.

3.2.4 Catalase enzyme activity

Catalase activity was determined in S344, YJK1272 and YJS after 0, 14 and 23 hours of growth in SD media at 30^{o}C while shaking (250 rpm). Before harvesting cells, ODs were measured at each time point and compared to the growth curve data to ensure that samples were at the right growth stage. 50 ml per strain were split and proteins were extracted immediately from one half while other half was washed twice with 0.9% (w/v) NaCl, treated with 2 mM TBHP, to prevent excessive killing in the sensitive strain, and incubated for one hour in 1xPBS. Whole-cell proteins were extracted following the Y-PER Plus Dialyzable Yeast Protein Extraction protocol (PIERCE) with one modification: 5 units of zymolase were added to the mixture to aid in cell lysis followed by 45 minutes incubation in a 30^{o}C water bath. Whole protein concentrations were determined spectrometrically with Bradford reagent (Sigma) (27).

Catalase enzyme activities in induced and non-induced samples were determined at room temperature using a previously described phosphate buffer-based assay (15). All reactions were started by adding 10-40 μl protein extract to 10 mM H_2O_2 in a total reaction volume of 200 μl. One catalase unit is defined as the decomposition of 1 μmol H_2O_2 per minute and mg protein at 240nm (ϵ=39.4$M^{-1}cm^{-1}$) (199). Commercially available catalase from *Aspergillus niger* (Calbiochem) served as positive control to record a standard curve. Four different amounts of *A. niger* catalase (1, 5, 10, and 15 units) were tested for decomposition of 10 mM H_2O_2 in phosphate buffer.

3.2.5 Semi-quantitative expression profiling of OSR and GSR candidates

Cells were harvested for RNA extraction at 0, 14, and 23 hours and ODs verified. RNA was extracted from induced (2 mM TBHP) and non-induced cells following the cold yeast RNA miniprep protocol from the Breeden lab (`http://www.fhcrc.org/science/labs/breeden/Methods/RNA_miniprep.html`). The amount of RNA in each sample was determined spectrometrically and 10 μg RNA per sample were

digested with four units of RNase-free DNase I (New England BioLabs) for 10 minutes at 37^{o}C. 1 μg of digested and undigested RNA was electrophoretically separated to confirm the absence of DNA. Upon successful DNA removal, cDNA synthesis was carried out on 1 μg DNase digested RNA using the iScript cDNA synthesis kit in a 20 μl reaction volume (Bio-Rad). To control for amplification of cDNA rather than genomic DNA, PCR was conducted on samples that were treated with and without reverse transcriptase (RT) (Bio-Rad). PCR amplification of cDNAs was conducted in a total volume of 25 μl using the TaKaRa Ex Taq kit (TaKaRa) on 2 μl cDNA and a final primer concentration of 0.6 μM (Table 3.1). The basic PCR regime consisted of 5 minutes initial denaturation at 95^{o}C, followed by 25-35 cycles of 30 seconds at 95^{o}C, 30 seconds at the primer-specific annealing temperature (T_A) (Table 3.1), and 45 seconds at 72^{o}C, concluding with 10 minutes extension at 72^{o}C. 10 μl PCR product were separated in a 1% agarose gel and brightness visually compared between strains and time points.

3.2.6 Statistical analyses

Biological triplicates were carried out for each experiment. The results from the conditioned media and co-culture experiments were compared in a one-way analysis of variance (ANOVA) with Bonferroni correction. Experiments that compare a specific treatment or enzyme activity at a certain time point, including the dose-response profile, growth and survival during batch-culture, and the catalase activity assays, were analyzed using two-way ANOVAs with Bonferroni correction. Linear regression and determination coefficient (R^2) were calculated for the killing rate assays and the *A. niger* catalase standard curve. The survival data were subjected to curve fitting using linear and nonlinear regression equations, using the Akaike information criterion to determine goodness of fit. All statistical analyses were conducted using Prism 4.0a (GraphPad Software, Inc.).

3.3 Results

3.3.1 YJK1272 and YJS have similar dose-response profiles in TBHP and H_2O_2 but differ from S344

TBHP is commonly used as a substitute for H_2O_2 in studies investigating oxidative stress. To ensure that both peroxides elicit the same phenotype, S344, YJK1272 and YJS were exposed to increasing concentrations of TBHP and H_2O_2. To exclude the possibility that the phenotype is influenced by the tert-butyl group rather then the reducing actions of the peroxide bond, TBA was used as control. YJK1272 and YJS survived both peroxide treatments significantly better than S344 ($P < 0.0001$; Figure 3.1A and B). S344 and YJK1272 differed at mid-range concentrations of 10 mM TBHP ($P < 0.05$), 15 mM TBHP ($P < 0.001$) and 20 mM TBHP ($P < 0.05$). S344 and YJS differed at 15 mM TBHP ($P < 0.05$). YJK1272 and YJS did not differ from each other. In H_2O_2, YJK1272 and YJS survived at all concentrations better than S344 ($P < 0.001$). Additionally, YJK1272 and YJS differed at 15 and 20 mM from each other ($P < 0.05$, $P < 0.001$). Exposure to TBA had no effect on survival of any of the strains at any concentration (Figure 3.1C). Given the similarity in survival phenotypes between TBHP and H_2O_2, TBHP was used for all further experiments because of its higher stability and safety.

3.3.2 Survival declines immediately after addition of TBHP but is alleviated in S344 by a factor secreted by YJK1272

Survival in TBHP over time varied significantly between strains and time points ($P < 0.0001$; Figure 3.2A). The observed number of cells at time point zero (immediately after addition of TBHP) was much smaller in S344 than in YJK1272 and YJKS. S344 cells started to die immediately after addition of TBHP (time = 0 minutes). The y-intercept of S344 (0.8399 ± 0.0541) was significantly smaller than that of YJK1272 and YJS (1.074 ± 0.0869, 1.069 ± 0.0924). Survival declined with time

for all strains (S344: $P < 0.01$, YJK1272 and YJS: $P < 0.05$). Survival declined significantly more rapidly in S344 (slope = -0.009536 ± 0.001500) than in YJK1272 (YJK1272=-0.007679 ± 0.002410) or YJS (YJS=-0.008024 ± 0.002562).

When strains were cultured in conditioned medium or grown in co-culture in the presence of TBHP, survival of S344 improved slightly compared to the control. Yet, only in co-culture with YJK1272 was the difference significant ($P < 0.05$). YJK1272 survival does not vary significantly between treatments (Figure 3.2B).

3.3.3 TBHP survival differs in the exponential growth phase but not in stationary phase

The growth of each strain in synthetic defined media was recorded as a measure of optical density. Strains exhibited the expected growth curve pattern, comprising a lag phase, exponential growth, and a stationary phase (Figure 3.3A). Entrance into exponential growth occurred at around seven hours post inoculation and stationary phase was reached after 20 hours. Growth curves differed significantly between strains ($P < 0.0001$). With the onset of exponential growth, YJS grew faster than YJK1272 and S344 (heterosis). S344 and YJK1272 grew with a comparable rate at any time point (Figure 3.3A).

Survival of 20 mM TBHP changed during batch-culture growth ($P < 0.0001$; Figure 3.3B). During lag phase, all three strains exhibited low survival. Upon entering exponential growth, YJK1272 and YJS displayed a sudden increase in survival compared to S344, whose survival only gradually increased. In stationary growth phase, all three strains survived treatment with TBHP at comparable levels. During lag phase survival of YJS was significantly lower than S344 and YJK1272 ($P < 0.001$, $P < 0.05$). For YJK1272, survival increased from 0.2 to 0.8 between 6 hours and 10 hours. Survival of YJS increased from 0.05 to 0.9 between 9 hours and 15 hours. Best curve fits for survival data were achieved using the Boltzman sigmoidal

equation with R^2 being 0.7463 for S344, 0.665 for YJK1272 and 0.9267 for YJS. To obtain maximum phenotypic differentiation all subsequent assays were conducted 14 hours post inoculation. This includes phenotyping of segregants and reciprocal hemizygozity analyses of parental alleles in an effort to identify the genetic bases of high peroxide survival in the clinical isolate.

3.3.4 Catalase enzyme activity is low and indistinguishable during exponential growth

A standard curve of H_2O_2 decomposition was recorded for 1, 5, 10, and 15 units of commercial *A. niger* catalase. The best-fit coefficient (R^2=0.946) indicated that the catalase enzyme assay accurately determined catalase activity (Figure 3.4A). Based on the equation for the linear curve-fit (y=0.054x) catalase enzyme activities were calculated in whole-protein extracts of S344, YJK1272 and YJS whose ability to decompose 10 mM H_2O_2 were measured over one minute.

Catalase enzyme activities for S344, YJK1272 and YJS were determined at critical points along the growth curve, including at the very beginning, at mid-log and in stationary phase. Enzyme activities were less than half a unit in all three strains, at all time points, in induced or non-induced samples, with one exception (Figure 3.4B). The enzyme activity plots showed increased activity in YJS during stationary phase after induction with TBHP but not without induction. A t-test revealed that this difference was significant ($P < 0.05$). Comparing all strains and time points with each other in a two-way ANOVA with Bonferroni correction showed that only the difference in catalase enzyme activity between S344 without TBHP and YJS with TBHP ($P < 0.001$) was significantly different.

3.3.5 Expression profiles of OSR and GSR markers are indistinguishable during exponential growth

Semi-quantitative expression profiles of key components of the OSR and GSR were recorded for non-induced and induced samples of S344, YJK1272, and YJS at 35

PCR cycles. Successful cDNA synthesis was established by the presence of PCR fragments of expected size in the positive *ACT1* control +RT and the absence of products in the negative control -RT (Figure 3.5). Fragments in *ACT1* +RT were of comparable brightness with the exception of YJK1272 +TBHP in lag phase, which was very weak. No fragments were detected in the negative controls of the other genes (data not shown). PCR amplifications of genomic DNAs were successful in all cases yielding fragments of expected sizes.

Three OSR candidates were tested (*YAP1*, *CCP1*, *TRX2*). *TRX2* derived cDNA levels were at equivalent levels in all samples. *YAP1* expression was barely detectable and no expression could be detected for *CCP1* during mid-log phase, the phase of interest due to the large phenotypic difference. *YAP1* and *CCP1* cDNA levels were visible in lag phase and stationary phase, but there was no correlation between intensity and strain or treatment. *YAP1* expression appears to be higher in the hybrid than in the parents.

GSR candidates that were investigated include *MSN2*, *CTT1* and *CTA1*. No expression could be detected for either catalase gene (*CTT1*, *CTA1*), except for *CTA1* from YJS +TBHP in lag phase. Yet, the amplicon size differed from that of the genomic control indicating non-specific amplification. *MSN2* expression was consistently stronger in lag phase than in mid-log or stationary phase. No expression differences could be detected for *MSN2* among strains and treatments, except for YJK1272 +TBHP in lag phase and YJS -TBHP where no expression could be detected.

HSP82, encoding the stress-induced isoform of Hsp90, expression was comparable for all strains and treatments during mid-log phase but differed during lag and stationary phase. During lag phase, S344 and YJS +TBHP exhibited strongest expression. In stationary phase, expression in YJS -TBHP was stronger than in the other samples, which exhibited comparable expression levels.

3.4 Discussion

Dose response profiles, killing rate, conditioned media and co-culture assays allow the following conclusions about the nature of the phenotype: (i) killing is due to the peroxide group; and not the tert-Butyl group, (ii) YJK1272 becomes resistant to TBHP right at the beginning of mid-log growth, the hybrid YJS towards the end of it and both strains survive TBHP treatment better than S344 and (iii) a YJK1272-secreted factor improves S344 survival.

The results obtained from comparative dose-response profiles of TBHP and H_2O_2 in combination with the change in survival from exponential to stationary growth, exclude candidates that have previously been shown to elicit different H_2O_2 and TBHP survival phenotypes and whose degree of survival depends on growth stage. Those candidates include *RAD9*, a DNA damage-dependent checkpoint protein, and the glutaredoxins (*GRX1*, *GRX2*) (Table 1.1) (99, 198). The *rad9* mutant is an unlikely candidate since H_2O_2 and TBHP affect it in different ways. H_2O_2 kills the *rad9* mutant but TBHP has no effect (99). The data presented here show similar effects of H_2O_2 and TBHP on strain survival, excluding the *rad9* mutant. The *grx1 grx2* double mutant is sensitive to H_2O_2 and TBHP, suggesting that *GRX1* and *GRX2* could have impaired function in S344 (198). The results collected here for survival during different growth stages, rule this scenario out as S344 survives TBHP in stationary phase but the *grx1 grx2* mutant is sensitive to oxidative stress during stationary growth.

Recording a growth curving and measuring survival during different stages showed that the phenotypic difference is largest during exponential growth and all strains survive oxidative stress during stationary phase at comparable levels. This result allows two conclusions. First, the mechanism causing increased survival in YJK1272 and YJS requires cells to be in a metabolically active state. Second, cellular processes

acting during stationary phase that render cells resistant to various stresses do not influence the phenotype. Extending the second point would also imply that the GSR is unlikely to be responsible for the phenotypic difference. The GSR is initiated when yeast cells are exposed to a multitude of different stresses, as is the case during stationary phase (270, 310).

Catalase enzyme activities were measured during different stages of the growth curve and were shown to be comparably low in all strains during the critical phase of exponential growth. The low enzyme activities during exponential phase are in concordance with previous findings that expression of both catalase enzymes is repressed in the presence of glucose, which is present during mid-log phase (60). These data, in combination with the catalase expression results described below, strongly indicate that the H_2O_2 detoxifying catalases are not responsible for the phenotype under investigation.

Expression profiles of GSR and OSR transcription factors and detoxifying molecules did not differ between the parental strains and their hybrid during exponential growth, the phase critical for the phenotypic difference observed. Candidate gene expression is either not detectable or does not differ between parental strains and treatments during exponential growth. Both regulators of OSR and GSR, *YAP1* and *MSN2*, are expressed at comparable levels. Phenotypic differences could still be due to structural variation but both molecules are highly conserved between S344 and YJK1272. Expression levels for the cytosolic (*CTT1*) and the peroxisomal (*CTA1*) catalases are, as expected, below the level of detection (60). Interestingly, while *HSP82* levels are uniform during mid-log phase, S344 and YJS seem to respond with *HSP82* up-regulation when exposed to TBHP in lag phase. The expression data corroborate the growth phase and survival data, suggesting that GSR and OSR are of little impact on survival of TBHP.

The secreted factor that improves survival of S344 is most likely to be of short-

lived nature. S344 survival appears to increase slightly in the conditioned media and co-culture experiments compared to the control but only in the co-culture assay is the difference significant. This indicates that the factor acts immediately after addition of TBHP and declines during the one hour incubation period so that is has only a minimal (non-significant) effect in the conditioned media. The factor's character remains to be established but potential candidates are the quorum sensing molecules tyrosol and phenylethanol (50, 328).

After ruling out the most likely candidates for increased peroxide by showing that catalase activity is negligible and that expression levels of oxidative and general stress responses are comparable between parental strains, it can be concluded that novel mechanisms are responsible for the differential survival observed. Genetic analyses will need to be conducted to identify the cause of increased peroxide survival. The factor/mechanism is predicted to be at the beginning of a pathway or highly connected at the center of a metabolic network as the phenotypic difference is not only quite dramatic but depends strongly on the cell to be metabolically active.

Table 3.1: Primers used for semi-quantitative expression profiling of OSR and GSR candidate genes. All primer pairs, with the exception of the pair used to amplify *ACT1* (83) were developed as part of this investigation.

Gene	Primer sequence (3' → 5')	T_A (^oC)	Fragment size (bp)
ACT1	F: TACCCAATTGAACACGGTAT		
	R: CTGAATCTTTCGTTACCAAT	58	564
CTT1	F: GAAGACAACGACGAAGTATCTG		
	R: CTCTGTATAATCCTCTTAGTC C	51	853
CTA1	F: CAATCCCGCTATCAGAGATG		
	R: GTCTCTTCCAGATTGCTGTC	53	786
CCP1	F: AAGGACCCTGGAGCGAAAAGTA		
	R: TCCAGAGTTCTTCAAGTGGGTC	50	871
TRX2	F: GGTCACTCAATTAAAATCCGC		
	R: ATAGCAGCTGGGTTGGCACCG	53	285
YAP1	F: AGGGTTCAAAATCTCGTCACG		
	R: AACCAATCCATCGAAGTGGA	50	706
MSN2	F: CGTGGAGAATAATAACCCAA		
	R: GTCTATGTTCAGTGAATTAAAATA	50	709
HSP82	F: TGGCTAGTGAAACTTTTGA		
	R: AAGGCTTAGTCTTGTTTAG	50	825

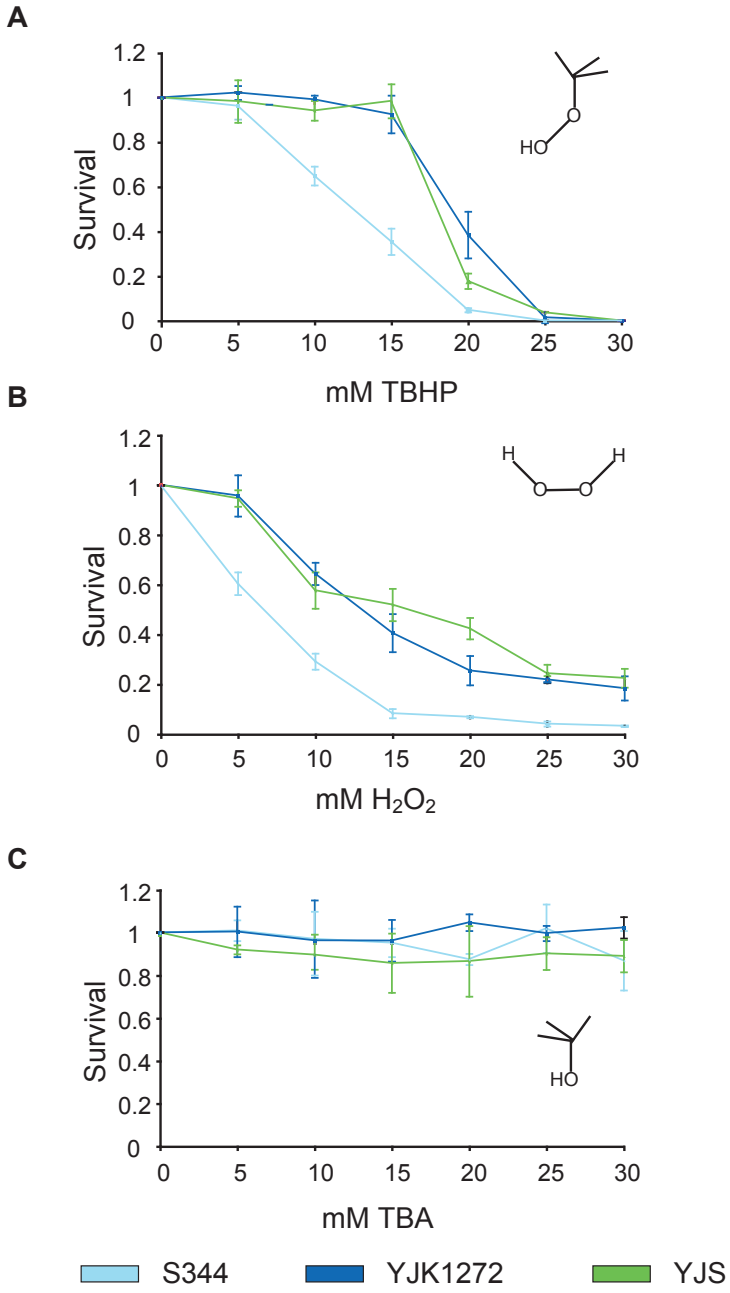

FIGURE 3.1**:** To record dose-response profiles strains YJK1272, S344 and YJS were exposed to TBHP, H_2O_2 and TBA concentrations ranging from 0 to 30 mM and survival measured in triplicates. The X-Y straight marked scatter plot shows the means and one standard deviation at each concentration. Each strain is represented in a different color (light blue=S344, dark blue=YJK1272, green=YJS). The skeletal formulas inserted in the diagrams illustrate the peroxide bond in (A) TBHP and (B) H_2O_2 and the tert-Butyl group in TBHP and (C) TBA.

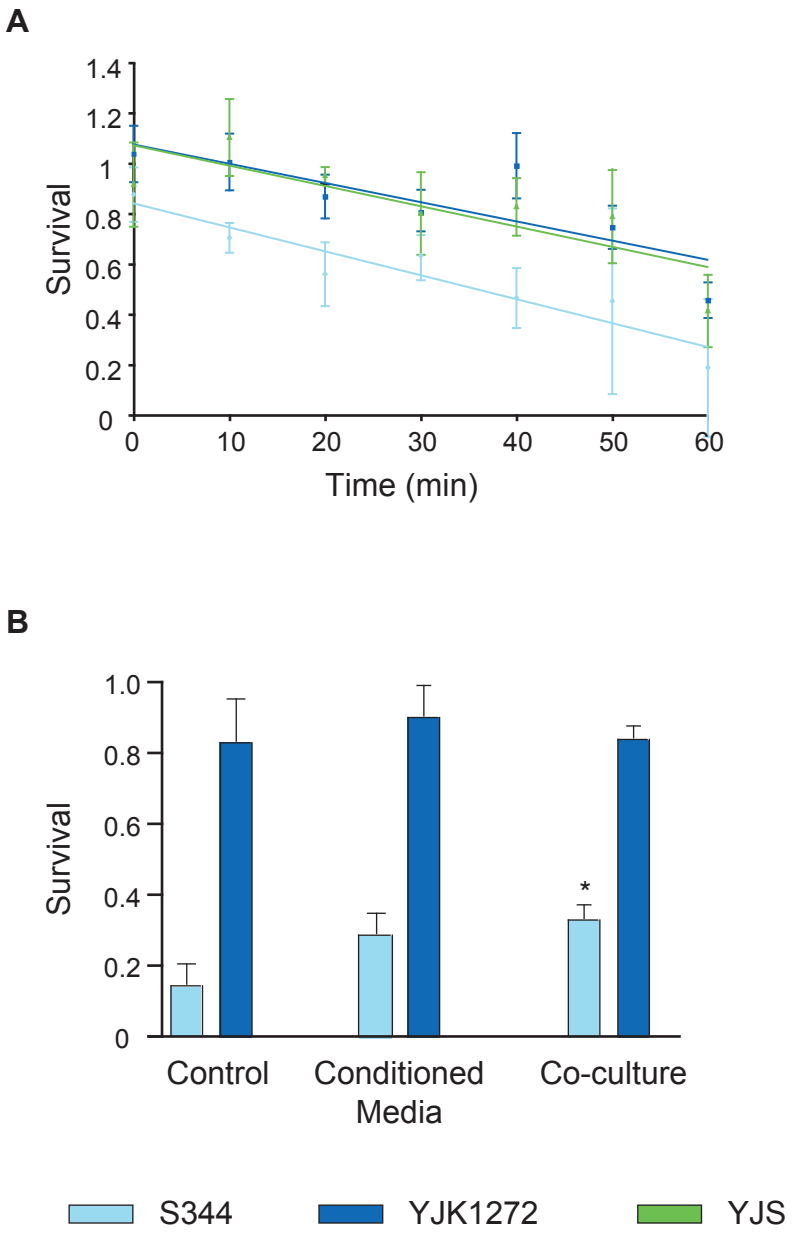

FIGURE 3.2: Killing curve recorded for TBHP and survival in conditioned media and co-culture. (A) Time course of survival in 16 mM TBHP. Triplicates of each experiment plotted with one standard deviation and the linear regression line are shown in the strain's corresponding color. (B) Comparison of YJK1272 and S344 in conditioned media and co-culture. Triplicates with one standard deviation are shown.

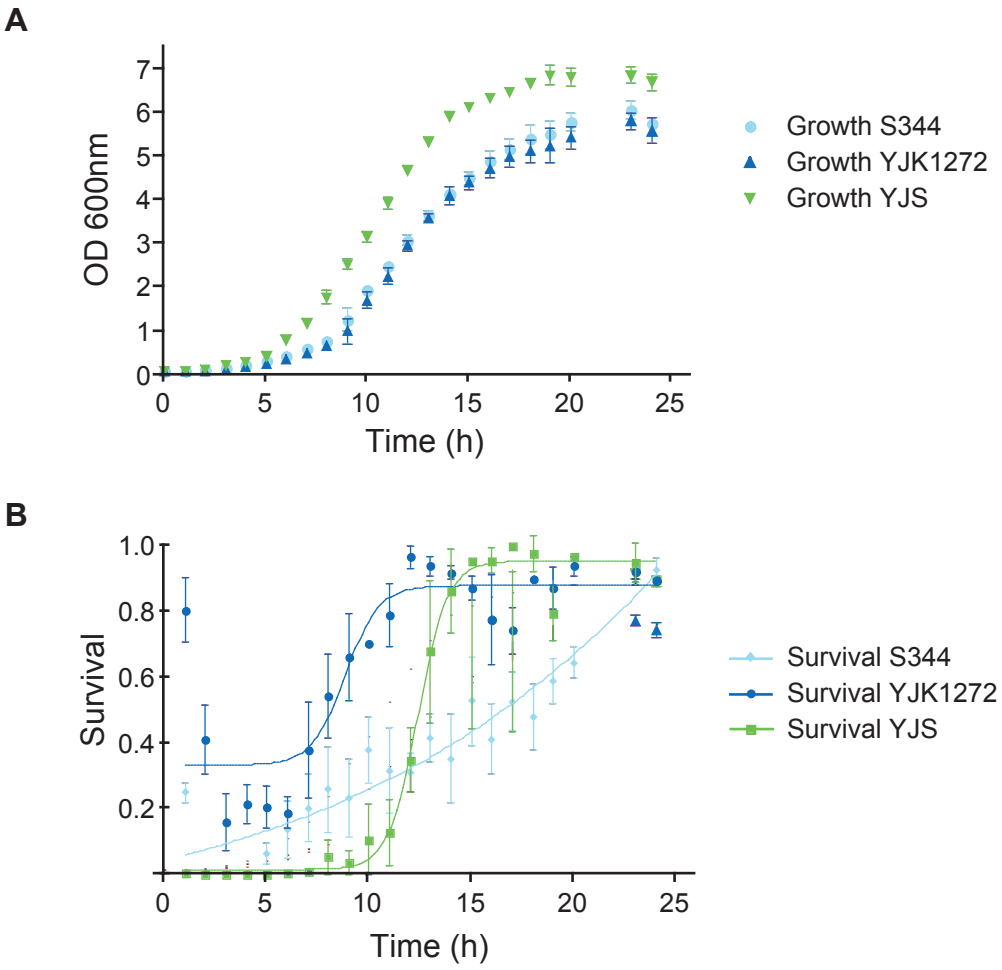

FIGURE 3.3: (A) Growth in SD media was measured in hourly intervals three times for S344 (light blue), YJK1272 (dark blue) and YJS (green). Shown are means and one standard deviation of OD measures. (B) Hourly records of TBHP survival (curve-fitting line). The diagram is based on three replicates and one standard deviation.

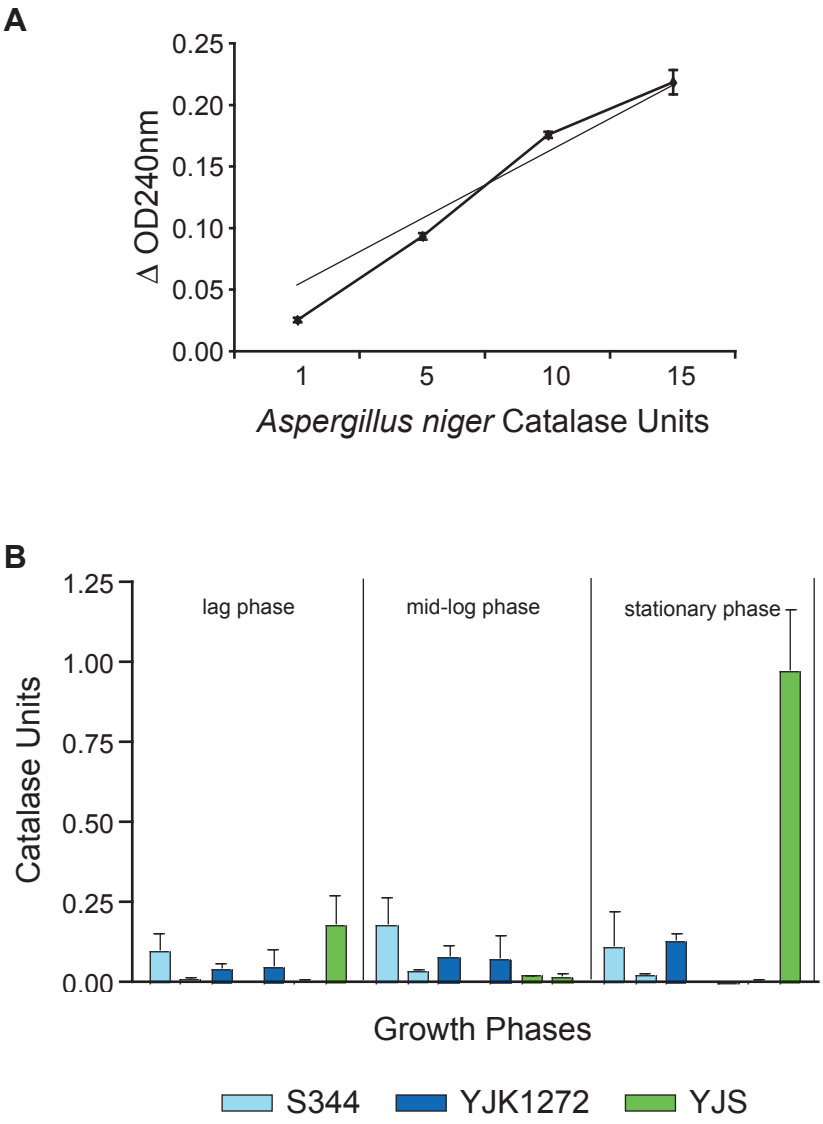

FIGURE 3.4**:** Catalase activities were recorded for S344, YJK1272 and YJS during lag, exponential and stationary growth in SD media and are represented here together with the standard curve. (A) *A. niger* catalase standard curve. The straight marker line of triplicates with one standard deviation is blue and the linear regression line is black (R^2=0.946). (B) *S. cerevisiae* strains are color coded as before and the diagram is divided between the three growth phases. The left column of each pair, that represents one strain during a certain phase, represents the non-induced the right column the induced sample.

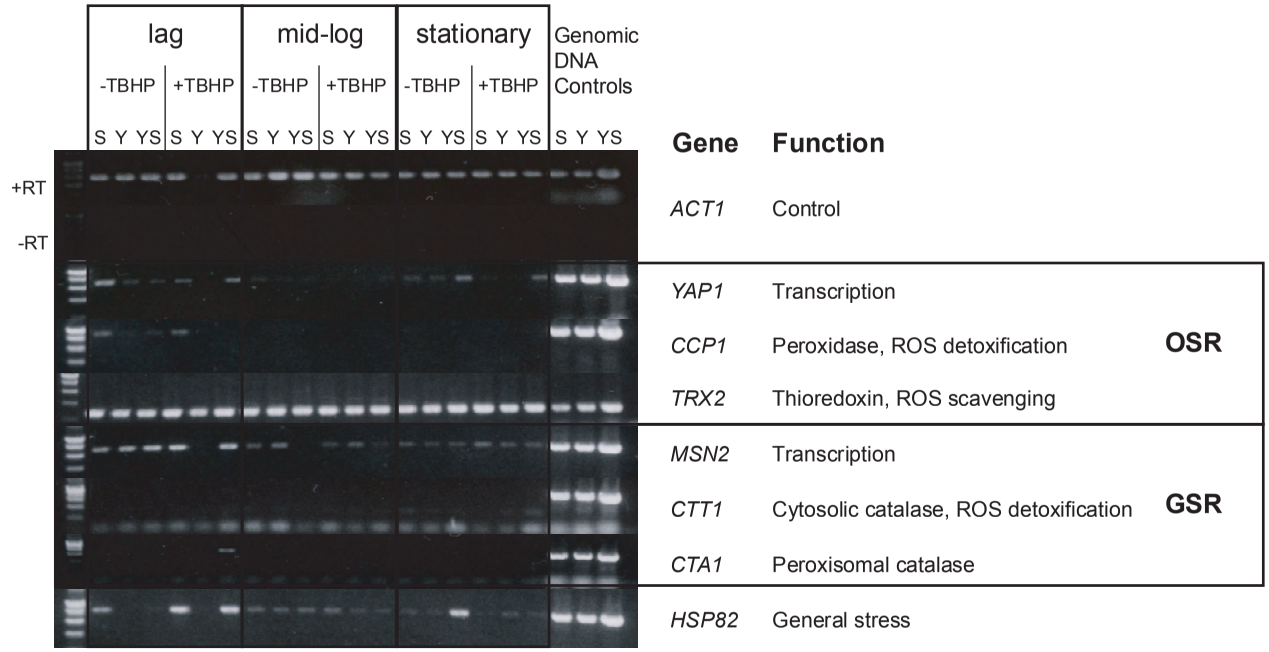

FIGURE 3.5: Semi-quantitative expression profiles of candidate enzymes, molecules and transcription factors of the general and oxidative stress response (GSR and OSR) for S344, YJK1272 and YJS during lag, exponential and stationary growth. Strains are encoded as follows: S=S344, Y=YJK1272 YS=YJS in each lane. The first lane contains 5 μl of DNA Ladder I (GeneChoice). For each time point the non-induced samples are loaded to the left and the induced samples to their right. At the right site of the gel, candidate gene amplicons from genomic DNAs of S344, YJK1272 and YJS are loaded to illustrate the expected amplicon size. Each row shows the PCR fragments obtained in 35 cycles for each gene, strain and treatment. Genes and their respective function are indicated to the right of the diagram. For the actin gene, the negative control (no addition of reverse transcriptase to the cDNA synthesis reaction; -RT) is shown. This has been done but omitted from the figure for all other genes.

4

A Quantitative Trait Nucleotide in the Zinc Cluster Protein Encoding *RDS2* Gene Increases Peroxide Survival in a Clinical *S. cerevisiae* Background

4.1 Introduction

Continuous phenotypic variation is a central attribute of life. Unlike Mendelian traits that are governed by a single gene, quantitative traits are affected by multiple genes. These genes are embedded in quantitative trait loci (QTLs) (113), whose identification is a central problem of quantitative genetics. The primary method that has been used to identify QTLs is linkage mapping, which localizes genes by segregation (linkage) of a Mendelian marker, such as morphology, chromosomal deficiencies or DNA sequence polymorphisms, with the trait of interest (6, 185, 242, 243, 302). A wide variety of QTLs have been identified by linkage mapping, including germination rate, size, and pest resistance in tomato (103, 106), potato (32, 190), and maize (44, 113), as well as milk production and meat quality in dairy cattle (115) and swine (298). Because linkage mapping is hampered in humans due to family sizes, non-designed crosses and too few classical genetic markers, association mapping has been

developed as an alternative. This method compares frequencies of genetic variants among affected and unaffected individuals and relies on linkage disequilibrium (LD) (23). Association mapping facilitated the identification of loci affecting birth weight, and susceptibility to Alzheimers disease, and colorectal and breast cancer in human (18, 90, 105, 150).

To raise the likelihood of QTL detection, often individuals of the same extreme phenotype are selected from the segregating population for selective genotyping (185). Genotyping can be done one individual at the time, as single segregant analysis (SSA) or by pooling DNA from individuals with similar trait values, often referred to as bulk segregant analysis (BSA) (10, 219, 254). Both experimental approaches traditionally utilized restriction fragment length polymorphisms (RFLPs) or random amplification of polymorphic DNA (RAPD). Yet with the advent of genome sequencing and high-throughput microarray technology, microarray-assisted QTL mapping has largely replaced those methods in applicable organisms. One such organism is in the genetic model system *S. cerevisiae*, which has quickly established itself as a useful model to study quantitative inheritance. The standard expression microarray S98 GeneChip from Affymetrix has often been used for microarray-assisted QTL mapping in *S. cerevisiae*. S98 has been developed based on the S288c genome sequence (123). Hence, S288c hybridizes equally well to all probes on the array but a strain that differs in its sequence from S288c will hybridize less efficiently. The probes that yield different hybridization signals between S288c and the other strain used for mapping are considered informative single feature polymorphisms (SFPs) and can be utilized as QTL mapping markers (281).

Traits that have been mapped by SSA hybridization to the S98 GeneChip include sporulation efficiency (82), gene expression and regulation (30), DNA damage repair (81), and high-temperature growth (299). Although the number of segregants hybridized to the S98 array differed greatly, all studies were successful in

identifying linkage to one (81) or multiple QTLs (30, 82, 299). To illustrate the difference in genotyping efforts, Brem et al. hybridized four segregants of one tetrad (30), Deutschbauer and Davis and Steinmetz et al. genotyped 19 segregants of extreme phenotype (82, 299), and Demogines et al. hybridized 123 segregants (81). Microarray-assisted QTL mapping yields QTLs of comparable sizes to other genotyping methods, such as short tandem repeat (STRs) but provides a more comprehensive analysis of the whole genome with less labor. To illustrate the difference, 319 segregants were genotyped for 264 STR markers, which are 14.7 cM apart, resulting in five QTLs ranging from 13 kb to 72 kb. While hybridization of 19 segregants to the S98 array, on which markers are separated by 1.2 cM, was sufficient to map two high-temperature QTLs (8 kb and 52 kb) (151, 299).

The first study to apply microarray-assisted BSA to bakers yeast as a demonstration of technique confirmed the large effect the previously identified *FLO8* gene has on variation of cell morphology (29, 194). A second BSA "proof of principle" study mapped known genes encoding drug resistance and uncovered genetic changes in experimentally evolved cells (281). A third study employed BSA to map sporulation efficiency and detected one QTL containing four linked genes, all of which affect the phenotype (16). These three studies employed the S98 GeneChip from Affymetrix and mapped QTLs of comparable sizes to the SSA studies (0.2-24 kb (281), 6-21 kb (29), >50 kb (16)). In addition to using S98, the novel GeneChip Tiling Array has successfully aided in the mapping of two QTLs (36kb and 118kb) that influence DNA repair (81).

The level of resolution to which *S. cerevisiae* quantitative traits have been mapped varies. Some traits, like small molecule perturbations and ethanol resistance, have been mapped to the level of candidate QTLs, which are genomic regions that are significantly linked to the genotype markers but have not been confirmed by genotyping individuals with independent markers for this region. Experimental validation and

identification of causative quantitative trait nucleotides (QTNs) has been achieved for sporulation efficiency, high-temperature growth and DNA damage repair. DNA repair is largely affected by the substitution I791S in *RAD5* (81). The two studies investigating sporulation efficiency identified adenine insertions upstream of the *RME1* and *RAS2* start codons, substitutions E1493Q in *TAO3*, and D30G in *MKT1* as QTNs (16, 82). High-temperature growth is also affected by a QTN in *MKT1* (D30G) as well as a S258N substitution in *END3* (288). Note that the same substitution in *MKT1* affects two different traits. *MKT1* encodes a nuclease that has a temperature-dependent effect on RNA replication and regulates *HO* mRNA translation (305, 330). The presence of upstream adenine insertions in *RME1* and *RAS2* emphasizes that QTNs are not necessarily non-synonymous polymorphisms in open reading frames (ORFs), complicating identification by candidate gene screens that are focused on sequence divergence inside ORFs.

Although yeast geneticists have access to a large tool box that includes multiple genome sequences (84, 123, 323), different microarray platforms (73, 333), and easy molecular manipulation of yeast cells, QTNs could only be experimentally verified for three traits. Experimental proof that establishes an association between a specific nucleotide and a quantitative trait, by site-directed mutagenesis, is technically challenging. To illustrate the magnitude of the challenge and the aptitude of yeast as a quantitative genetics model system, the only other eukaryote in which experimental validation of a QTN has succeeded is the nematode *Caenorhabditis elegans*. Complementation allowed for the identification of the substitution F96L in the calpain-like protease *tra-3* of *C. elegans* that attenuates growth at lower temperatures (168).

The ability of *S. cerevisiae* to survive oxidative stress is of quantitative nature. Investigations on populations derived by experimental evolution in the laboratory and a cross between a laboratory and a clinical strain indicated segregation of multiple loci (249, 338). Witten, Chen and Cohen evolved two yeast strains for oxidative

stress resistance by applying a rapid selection scheme. Both strains acquired the same major-effect mutation but differ in the nature of segregating modifiers, whose identities remain unknown. The authors concluded that the remaining segregating loci are of minor effect and have epistatic interactions (338). Perlstein et al. tested growth inhibition in F_1 segregants in response to 23 small molecules, including H_2O_2, and came to the conclusion that two loci affect oxidative stress resistance (249). Although both studies showed that the yeasts ability to survive oxidative stress is a polygenic trait, the causative genetic factors remain elusive. This investigation utilizes the naturally occurring variation in two *S. cerevisiae* isolates to elucidate the, as of yet unknown, quantitative architecture of peroxide survival, which affects *S. cerevisiae* ecology and fungal pathogenicity.

4.2 Materials and Methods

4.2.1 Yeast strains and media

All strains included in this study (Table 4.1) were kept in cryo-storage in 15% (v/v) glycerol at -80^{o}C and cultured on YPD plates (Chapter 2) prior to experimentation. For RHA, Hygromycin B (300 μg/ml) or G418 (200 μg/ml) were added to YPD plates (Chapter 2) after autoclaving. SD media plates used for LYS5MX4 transformations contained 2% (w/v) glucose, 37.8 mM $(NH_4)_2SO_4$, 1.7 g/l YNB without amino acids and ammonium sulfate, and 2% (w/v) agar. For high-throughput phenotyping, 1 or 1.2 mM H_2O_2 were added to 50^{o}C SD agar. Concentration of H_2O_2 in the stock solution was determined spectrometrically at λ=240nm (ϵ=$39.4 M^{-1}cm^{-1}$) and adjusted accordingly (199). Plates were stored in the dark for no more than 5 days. α-aminoadipate (α-AA) plates were prepared as described before (346) with two modifications: the YNB-dextrose-lysine mixture was not autoclaved but filter sterilized and the pH of the α-AA solution was adjusted to 5.5 instead of 6.

4.2.2 DNA amplifications for candidate gene genotyping and transformation

The PCR regime used for all reactions comprised a 3 minute initial denaturation at 95^{o}C, followed by 37 cycles of 30 seconds denaturation at 95^{o}C, 30 seconds annealing, and 45 seconds extension at 72^{o}C, concluding with 10 minutes extension at 72^{o}C. Annealing temperatures (T_A varied depending on the primers used (see below). MX4 cassettes were PCR amplified as follows: initial denaturation at 94^{o}C for 3 minutes was followed by ten cycles of 94^{o}C for 20 seconds, 55^{o}C for 15 seconds, and 72^{o}C for 1 minute 30 seconds. These were followed by 25 cycles of 94^{o}C for 20 seconds, and 72^{o}C for 1 minute 30 seconds. These parameters were modified from a previously published method (125). Reactions were carried out using the TaKaRa Ex Taq kit containing 0.6 μM of each primer, unless specified otherwise. The final volume of each PCR was 25 μl, except for MX4 amplifications, which were 50 μl. Allele-specific PCR to fine-map the QTL on chromosome XVI was carried out in two 25 μl PCR reactions per segregant containing 10xThermoPol reaction buffer, 0.5 μM of each primer, 200 mM dNTPs (Invitrogen), and 0.625 U $Vent_R$ (exo) DNA Polymerase (New England BioLab).

4.2.3 Diagnostic RFLP assays

Diagnostic RFLPs that distinguish between the parental alleles were used to genotype F_1 segregants for candidate genes, to detect linkage between candidate QTLs and peroxide survival in BCI high- and low-survival segregants, and for fine-mapping the QTL on chromosome XVI in F_1 and BCI high- and low-survival segregants. 5 μl PCR product were tested for positive amplification in 1% (w/v) agarose. All digests contained 5 μl PCR product, 10x reaction buffer, sterile water and enzyme in a total reaction volume of 10 μl. Upon completion, fragments were separated for 30-45 minutes in a 1.5% (w/v) agarose gel at 120 V in 1xTAE buffer. Segregant and parental fragments were compared and genotypes assigned accordingly.

4.2.4 Lithium acetate transformation

The high efficiency lithium acetate (Li/Ac) transformation protocol (117), with modifications, was used to generate reciprocal hemizygotes or allele replacement strains (Table 4.1). The washed and pelleted cells were diluted in 400 μl 0.1 M LiAc and 50-100 μl of this suspension used for transformation. After adding the transformation mix, samples were incubated for 30 minutes at 30^{o}C and for 15-20 minutes at 42^{o}C in water baths. Transformed cells were centrifuged for 15 seconds at 6000 rpm and resuspended very carefully in 600 μl YPD, when transformed with hphMX4, kanMX4 or pAG26 (hphMX4CEN), or 600 μl sterile water, when transformed with LYS5MX4 or PCR product. Cells transformed with drug cassettes or plasmids were allowed to recover for 2 hours at 30^{o}C while shaking (200 rpm) and spread onto selective media. Cells transformed with LYS5MX4 were spread onto SD media and cells transformed with PCR products onto α-AA plates. Plates were incubated for up to 3 days at 30^{o}C. Each transformation reaction was done with 100-400 μl ethanol purified PCR product in 25-50 μl sterile water.

4.2.5 Heritability of peroxide survival and candidate gene genotyping

The genetic bases of peroxide survival were investigated using strains YJK1272, S344, derivatives of YJM789 and S288c, and their hybrid YJS (Table 4.1). For easier understanding and whenever possible, strains are referred to as Y when derived from YJM789 and S for strains isogenic with S288c. Furthermore, genotypes or alleles will be called Y for wild type and y for allele replacements that carry the S SNP in a Y allele, same for S and s. To assess the phenotypic nature of peroxide survival and identify its mode of inheritance, YJK1272, S344, their hybrid YJS, and 200 F_1 segregants were phenotyped using the CFU assay (20 mM TBHP) on yeast cells that were grown for 14 hours (Chapter 2). The hybrid was sporulated and tetrads treated as described earlier (Chapter 3). To estimate the effective number of loci segregating

in the S344xYJK1272 cross, the Castle-Wright estimator (n_e) and its standard error were calculated based on the phenotypic variance observed in the F_1 as described by Lynch and Walsh p. 234 (200).

200 F_1 segregants were genotyped for candidate genes *CTA1*, *CTT1*, *CCP1*, and *SOD1* using diagnostic RFLPs (Table 4.2) or allele-specific multiplex PCR (Table 4.3). The latter was only used to genotype *CTA1*, *CTT1*. PCR amplicons for RFLP digests were generated at T_A=53^{o}C from 2 μl of a 1:100 dilution of genomic DNA prepared using the CTAB method and digested for 2 hours at 37^{o}C in an incubator (*Nci*I, *Ssp*I, *Sau*3AI) and at 25^{o}C in a water bath (*Sma*I) (Table 4.2) (108). Restriction fragments were separated immediately after digest and compared to parental controls.

Allele-specific primers were designed to meet two criteria, amplification of only one or the other parental allele, and generation of differently long PCR products. Catalase gene sequences of S288c and YJM788 were aligned and screened for polymorphisms. Allele-specificity was achieved by a mismatch at the final 3' position of each primer and length variation based on the distribution of polymorphisms. A set of allele-specific multiplex primers comprised four primers that would either amplify only the S alleles or only the Y alleles of each gene (Table 4.3). 2 μl of a 1:100 dilution of genomic DNA extracted with the CTAB method (108) were added to *CTA1* and *CTT1* multiplex PCR, which was carried out at T_A=60^{o}C with final primer concentrations of 0.525 μM (Table 4.3). Multiplex PCR fragments were separated in a 1.5% (w/v) agarose gel and F_1 segregants scored based on parental electrophoresis patterns.

4.2.6 Backcross design and segregant phenotyping

Three backcross lines (BCI, BCII, BCIII) were set up by crossing high-survival F_1 segregants F_1-2D (survival=0.79, drug marker hphMX4), F_1-10B (0.91, hphMX4),

F_1-19C (0.99, kanMX4) with strains S344 (kanMX4) or S347 (hphMX4) (Table 4.1). Double-drug resistant hybrids were sporulated and tested for drug marker segregation like YJS (Chapter 3). Additionally, a second backcross to S344 was conducted using BCI segregant BCI-2C (0.89, hphMX4).

Backcross segregants were phenotyped with the CFU assay (Chapter 2) and a spot dilution assay for high-throughput preliminary screening developed by Randy Strich (pers. comm.). Briefly, 5 μl of ten-fold dilutions of S344, YJK1272 and eight back cross segregants, ranging from 1x10^7 to 1x10^2 cells/ml, were spotted onto synthetic defined media plates containing 1 mM or 1.2 mM H_2O_2. Plates were incubated for 48 hours at 30^{o}C and the phenotype of putatively resistant segregants, those resembling YJK1272, was confirmed and quantified using the CFU assay.

4.2.7 Microarray-assisted QTL mapping

CustomArray 4x2k oligonucleotide microarrays from Combimatrix served as SSA genotyping platform. Pairs of oligonucleotides, one of which matches one parent while its partner has 2 internal mismatches, were identified by sequential comparisons between both parental genome sequences (123, 323). The YJM789 genome (Genbank accession number AAFW000000) was fragmented into 25mers, window size 5 bp, which were searched against the S288c genome from SGD's FTP server. Those that had 2-5 mismatches in S288c were retained and new oligomers picked based on those locations in YJM789, located -5 bp to +5 bp relative to the original oligomer. These secondary olignucleotides were searched against the S288c genome sequence and those with exactly one match but at least two internal mismatches were retained and searched against the YJM789 genome. The search was repeated with S288c oligonucleotides. Mismatch oligonucleotides were analyzed for melting temperature, GC-content and self-complementarity. For each parameter, a weighted penalty score was applied to every oligonucleotide reflecting its deviation from the mean. In

addition to these physical parameters, the genomic location of the oligonucleotide was considered. Selected oligonucleotides were 25 bp long, differed by 2 internal mismatches between the parents, scored low penalties and were evenly distributed across the genome.

Genomic DNA for microarray hybridizations was extracted using the Genomic-tip 100/G from Qiagen according to the manufacturer's instructions. For SSA, genomic DNA from 22 high-survival BCI segregants were digested and labeled as described by Muller and McCusker (230). Hybridizations and microarray stripping were carried out according to Combimatrix standard protocols and arrays re-used twice. Three BSA hybridizations to the S98 array were conducted by mixing 47 F_1, 22 BCI and 24 BCII high-survival segregant genomic DNA. DNA concentrations were determined spectrometrically and DNA mixed in equal proportions. A total of 20 μg genomic DNA was digested with 1U DNase I (New England BioLabs), 10 μg of which was labeled with Biotin-N6 (Enzo Life Sciences) and hybridized (334). Parental controls were included in SSA and BSA hybridizations.

To verify oligonucleotide sequences on the S98 and the 4x2k arrays all probes were BLAST searched against the Sanger Center *S. cerevisiae* trace archive (`http://www.sanger.ac.uk/Projects/S_cerevisiae/`) (7). Probes without a single match were excluded from both analyses.

Informative probes from the S98 GeneChip were extracted by searching the CEL file using the EMBOSS program fuzznuc (262) against the S288c genome from the SGD FTP directory and the YJM789 genome from GenBank. Probes were divided into those that (i) match neither genome, (ii) match both strains, with one mismatch, (iii) have one mismatch with S288c but none with YJM789, (iv) match both genomes exactly, (v) match S288c exactly and have one mismatch in YJM789, (vi) match S288c exactly and have two mismatches in YJM789. Probes from these searches were divided into control (i+iv) and informative probes, which perfectly match the

S288c genome but have one or two mismatches to the YJM789 genome (v+vi). The latter will be referred to as one-mismatch and two-mismatch probes. The controls (i+iv) were used to normalize signal strength between arrays and to estimate variation in signal strength from probe to probe and the putative effects of melting temperature. The melting point of each probe was calculated using standard procedures with parameters from Breslauer (24, 31, 272). Since melting temperature and hybridization value were positively correlated with each other, hybridization values were adjusted using linear regression. Following normalization, the hybridization values of the parental strains were compared with each other to identify informative probes whose hybridization signals are more similar to either parent or intermediate. These S98 single feature polymorphisms (SFPs) were then extracted from the F_1, BCI and BCII analyses (16).

SFPs from 4x2k arrays were determined based on hybridization signals, which were expressed as FGmeans (number of pixels obtained for each probe). FGmeans of each oligonucleotide pair were subtracted from each other (Y-S) so that a score >0 suggests preferential hybridization to S and <0 to Y. One standard deviation (SD) and one half SD were subtracted from the FGmeans difference. Scores were applied to the FGmeans-SD depending if the difference was <-10, <0, 0, >0, or >10. Finally, a weighted score was applied to each probe depending if its neighboring probe had the same parental genotype or not, resulting in the 4x2k set of SFPs. 1 SD and 0.5 SD were analyzed in parallel.

Candidate QTLs were identified based on four genotype data sets. Analysis A encompasses S98 one-mismatch SFP and B S98 two-mismatch SFPs in 22 high-survival BCI segregants. The 4x2k SFPs from 22 single spore hybridizations were split into two sets and searched for lack of recombination between S and Y. Blocks were assembled that were enriched for Y, i.e. more than 50% of the analyzed 22 spores had the Y genotype and divided into blocks allowing for gaps (4 out of 5

SFPs are Y) or not gaps ($\geq$ 3 consecutive Y SFPs) were summarized as analysis C and D.

To test for genetic linkage between candidate QTLs and peroxide survival, diagnostic RFLPs were applied to 22 high-survival and 20 low-survival BCI segregants. PCR amplicons were digested for 2 hours in a 37^{o}C incubator and completed reactions inactivated by heating to 65^{o}C for 20 minutes. Linkage was assessed using a chi-square test (Table 4.5).

4.2.8 Fine-mapping of a QTL on chromosome XVI

Fine-mapping of a QTL on chromosome XVI was conducted on the same panel of 22 high- and 20 low-survival segregants from BCI. High-survival segregants were scored for the presence of Y and S alleles at seven different markers spanning the QTL and low-survival segregants for four of the seven markers. The seven markers comprised three diagnostic RFLPs and four allele-specific PCR reactions. RFLP digests containing *Dra*I, *Eco*NI, and *Hae*III (Table 4.6) were incubated for 2 hours at 37^{o}C and heat inactivated for 20 minutes at 65^{o}C (*Dra*I, *Eco*NI) or 80^{o}C (*Hae*III). Diagnostic RFLPs were also tested on 47 high-survival and 16 low-survival F_1 segregants. A set of allele-specific PCR primers comprised three primers, two of which are specific due to a mismatch at the final 3' position and a third general primer to amplify in the opposite direction from the mismatch primer (Table 4.6). Two PCR reactions per segregant were analyzed, each containing one allele-specific and the general primer. Amplicons were separated in a 1% (w/v) agarose gel and scored for presence/absence of fragments in both reactions. S344 and YJK1272 served as positive controls for diagnostic RFLPs and allele-specific PCR.

4.2.9 Reciprocal hemizygosity analyses (RHA)

Preliminary experiments showed that hybrid strains hemizygous at *RDS2* and *COX11* (wild type allele/kanMX4 or hphMX4) were significantly more sensitive to 20 mM TBHP than the parental strains or the hybrid (data not shown). Consequently, all RHA competition CFU assays were done in 16 mM TBHP. In preparation of systematic RHA, hphMX4 and kanMX4 were tested for putative effects on peroxide survival. Two diploid S and Y strains, that each had their *GAL2* ORFs replaced with kanMX4 and hphMX4 were co-cultured in 16 mM TBHP, processed in the CFU assay and plated on selective media as described before (Chapter 3) (Table 4.1) (125, 320). The mean of four replicates and its standard error (SEM) were calculated and compared with Student's t-test.

Reciprocal hemizygotes were constructed using published strains and primers (299). The ORFs of target genes in the S and Y background (Table 4.1) were replaced with hphMX4 and kanMX4 as described by Steinmetz et al. (125, 299, 320). Both cassettes were maintained on plasmids pAG32 (hphMX4) and pFA6 (kanMX4) and multiplied in *Escherichia coli* DH5α cells (Invitrogen) (125, 320). To extract plasmids, *E. coli* cells were grown overnight in 3 ml Luria-Bertani broth with Ampicillin (1% (w/v) tryptone, 0.5% (w/v) yeast extract, 1% (w/v) NaCl, 100mg/l Ampicillin) at 37^{o}C and plasmid mini preparations conducted using the S.N.A.P. miniprep kit according to Invitrogen's instructions. For PCR amplification of hphMX4 and kanMX4, the published (299) primer pair JM41 and JM42 (Table 4.9) was modified for specific replacement of wild type ORFs by adding JM41 to the 3' end of the primer targeting -50 bp to -1 bp upstream of the ORF and attaching JM42 to the 3' end of the reverse complemented sequence targeting +1 bp to +50 bp. 1 μl of a 1:100 plasmid solution was used to amplify hphMX4 and kanMX4. Successful amplification of hphMX4 and kanMX4 was verified prior to transformation, carried

out using the Li/Ac protocol. Putative RHA transformants were tested with primer pairs FT167/YFG_-500F and JM37/YFG_+500R at T_A=50^{o}C (Table 4.9). The YFG primer was designed to anneal specifically to a region 500 bp up- or downstream of the target gene. Removal of the target ORF was PCR verified (Table 4.9) (125).

Positive transformants were sporulated and crossed as described before to obtain reciprocal hemizygotes (299), which were then tested for survival competitively in 16 mM TBHP using the CFU assay. Each comparison was conducted three times and statistically analyzed with a paired T-test with Bonferroni correction.

4.2.10 Characterization of RDS2

The effect of the candidate gene *RDS2* on peroxide survival was investigated using three different comparisons. (i) Wild isolates of *S. cerevisiae* that have S or Y like *RDS2* alleles were compared with each other and S344 and YJK1272, (ii) homozygous *RDS2* deletions in S344 and YJK1272 were examined for survival, and (iii) S and Y strains with single nucleotide polymorphism replacements in *RDS2* were compared to the wild type strains.

The Saccharomyces_cerevisiae_WGS database at GenBank has been mined with blastn with 50 bp long sequences of *RDS2* of either parental allele containing one of the two non-synonymous polymorphisms using MEGABLAST (7). The wild *S. cerevisiae* strains identified as having one or the other allele, were tested three times for survival in 20 mM TBHP using the CFU assay. The following comparisons were analyzed using one-way ANOVAs with Bonferroni correction: S344 vs S allele strains, YJK1272 vs. Y allele strains, S344 vs. Y allele strains, and YJK1272 vs. S allele strains.

To identify patterns of evolutionary conservation, Rds2 was BLAST searched against the protein translations of the genomes of *C. glabrata*, *Ashbya gossypii*, *Kluyveromyces lactis*, *C. albicans*, *A. fumigatus*, *A. nidulans*, *Neurospora crassa*,

Ustilago maydis and *C. neoformans* deposited at NCBI GenBank and the alignment visually analyzed.

Homozygous *RDS2* deletions in either parental background were generated by mating two strains with heterozygous deletions of *RDS2* with hphMX4 and kanMX4 (from RHA) with each other and screening the diploids for lysine prototrophy and double drug resistance. Two transformants of each parental background were analyzed and the four homozygous deletion strains tested for survival in 16 mM TBHP three times. Means and standard error were calculated and compared with Student's t-test.

Homologous allele replacements of the C751G SNP in *RDS2* were carried out in the lysine auxotrophic haploid strains S1288 and YHS633 (Table 4.1), employing the lysine/α-AA counter-selection system (158). The two-step process entailed replacement of the region between nucleotides 701 and 830 inside the *RDS2* ORF with LYS5MX4 (pSA39) (158) and removal of LYS5MX4 with a PCR product containing the other parent's SNP. 1 μl of a 1:100 dilution of pSA39 was added to reactions amplifying LYS5MX4 together with primers JM41_AS751-828_F and JM42_AS751-828_R (Table 4.9) (125, 158). Successful integration of *LYS5* and removal of the *RDS2* target region was tested with primer pairs FT167 / RDS2_-500F and JM37 / RDS2_+500R at T_A=50^{o}C and primers RDS2_701F and RDS2_830R at T_A=53^{o}C (Table 4.9). 1 μl genomic DNA, prepared using the ten-minute protocol (147), was added to generate PCR products for homologous allele replacement and to test for successful replacement and marker removal.

Homologous allele-replacement PCR products were generated by combining two short fragments that were amplified off parental DNA with the following primer combinations: RDS2_550F / RDS2_755_Y_R [i] and RDS2_751_Y_F / RDS2_1000R [ii] were used on S1288 and RDS2_550F / RDS2_755_S_R [iii] and RDS2_751_S_F / RDS2_1000R [iv] on YHS633. PCR products [i] and [iv], and [ii] and [iii] were

mixed and 1 μl amplified with primers RDS2_550F and RDS2_1000R (Table 4.9). All reactions were done at T_A=52^{o}C. This PCR product worked less efficient in the Y background. Hence, a second PCR product, with longer regions of homology, was produced by replacing primer RDS2_550F with RDS2_102F and RDS2_1000R with RDS2_1315R, resulting in transformant YSD52 (Table 4.1).

The LYS5MX4 replacement transformation was done as co-transformation with 2 μl plasmid pAG26 (hphMX4 CEN *URA3*) (125). After 3 days of incubation at 30^{o}C, drug-resistant transformants were replica plated onto α-AA plates and incubated at 30^{o}C for 2 days. Putative transformants were tested for correct SNP replacement by restriction digest with *Bbs*I and sequencing (Chapter 2). PCR amplicons for the *Bbs*I digest were generated using primers RDS2_102F and RDS2_966R at T_A=50^{o}C and 8 μl PCR product were digested with 10x reaction buffer and 1U *Bbs*I in a total volume of 10 μl and separated in 1.5% (w/v) agarose. Sequencing was carried out using primers RDS2_102F, RDS2_966R, RDS2_550F, RDS2_1000R, RDS2_701F, and RDS2_1315R (Table 4.1). Two independent transformants were created for either wild type background.

To diploidize haploid strains with allele replacements (YSD1, 3, 36, and 52) and the wild types (S1288, YHS633), all of which are MATα *lys5*, two crosses were conducted (Table 4.1). S1288 and YSD1 were crossed with YSD-S1. YHS633 and YSD36, were crossed with YSD-Y1. Prior to mating, YSD-S1 and YSD-Y1 were sporulated (Chapter 3). Diploids were selected for Hygromycin B drug resistance and lysine prototrophy and single colonies isolated, sporulated and between 40 and 60 tetrads dissected. Those tetrads were subjected to tester matings on SD and YPD + Hygromycin B. The MATa *lys2* segregants were then mass-mated to the transformed and wild type strains to generate diploids (Table 4.1). Additionally, matings were carried out to generate strains that are heterozygous for the polymorphism and hybrid strains that are homozygous for one or the other SNP (Table 4.1).

All strains were screened for survival in 16 mM TBHP up to ten times. Differences between genotypes were assessed using one-way Anova with Bonferroni correction and Dunnett's Test and the Wilcoxon Signed Rank Test to detect differences in peroxide survival between strains with different genotypes. The percent phenotypic contribution was calculated as 100 x (Survival(Y y/y)–Survival(Y Y/Y))/(Survival(S S/S)–Survival(Y Y/Y)) (82).

4.3 Results

4.3.1 High peroxide survival is a dominant quantitative trait and not linked to candidate genes

To determine if peroxide survival is dominant or recessive, survival of YJS was compared with that of S344 and YJK1272. The hybrid phenotype resembled that of YJK1272. Both strains survived peroxide treatment significantly better than S344 ($P < 0.01$) (Figure 4.1A). Hence, high peroxide survival is a dominant trait. To establish if peroxide survival is of Mendelian or quantitative inheritance, YJS was sporulated and F_1 segregants phenotyped. 68 tetrads, giving rise to four viable spores exhibiting 2:2 segregation of drug resistance were obtained. 200 F_1 spores, from 50 tetrads, were tested for survival in 20 mM TBHP (Figure 4.1B). The phenotypic spectrum ranged from 0 to 1 and resembled a bell-shaped curve, which is diagnostic of a quantitative trait. On both ends of the curve, F_1 segregants were observed whose phenotypes exceeded the parental means (S344=0.14 $\pm$ 0.036 SEM, YJK1272=0.83 $\pm$ 0.072), indicating transgressive segregation.

47 F_1 segregants (approx. 25%) exhibited high-survival ≥ 0.8 (YJK1272-like), and 16 segregants low-survival ≤ 0.2 (S344-like). The phenotypic variance amongst F_1 segregants (0.0587) was used to estimate that 10 $\pm$ 2 loci segregated in the cross, confirming the quantitative nature of peroxide survival. The high- and low-survival segregants were included in the ensuing QTL mapping and fine-mapping efforts.

To determine if the phenotype is due to the known peroxide resistance determinants *CTA1*, *CTT1*, *CCP1*, and *SOD1*, a primary candidate gene screen was conducted. The parental alleles of *CTT1*, *CTA1*, *SOD1*, and *CCP1* vary by a number of non-synonymous and synonymous single nucleotide polymorphisms (SNPs) in their ORFs and in the 1,000 bp up- and downstream regions (Table 4.2). The RFLP assay was applied to all 200 F_1 segregants to genotype *SOD1* and *CCP1*, and to 92 segregants to genotype *CTA1* and *CTT1*. Allele-specific multiplex PCR was used to assay *CTA1* and *CTT1* alleles in 108 segregants. However, no association between a parental allele and the phenotype could be detected. The genes segregated at random with respect to peroxide survival; therefore the phenotype is not linked to the candidate genes (Figure 4.1C).

4.3.2 Backcross analysis

A QTL mapping population was derived by setting up three backcross lines. Three high-survival F_1 segregants (survival=0.79, 0.91, 0.99) were crossed to the low-survival parent S344/S347. In each case the backcross hybrid displayed lower survival than the F_1 segregant but survived better than the S parent (BCI=0.49, BCII=0.54, BCIII=0.59). Survival declined even further in the second backcross hybrid (0.33), developed from a high-survival BCI spore (0.89) (Figure 4.2A). The second backcross derived from BCI was not analyzed further. The three first backcross hybrids were sporulated and a total of 1,246 backcross segregants were phenotyped for peroxide survival using the CFU and plate assay. A primary CFU assay was conducted on 199 BCI, 197 BCII, and 86 BCIII segregants (Figure 4.2B). None of the backcross lines contained sufficient numbers of high-survival segregants for QTL mapping. The frequencies of high-survival segregants in each line were lower than the 1 in 4 observed in the F_1. BCI contained 1 in 12, BCII 1 in 22, and BCIII 1 in 86 high-survival segregants. Line II and III encompassed more low-survival segregants than the F_1.

In each back cross line the phenotypic variance (0.0418, 0.04, 0.0315) decreased relative to the F_1 (0.0587) and the peak of the bell-shaped curve shifted to the left (low-survival) end of the distribution.

To obtain more high-survival backcross segregants for selective genotyping 72, 600, and 92 additional segregants from lines BCI, BCII, and BCIII were phenotyped using the plate assay. Of these, 15 (BCI) and 63 (BCII) had their survival phenotype verified using the CFU assay and 8 and 11 met the cut-off value of 0.8. The high-survival segregants identified by CFU and plate assays in BCI (22) and BCII (24) were subsequently used for QTL mapping and low-survival segregants (BCI: 20, BCII: 31) for linkage analysis and QTL fine-mapping. None of the 92 additional segregants tested in line BCIII showed Y-like survival. Due to this extremely low frequency, phenotypic and genotypic analyses of BCIII were discontinued.

4.3.3 QTL mapping

The S98 array contained 141,644 probes that matched the S288c and YJM789 genomes perfectly (zero-mismatch), 10,160 probes matched S288c perfectly and had one mismatch in YJM789 and 1,075 probes with two mismatches. After comparing those probes with the Sanger Center *S. cerevisiae* trace archive to filter out sequence errors, 384 of the one-mismatch and 94 of the two-mismatch probes were removed from the analysis. The remaining 9,776 one-mismatch and 981 two-mismatch probes ranged in GC content from 16-80% and in melting temperatures from 45-81^{o}C.

After normalization, analysis of hybridization values showed the following correlations. The zero-mismatch probes, which matched both parental genomes perfectly, were a measure of differences in hybridization signals between arrays (Figure 4.3). Zero-mismatch probe values were comparable in S344, YJK1272 and F_1 but were much lower in BCI, indicating that this hybridization reaction did not work as well. One- and two-mismatch probes resembled the zero-mismatch hybridization values in

S344 but YJK1272 hybridized only about half as well to these probes. The one- and two-mismatch probe signals in the F_1 were intermediate between the signals observed for the parental controls, confirming the origin of about half the genome from either parent. Although hybridization of BCI was overall lower, one- and two-mismatch probes hybridized almost as well as the zero-mismatch probe. The difference in hybridization signal between the zero-mismatch control and the informative probes was smaller than in YJK1272 and F_1, resembling the S344 pattern and reflecting the backcross nature of this line. The observed differences in normalized hybridization signals between the parents and the segregants indicated that the BSA was successful. Spacing between SFPs differed between the one-mismatch analysis A (0.4 cM) and the two-mismatch analysis B (4 cM). Note, that due to the design of the S98 array, markers are not evenly spaced across the genome.

A total of 1,127 oligonucleotide pairs were spotted onto the 4x2k array. 37 of those were excluded from the analyses due to sequencing errors, resulting in 1,090 SFPs. Subtraction of 1 or 0.5 SD from the difference in hybridization means yielded similar patterns, so the 0.5 SD calculations were used to extracts SFPs for analyses C (4 out of 5 Y SFPs) and D ($\geq$ 3 consecutive Y SFPs). SFPs were spaced on average 3.5 cM apart and covered about 11.5 Mb of the genome. Genomic regions that were not covered, by design, included the rDNA array, the telomeres and repetitive sequences.

Analyses A, B and C yielded similar numbers of regions in the genome derived from Y (21, 18, 19) (Figure 4.4A-C). Analysis D resulted in 10 Y-derived regions (Figure 4.4D). Given the stringency of analysis B (two-mismatch SFPs), QTLs were considered high quality when they were identified in B and one or more other genotyping analysis (Table 4.4). Seven candidate QTLs matched this criterion. Those are located on seven chromosomes and differ in length from about 25 cM to 137 cM. None of them included a ROS candidate gene from the primary gene screen (Table

4.4).

To assess the reliability of BSA and SSA and detect differences in their ability to detect QTLs, five candidate QTLs were tested with diagnostic RFLPs (Table 4.5, Figure 4.4). These five QTLs were identified in different analysis. Two were identified only in B (ChrXI) or C (ChrIX), one was identified in A and C (X), one in A and B (X) and one in A, B and C (XVI). RFLPs were scored for 22 high-survival and 20 low-survival BCI segregants. For the QTLs on chromosomes IX, X, and XI high- and low-survival segregants inherited about 50% of their alleles from YJK1272 (Table 4.5). The genotype data for the QTL on chromosome XVI exhibited a different pattern. 77% of the high-survival segregants inherited this genomic region from YJK1272. Only 21% of the low-survival segregants inherited the Y allele. The chi-square test for the QTL on chromosome XVI was significant (χ^2=144, $P < 0.0001$). The allele distribution at this locus was further determined in high- and low-survival segregants in the F_1 and BCII lines. 60% of the high-survival F_1 segregants (χ^2=4, $P < 0.05$) carried a Y allele as opposed to 19% of the low-survival segregants (χ^2=38, $P < 0.0001$). 66% of the high-survival BCII spores (χ^2=90, $P < 0.0001$) had the Y allele but only 3% of the low-survival segregants (χ^2=26, $P < 0.0001$) tested positive for the Y allele. Interestingly, the F_1 segregant that was used to derive BCIII did not have the Y allele at this locus.

4.3.4 Fine mapping and characterization of a QTL on ChrXVI

Recombination mapping was conducted on a 250 kb (∼86 cM) (226) interval on chromosome XVI that tested positive for genetic linkage in the RFLP screen. The mapping population comprised 22 high- and 20 low-survival segregants from the BCI line, which were genotyped with allele-specific PCR primers and diagnostic RFLPs (Table 4.6). Genotyping by allele-specific PCR was unambiguous and restriction fragments of segregants resembled that of either parental control. Genotype data

could be obtained for all seven markers tested for 21 of 22 high-survival BCI segregants and for four of seven markers for the other one. For the 20 low-survival BCI segregants data were obtained for all four markers tested for 19 and for three markers for the other one (Table 4.7).

Seven recombination events in the high-survival group and two in the low-survival group were detected. Two recombination events in the high-survival group at markers ChrXVI_300 and ChrXVI_322 narrowed the region of interest to 23.2 kb (∼7.9 cM). Markers ChrXVI_300, ChrXVI_322, ChrXVI_335, and ChrXVI_350 were tested in 42 high-survival and 16 low survival F_1 segregants as well (Table 4.7). Complete data were obtained for 40 high-survival segregants, with missing data for one and two markers of the remaining two segregants. In the low-survival group, complete data for all but one segregant were obtained, while the remaining segregant was genotyped for three of four markers. Two recombination events (ChrXVI_335, ChrXVI_350) were detected among the high-survival F_1 segregants and none in the low-survival spores.

The region identified by recombination mapping contains 14 genes (Table 4.8). Preliminary experiments showed that neither kanMX4 nor hphMX4 affected peroxide survival (Figure 4.5). Four RHA comparisons were conducted for each gene, 56 for the entire locus. Yet, no significant difference in survival between one or the other parental allele in a hybrid background of any of the 14 genes could be statistically verified (Figure 4.6).

In a secondary candidate gene screen, all genes in the QTL were compared for DNA sequence similarity between the parental strains and gene functions related to stress response (Table 4.8). Four genes are identical between the parental strains, four contain only synonymous polymorphisms and six contain non-synonymous polymorphisms in addition to synonymous polymorphisms. The strongest candidate based on sequence and function was *RDS2*. It is a zinc cluster transcriptional activator in-

volved in resistance to ketoconazole and the null mutant is calcofluor white sensitive (`www.yeastgenome.org`) (4).

4.3.5 Identification of a causative nucleotide in RDS2

The *RDS2* ORF is 1,341 nucleotides long and contains four synonymous SNPs at positions 42, 762, 828 and 1158 and two non-synonymous SNPs at positions 505 and 751. One non-synonymous SNP (A505G) results in a substitution from threonine (Thr) in S288c to alanine (Ala) in YJM789 at amino acid position 169. The other (C751G) leads to the substitution of histidine (His) in S288c with an aspartic acid (Asp) in YJM789 at amino acid position 251.

BLAST searches of *RDS2* alleles against the *S. cerevisiae* trace archive led to the identification of eight strains that have one or the other SNP at position 505 and 751. Six share the S allele: RM11 (grape), Y55 (wine), L-1528 (wine), DBVPG6765 (unknown, ex. *S. boulardii*), DBVPG1853 (White Tecc wine), and DBVPG1788 (soil). Two have the Y allele: YPS606 (oak tree) and SK1 (soil). Hence, both SNPs segregate in the *S. cerevisiae* population. No recombination events between the two polymorphisms were detected in the wild strains. Yet, strains varied in peroxide survival depending on their *RDS2* configuration (Figure 4.7A ($P < 0.001$)). RM11 was the only S allele strain that survived TBHP treatment better than S344 or any other S allele strain. The RM11 phenotype resembled that of YJK1272. The other five S allele strains were statistically indistinguishable from S344 and demonstrated less survival than YJK1272 ($P < 0.001$). The two Y allele strains exhibited intermediate phenotypes.

The region of *RDS2* encompassing the C751G polymorphism is evolutionary conserved. Sequence similarity is highest amongst the Saccharomycetaceae. *C. glabrata*, *A. gossypii* and *K. lactis* have alignment scores > 200 across almost the entire molecule. With increasing evolutionary distance from *S. cerevisiae*, protein con-

servation declines but the C-terminal region of Rds2, containing the His → Asp substitution, is highly conserved across all nine fungal genomes (Figure 4.7B). The three Saccharomycetaceae species share the Asp of YJK1272. All other ascomycetes, as well as the basidiomycete *U. maydis*, have glutamic acid at position 251. *C. neoformans* has a serine at this position. The evolutionary conservation of an acidic amino acid in the C-terminal region of Rds2 strongly suggested this residue to be of functional importance.

Homozygous deletions of *RDS2* in diploid S and Y backgrounds were tested for survival. Deleting *RDS2* resulted in reduced peroxide survival in the Y strain but had no effect on the S strain, which survived like wild type (Figure 4.8A). The two homozygous deletion strains of the Y background exhibited a slight, although not significant ($P = 0.0810$) decrease of survival compared to YJK1272. Both Y deletion strains resembled the phenotype of the hybrid YJS that survived less well than YJK1272 in 16 mM TBHP. The reduced survival of Y deletion mutants but not S deletion mutants, indicated that *RDS2* is the gene underlying this QTL and that its downstream targets or interactions differ in S344 and YJK1272.

C751G is the SNP in the highly conserved region of *RDS2* and hence efforts focused on this SNP rather than on A505G. The C and G at position 751 were exchanged between S344 and YJK1272 using site-directed mutagenesis and resulted in two transformants. Introducing the G into the S strain did not alter the survival phenotype. Both diploidized transformants responded to TBHP like the S wild type. Introducing the C from the S strain into the Y strain leads to reduced survival in TBHP ($P < 0.05$). Both transformants exhibited reduced survival when compared to the wild type (Figure 4.8B). Furthermore, testing homozygous Y and S strains that are heterozygous for C751G demonstrated decreased survival in the Y strains (Figure 4.8B). Homozygous Y with the Y/y allele combination survived treatment better than the homozygous S with S/s alleles ($P < 0.001$) but less well than the

wild type (Y/Y) ($P < 0.05$). This result shows that, although the phenotype appears to be dominant, the causative QTN in *RDS2* is recessive. Testing hybrid backgrounds that were homozygous for either polymorphism confirmed the findings from the allele replacement experiments (Figure 4.8C). Hybrids homozygous for the Y/Y alleles survived treatment better than hybrids homozygous for the S/S alleles ($P < 0.01$, $P < 0.001$) or YJS ($P < 0.05$). Hybrids homozygous for the S/S alleles were statistically indistinguishable from YJS. Based on survival data of the Y strain that is homozygous for the y/y alleles it can be concluded that the S288c-derived allele decreased survival in the Y background by 15%. Combined evidence from survival data of homozygous deletion and allele replacement strains demonstrated that C751G is a QTN influencing peroxide survival in clinical a strain of *S. cerevisiae*.

4.4 Discussion

The identification of a QTN that increases survival of oxidative stress, a trait predominantly associated with clinical *S. cerevisiae* isolates, was facilitated by a combination of classical genetic approaches, a novel synthesis of selective genotyping methods, and a secondary candidate gene screen that implemented evolutionary conservation.

The primary candidate gene screen excluded genes involved in oxidative stress response. The absence of genetic linkage between the catalase genes and peroxide survival complements the results obtained in Chapter 3. Catalase activity was exceedingly low during exponential phase and the parental strains and the hybrid did not differ in catalase activity at that time point. Catalase expression levels could not be detected during exponential growth in the S and Y background and their hybrid YJS. The genetic data attained here strengthen the conclusion that a novel, non-catalase based, mechanism is acting.

A secondary candidate gene screen, employing sequence conservation across fungi and gene function, resulted in the identification of *RDS2*. Two other approaches that

have been successful in identifying yeast QTGs are candidate gene screens based on gene function alone (81, 281) or reciprocal hemizygosity analysis (16, 82, 299). The latter has been applied to the problem of peroxide survival as well. Yet, it relies on a large number of experimental replicates for the statistical analyses to be powerful enough to detect subtle differences in allele contribution. Focusing on select putative peroxide QTGs and conducting more replicates for each would have strengthened the RHA effort.

The basis for successful mapping of *RDS2* was provided by a novel combination of SSA and BSA for selective genotyping of high-survival segregants. SSA via custom-designed Combimatrix 4x2k arrays provides an economic application that facilitates genotyping of segregants of any cross between strains whose genomes have been sequenced. This method will be even more useful as the Sanger Center *Saccharomyces cerevisiae* sequencing project produces more and more genome data. To date, the genomes of 14 wild *S. cerevisiae* strains have been sequenced by the Sanger Center and 22 more genomes are in the pipeline. The ecological and genetic diversity captured by this massive sequencing effort, together with ongoing sequencing projects at other institutions, is unsurpassed in eukaryote genomics. More than 1,000 potential crosses between genome strains can be exploited for the study of diverse phenotypes that are important to yeast biology or for yeast as a model system for human diseases. The resolution of the 4x2k arrays, designed and used here, suffered from sequencing errors in the S288c genome, the first ever eukaryotic genome to be sequenced (123). However, the S288c re-sequencing project at the Sanger Center (`http://www.sanger.ac.uk/Teams/Team118/sgrp/`) should remedy this situation soon, allowing for the design of more accurate probes.

SSA was combined with BSA. Previous BSA-based studies either confirmed the large effect of single genes (29, 281) or identified QTLs, whose candidate gene had already been identified or linked to the trait by other methods or studies (16, 81).

This study is the first to identify a QTN using custom-designed arrays and BSA in a gene that had not been previously linked to oxidative stress in *S. cerevisiae*. Diagnostic RFLP verification of candidate QTLs indicated that QTLs identified in BSA are not necessarily linked to the phenotype. In fact, only the QTL that was recognized in both BSA and at least one SSA resulted in marker-trait linkage. The example of the QTL on ChrXVI suggests that BSA alone might not be sufficient to detect QTLs but can be economically supplemented by 4x2k SSA. Following this reasoning, candidate QTLs on chromosomes VII, XI, XII and XIV represent excellent choices for further study.

Candidate QTLs that were identified by A, B and either C and/or D were screened for preliminary candidate genes, whose functions would suggest an involvement in ROS defense. One of these high-quality candidate QTLs contains *MKT1* and *END2* (XIV) and another *HSP104* (XII). QTNs in the first two genes have been shown to affect high-temperature growth and sporulation efficiency and *HSP104* is a chaperone that refolds proteins in response to heat, ethanol and sodium arsenite (82, 275). These findings suggests that yeast responds to multiple stressors with a select set of proteins and emphasizes that the oxidative stress response may be more complex than appreciated.

Contrasting the quantitative architecture of peroxide survival obtained by natural and laboratory selection (338), reveals that different evolutionary trajectories can lead to the same, or a very similar, phenotype. Two *S. cerevisiae* strains were evolved from an ancestral strain with slow growth in H_2O_2, via a rapid selection scheme (36). Both evolved strains grew about twice as fast when challenged with H_2O_2 than the ancestral strain. Crossing the evolved strains with each other revealed that resistance is a quantitative trait and that the same major-effector mutation had been acquired by both evolved strains but that they differed in the nature of the modifiers (338). The identities of the major mutation and the modifiers remain unknown but sequence

analysis of *RDS2* in the evolved strains would establish if the C751G substitution is affecting selection for oxidative stress resistance in the laboratory.

Transgression in F_1 segregants confirms the actions of different modifiers in the S288c and YJM789 genomes. The presence of segregant phenotypes exceeding parental phenotypes indicates nonadditive gene action, i.e. epistasis and/or overdominance or the fixation of particular alleles with opposing effects in the parental lines (200). Epistatic interactions between QTNs have been identified in high-temperature growth (288) and sporulation efficiency (82). This investigation compared strains that are homozygous for either background but heterozygous for the C751G polymorphism. The Y background exhibits reduced survival when heterozygous for the QTN (Y/y), strongly suggesting epistasis between the S288c-derived allele and a locus in the Y background. This finding is supported by survival data from hybrids homozygous for either allele. A homozygous S/S hybrid resembles the heterozygous hybrid but the homozygous Y/Y hybrid exhibited increased survival. Deletion of *RDS2* or allele replacement does not affect survival of the S strain. This pattern suggests that downstream targets have diverged between S344 and YJK1272, and that the YJM789-derived allele can no longer interact with targets in S344. However, these might be the genes whose products are required for stress response. Evolutionary conservation of the acidic amino acid residue in fungi and the presence of a neutral histidine residue in S344 suggest that the aspartic acid residue is the evolutionary ancestral state.

RDS2 encodes a zinc cluster protein of the fungal-specific *GAL4* family (4). Zinc cluster proteins are intimately involved in the development of pleiotropic drug resistance (PDR), which is defined as the rapid acquisition of resistance to multiple drugs (169). *S. cerevisiae* zinc cluster PDR genes encode transcriptional activators, such as *PDR1* and *PDR3*, that initiate transcription of genes whose products have detoxifying function, such as drug transporters. Zinc cluster proteins contain N-

terminal zinc finger motif ($Zn(II)_2Cys_6$) and a C-terminal activation domain (227). Activation of Gal4, for example, occurs by phosphorylation of a serine residue at position 699 in the C-terminus (273).

The *rds2* deletion mutant is sensitive to calcofluor white and ketoconazole but resistant to osmotic stress and unable to grow on the non-fermentable carbon sources glycerol and lactose (4, 5, 222). In the deletion strain, the cell wall composition changed depending on the growth stage, suggesting that Rds2 regulates drug sensitivity by altering the permeability of the cell surface (222). This result offers an explanation why YJK1272 as well as S344 survived peroxide equally well in stationary phase but exhibited different phenotypes in exponential phase (Chapter 3).

Rds2 possesses a zinc finger motif, has DNA binding activity and binds to the promoters of metabolic genes when cells are grown in glucose (294). Upon shifting cells to the non-fermentable carbon source ethanol, however, Rds2 is phosphorylated by Snf1 and activates transcription of genes involved in gluconeogenesis, the tricarboxylic acid cycle and glucose metabolism (294). Interestingly, ethanol is toxic to yeast cells because it elevates ROS levels in the mitochondria creating oxidative stress (65). Other zinc cluster proteins that are phosphorylated in response to stress exerted by acids and differential nitrogen sources are War1 (175) and Put3 (152). Sites of phosphorylation in these PDR genes have not yet been determined but a lysine to glutamic acid substitution near the activation domain of Pdr3 results in increased drug resistance (238), indicating a critical role for the acidic amino acid residue in stress response.

Stress-induced phosphorylation and the presence of an aspartic acid residue in the putative C-terminal activation domain of Rds2 resemble activation by phosphorylation of D427 in Skn7. This OSR transcription factor acts as a response regulator in a phosphorelay signal transduction system (174). It could be hypothesized that that Rds2 D251 is the site of activation upon oxidative stress that is required for the

activation of detoxifying genes and Rds2 may even be part of a novel phosphorelay system.

This study provides genetic evidence for a novel function of *RDS2* in the oxidative stress response. The quantitative trait nucleotide C751G influences stress response in an as of yet unknown mechanism or pathway. Since both alleles are found in multiple strains sequenced as part of the Sanger Center initiative, it suggests that these alleles are differentially functional, and not that one allele is defective.

Rds2 is a fungal-specific transcription factor that regulates cell wall architecture and pleiotropic drug resistance. The presence of an aspartic acid residue in the activation domain, resembling Skn7, makes Rds2 a promising drug target. Two-component and phosphorelay signaling systems appear to be absent from mammals and are consequently considered potential drug targets in other fungi and cell wall synthesis is already utilized as a powerful drug target (48, 68, 146). The identification of a QTN affecting a virulence-related trait furthers our understanding of yeast biology and provides a novel target for the study of drug actions.

Table 4.1: Strains whose name begin with an S are derivatives of the laboratory background S288c and a Y denotes derivation from the clinical isolate YJM128. All strains are homothallic MAT a/α diploids unless indicated otherwise.

Strain	Derivative of	Genotype	Reference
Initial cross and backcross design			
YJK1272	YJM145	*gal2*Δ::hphMX4/*gal2*Δ::hphMX4	McCusker Lab Collection
YJK1274	YJM145	*gal2*Δ::kanMX4/*gal2*Δ::kanMX4	McCusker Lab Collection
S344	S288c	*gal2*Δ::kanMX4/*gal2*Δ::kanMX4	McCusker Lab Collection
S347	S288c	*gal2*Δ::hphMX4/*gal2*Δ::hphMX4	McCusker Lab Collection
YJS [1]	YJK1272 x S344	*gal2*Δ::hphMX4/ *gal2*Δ::kanMX4	[2]
F_1-2DxS344		*gal2*Δ::hphMX4/*gal2*Δ::kanMX4	
F_1-10BxS344		*gal2*Δ::hphMX4/*gal2*Δ::kanMX4	
F_1-19CxS347		*gal2*Δ::kanMX4/*gal2*Δ::hphMX4	
BCI-2CxS344		*gal2*Δ::hphMX4/*gal2*Δ::kanMX4	
Reciprocal hemizygosity analysis			
YJM155	YJM145	*lys2*/*lys2*	(213)
YJM385	YJM145	*lys5*/*lys5*	(213)
S1002	S25	*lys2*/*lys2*	(299)
S1003	S96	*lys5*/*lys5*	(299)
Homozygous *RDS2* deletions			
YSD-Y1	YJM155	*RDS2*/*rds2*Δ::hphMX4	
YSD-Y2	YJM155	*RDS2*/*rds2*Δ::hphMX4	
YSD-Y3	YJM385	*RDS2*/*rds2*Δ::kanMX4	
YSD-Y4	YJM385	*RDS2*/*rds2*Δ::kanMX4	

Continued on next page

[1] YJS indicates hybrid background

[2] If no other reference is indicated, this strain was developed as part of this study

Strain	Derivative of	Genotype	Reference
YSD-S1	S1002	*RDS2*/*rds2*Δ::hphMX4	
YSD-S2	S1002	*RDS2*/*rds2*Δ::hphMX4	
YSD-S3	S1003	*RDS2*/*rds2*Δ::kanMX4	
YSD-S4	S1003	*RDS2*/*rds2*Δ::kanMX4	
Y-rds2-1	YSD-Y1 x YSD-Y3	*rds2*Δ::hphMX4/*rds2*Δ::kanMX4	
Y-rds2-2	YSD-Y2 x YSD-Y4	*rds2*Δ::hphMX4/*rds2*Δ::kanMX4	
S-rds2-1	YSD-S1 x YSD-S3	*rds2*Δ::hphMX4/*rds2*Δ::kanMX4	
S-rds2-2	YSD-S2 x YSD-S4	*rds2*Δ::hphMX4/*rds2*Δ::kanMX4	
Allele replacements and combinations			
S1288	S288c	MATα *lys5*::loxP[3]	(158)
YHS633	YHS605	MATα ho::loxP *flo8*Δ::loxP *lys5*Δ::loxP	(287)
YSD1	S1288	MATα *RDS2*-Y751^{G}*[4]	
YSD3	S1288	MATα *RDS2*-Y751^{G}*	
YSD10	YSD1xYSD-S1	MATa *lys2 RDS2*-Y751^{G}*	
YSD23	S1288xYSD-S1	MATa *lys2 RDS2*-S751^{C}	
YSD26	YSD1xYSD10	*RDS2*-Y751^{G}*/*RDS2*-Y751^{G}*	
YSD30	YSD3xYSD10	*RDS2*-Y751^{G}*/*RDS2*-Y751^{G}*	
YSD34	YHS633xYSD-Y1	MATa *lys2 RDS2*-Y751^{G}	
YSD36	YHS633	MATα *RDS2*-S751^{C}*	
YSD37	S1288xYSD23	*RDS2*-S751^{C}/*RDS2*-S751^{C}	
YSD43	YHS633xYSD34	*RDS2*-Y751^{G}/*RDS2*-Y751^{G}	
YSD51	YSD36xYSD-Y1	MATa *lys2 RDS2*-S751^{C}*	
YSD52	YHS633	MATα *RDS2*-S751^{C}*	
YSD55	YSD36xYSD34	*RDS2*-S751^{C}/*RDS2*-Y751^{G}	

Continued on next page

[3] Haploid strains used for allele replacement experiments and tester matings are heterothallic

[4] Asterisk indicates allele replacement genotype

Strain	Derivative of	Genotype	Reference
YSD58	YSD36xYSD51	*RDS2*-S751^{C}/*RDS2*-S751^{C}*	
YSD62	YSD1xYSD23	*RDS2*-Y751^{G}/*RDS2*-S751^{C}	
YSD66	YSD3xYSD23	*RDS2*-Y751^{G}/*RDS2*-S751^{C}	
YSD70	YSD52xYSD51	*RDS2*-S751^{C}/*RDS2*-S751^{C}*	
YSD72	YSD52xYSD34	*RDS2*-S751^{C}/*RDS2*-Y751^{G}	
YJS79	YSD1xYSD51	*RDS2*-S751^{C}/*RDS2*-S751^{C}	
YJS80	YSD3xYSD51	*RDS2*-S751^{C}/*RDS2*-S751^{C}	
YJS81	YSD36xYSD23	*RDS2*-Y751^{G}/*RDS2*-Y751^{G}	
YJS82	YSD52xYSD23	*RDS2*-Y751^{G}/*RDS2*-Y751^{G}	
Tester matings			
S19	S1	MATα *ura3*	(287)
S25	S1	MATα *lys2-1*	(287)
S95	S288c	MATa *lys2*	McCusker Lab Collection
S96	S288c	MATa *lys5*	McCusker Lab Collection
YJM788		MATa *ura3*	McCusker Lab Collection

Table 4.2: PCR primer and RFLP enzymes for candidate gene genotyping of F_1 segregants.

Gene	Syn[1]	Non-syn[2]	± 1000 bp[3]	Primer	Primer sequence (3' → 5')	Enzyme [U][4]	Fragment sizes (bp)
CTA1	4	1	7/2	CTA1-2146F	CAATCCCGCTATCAGAGATG	*Nci*I [10]	S: 182, 604
				CTA-2932R	GTCTCTTCCAGATTGCTGTC		Y: 786
CTT1	0	2	2/6	CTT1-2318F	GAAGACAACGACGAAGTATCTG	*Ssp*I [2.5]	S: 128, 403, 322
				CCT1-3171R	CTCTGTATAATCCTCTTAGTCC		Y: 128, 725
CCP1	6	2	6/5	CCP1-891F	AAGGACCCTGGAGCGAAAAGTA	*Sma*I [10]	S: 256, 615
				CCP1-1762R	TCCAGAGTTCTTCAAGTGGGTC		Y: 871
SOD1	4	0	4/6	SOD1-930F	GCTGTAACTATGTTGCGGAAA	*Sau*3AI [2]	S: 170, 357
				SOD1-1457R	GTTAGACCAATGACACCACA		Y: 527

[1] Synonymous polymorphisms in ORF

[2] Non-synonymous polymorphisms in ORF

[3] Synonymous and non-synonymous polymorphisms ± 1000 bp

[4] Enzyme units

Table 4.3: Primer sequences for allele-specific multiplex PCR to genotype F_1 segregants for candidate genes *CTA1* and *CTT1*.

Genes	Primer	Primer sequence (3' → 5')	Fragment length (bp)
CTA1	CTA1-S-F	AACCACTATTTAAAGCCGCA	615
	CTA1-S-R	TGTTAGACATTTCGTTCTTTTC	
	CTA1-Y-F	AACCACTATTTAAAGCCGCC	
	CTA1-Y-R	TGTTAGACATTTCGTTCTTTTA	
CTT1	CTT1-S-F	TTGGGTAAAGTCATTGCAGAAT	1012
	CTT1-S-R	TATGTGCGCCACTTCACC	
	CTT1-Y-F	TTGGGTAAAGTCATTGCAGAAG	
	CTT1-Y-R	TATGTGCGCCACTTCACT	

Table 4.4: Physical locations, sizes and map lengths of seven candidate QTLs identified in analysis B and at least one other genotyping analysis. For comparison the chromosomal and physical location of ROS detoxifying candidate genes from the primary candidate gene screen are indicated.

Chromosome	Region (kb)	Physical size (kb)	Map length (cM)	Analyses
II	368,678 – 474,302	105.6	35.9	B, D
VII	769,508 – 1,071,337	301.9	102.6	A, B, C
XI	72,059 – 285,440	213.4	78.7	A, B, C
XII	77,543 – 277,809	200.3	68.1	A, B, C, D
XIII	195,745 – 598,203	402.5	136.8	A, B, C, D
XIV	403,929 – 634.658	230.7	78.4	A, B, C, D
XVI	220,020 – 291.835	71.8	24.4	A, B, C
IV *CTA1*	969,677 – 968,130			
VII *CTT1*	654,638 – 656,326			
X *SOD1*	623,003 – 622,539			
XI *CCP1*	566,840 – 565,755			

Table 4.5: PCR primers, diagnostic RFLPs and Y allele distribution in BCI high- and low-survival segregants QTL linkage analysis.

Chr[1]	Position[2]	Primer	Primer sequence (3' → 5')	T_A(^{o}C)	Enzyme [U]	Fragment length (bp)	High (%Y)[3]	Low (%Y)[4]
IX	361,265	chrIXNotIF	ATAGCGAGCCACCAACACCA	52	*Not*I [5]	S: 906	59	63
		chrIXNotIR	TACTCCTTGGAATCACTGGA			Y: 626, 280		
X	86,297	chrXAflIIF	ATGCCTGTGAGGTGTATGACC	53	*Afl*III [10]	S: 826	41	50
		chrXAflIIF	GATTTCCACTGCATTACCCA			Y: 245, 581		
X	136,654	chrXDrdIF	ACCCAGCAGAAAGCAAACAA	53	*Drd*I [2.5]	S: 530	52	50
		chrXDrdIR	GGACGTGAAGAACAAAAGGAA			Y: 153, 377		
XI	500,892	chrXINsiIF	GGTAATGATGGTGATTTTAGAT	50	*Nsi*I [5]	S: 275, 570	59	36
		chrXINsiIR	CGGTAGTTTGCTTTATGGATTCA			Y: 845		
XVI	335,021	chrXVIEcoNIF	ATGCTGGAGAGAAACCCAAA	52	*Eco*NI [7.5]	S: 852	77	21
		chrXVIEcoNIR	AAGAAAGAAATCCGTCCTATGA			Y: 338, 514		

[1] Chromosome

[2] Physical location of diagnostic RFLP on chromosome (kb)

[3] Percentage of high-survival BCI segregants that have the Y allele

[4] Percentage of low-survival BCI segregants that have the Y allele

Table 4.6: Allele-specific PCR primers and diagnostic RFLPs used for fine-mapping of the QTL on chromosome XVI.

ChrXVI[1]	Marker	Primer sequence (3' → 5')	T_A(^{o}C)	Enzyme [U]	Fragment length (bp)
100,561	ChrXVI_100F	ATCAAGAGGACCAAGACACCAT	59		1,072
	ChrXVI_100SR	AAATCATCTGGGATCACCTTC			
	ChrXVI_100YR	AAATCATCTGGGATCACCTTT			
199,940	ChrXVI_200SF	GGGAAGATTTGAGATAGTAGC	59		534
	ChrXVI_200YF	GGGAAGATTTGAGATAGTAGG			
	ChrXVI_200R	TAACAATAGAACAGGGAAGGTG			
252,116	ChrXVI_250SF	AATGCTGTTTGAGTAGGCAGG	59		518
	ChrXVI_250YF	AATGCTGTTTGAGTAGGCAGA			
	ChrXVI_250R	GCAAATAATGAGGAAACTTCAAATG			
299,677	ChrXVI_300SF	GCAGTTTTTTTCCCTATCTCTG	59		785
	ChrXVI_300YF	GCAGTTTTTTTCCCTATCTCTT			
	ChrXVI_300R	GCAGGATTATTGAAGCCGTA			
322,898	ChrXVI_322DraIF	TGCCAAACATGTCACTTACCC	50	DraI [1]	S: 162, 866
	ChrXVI_322DraIF	CTGCCTAATCTCAATCCATT			Y: 1028
335,021	ChrXVI_335EcoNIF	ATGCTGGAGAGAAACCCAAA	52	EcoNI [7.5]	S: 852
	ChrXVI_335EcoNIR	AAGAAAGAAATCCGTCCTATGA			Y: 338, 514
350,451	ChrXVI_350HaeIIIF	TCTGCCCAAGAGTGTATTG	50	HaeIII [2]	S: 198, 811
	ChrXVI_350HaeIIIR	TAGACGCTAAAAAGTTGAAT			Y: 1,009

[1] Position on chromosome XVI (kb)

Table 4.7: Genotyping results for seven allele-specific PCR and diagnostic RFLP marker used to genotype high- and low-survival segregants in the BCI and F_1 (Table 4.6).

ChrXVI[1]	H[2] BCI (Y/S)[3]	L[4] BCI (Y/S)	H F_1 (Y/S)	L F_1 (Y/S)
100	14/8			
200	0/21			
250	6/5			
300	17/4	3/16	26/16	3/13
322	17/4	4/16	25/16	
335	17/5	4/15	25/17	3/13
350	14/7	5/14	20/20	3/13

[1] Marker position on chromosome XVI as indicated in Table 4.6

[2] High-survival segregants

[3] Number of Y-derived alleles/S-derived alleles

[4] Low-survival segregants

Table 4.8: Genes found in the QTL on chromosomes XVI and their functions as described in the Saccharomyces Genome Database (`www.yeastgenome.org`). Genes are sorted into three groups depending on the presence of synonymous and non-synonymous polymorphisms in the open reading frame. Gene order in the QTL is: *RDS2*, *COX11*, *RPL5*, *SPO19*, *TAF14*, *TBF1*, *HHO1*, *NAN1*, *KAP120*, *SPC29*, *RNY1*, *TFB2*, *MEI5*, *VPS30*.

Gene	Function/Description
Identical DNA sequence	
COX11	Copper ion binding, cytochrome c oxidase
RPL5	RNA binding, protein component of the large ribosomal subunit
TFB2	General RNA polymerase II transcription factor
MEI5	Meiosis-specific protein, involved in meiotic recombination
Only synonymous polymorphisms	
SPO19	Meiosis-specific protein, involved in completion of nuclear division
TBF1	Telobox/containing general regulatory factor
KAP120	Karyopherin, structural constituent of nuclear pore
SPC29	Inner plaque spindle pole body compoment
Non-synonymous and synonymous polymorphisms	
RDS2	Zinc cluster transcriptional activator conferring ketoconazole resistance
TAF14	General RNA polymerase II transcription factor activity
HHO1	Linker histone required for nucleosome packaging
NAN1	U3 snoRNP protein, component of the small ribosomal subunit
RNY1	RNAse
VPS30	Subunit of phophatidylinositol 3-kinase complexes I and II

Table 4.9: Primers used for RHA and homologous replacement of C751G between S and Y strains.

Primer	Primer sequence (3' → 5')
Recriprocal hemizygosity analyses	
JM41	CAGCTGAAGCTTCGTACGC
JM42	GCATAGGCCACTAGTGGATCTG
JM37	CCTCGACATCATCTGCCC
FT167	GTATTCTGGGCCTCCATGTC
Homologous allele replacement	
RDS2_102F	TAGGTGCGTCAAGAGGGATA
RDS2_966R	TAACATCCTCTCGAAGCTCT
RDS2_550F	AGGAGTGGCAAGACAAGAAAAT
RDS2_1000R	AACACGATCATAAGATAATAACA
RDS2_701F	AACAATTCTTTTTAACAGCGG
RDS2_830R	TCCATGTAGTCTTGTAGTCT
RDS2_1315R	CAAAGGGATGAAATTCCCGA
RDS2_-500F	CTTATCATGACAATATTAGGGA
RDS2_+500R	TTCTTGTCTTCACCACGTCCAA
JM41_AS751-828_F	AGTCTCGAATTCTAGCGAATGCAAACGAAAACAGTGCACCGACACCGAAG CAGCTGAAGCTTCGTACGC
JM42_AS751-828_R	TGGATAGTGGTTTCAGAATCCTTTGCTTGGAAGACTGATTCATATATTTG GCATAGGCCACTAGTGGATCTG
RDS2_751_S_F	CAGAA**C**[1]ACCGGCTGAAATTGGTCATAAATGC
RDS2_751_Y_F	CAGAA**G**ACCGGCTGAAGTTGGTCATAAATGC
RDS2_755_S_R	CTTCGCATTTATGACCAA*C*[2]TTCAG
RDS2_755_Y_R	CTTCGCATTTATGACCAA*T*TTCAG

[1] Bold print indicates non-synonymous SNP at position 751 in *RDS2*

[2] Italics print indicates synonymous SNP at position 762 in *RDS2*

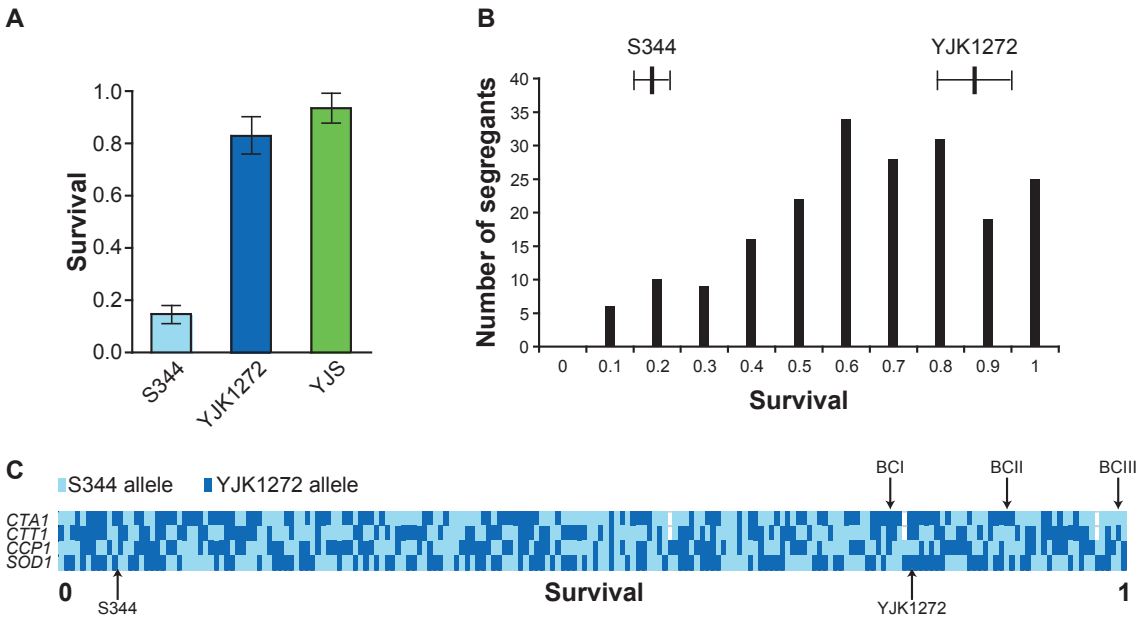

FIGURE 4.1: (A) Survival of parental isolates and their hybrid in the CFU assay (20 mM TBHP). The bar graph represents the mean of three experimental replicates per strain and its standard error. (B) The histogram shows experimental data collected for 200 F_1 segregants that are clustered by survival in bins of size 0.1. Parental means (bold vertical line) and standard errors (horizontal lines) are indicated above the histogram. (C) Candidate gene genotypes for 200 F_1 segregants. The presence of either parental allele of the four candidate genes *CTA1*, *CTT1*, *CCP1*, and *SOD1* is indicated by applying the appropriate parental color to each cell. Each row represents data for one gene and each column shows the genotype of each segregant. Segregants are sorted by survival from lowest (0) to highest (1), reflecting the phenotypic data from (B). Arrows below the chart point at segregants whose phenotypes are closest to the parental means. Arrows above the chart indicate the three F_1 segregants that were crossed to S344 to generate backcross lines I, II, III (BCI, BCII, BCIII). Gaps mark missing genotype data.

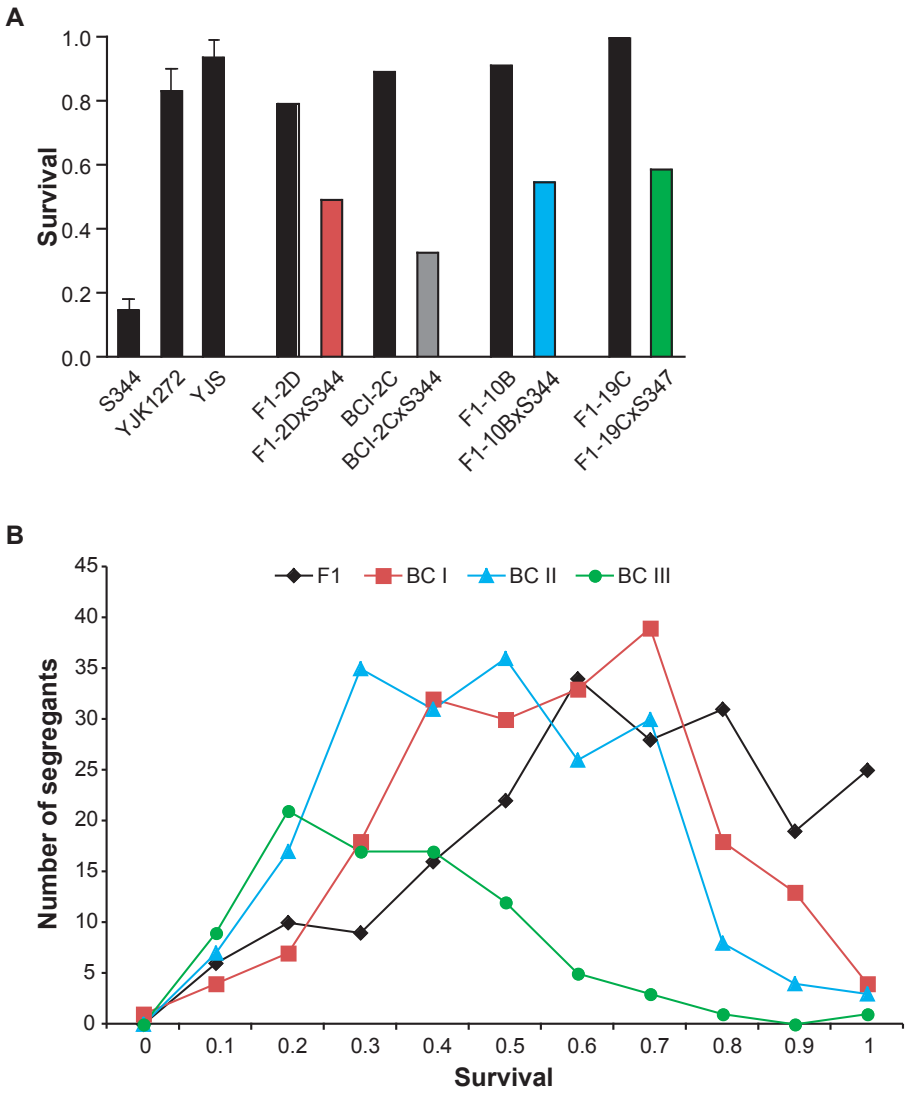

FIGURE 4.2: (A) The bar graph compares the parental and hybrid means (± SEM) (20 mM TBHP) to survival of F_1 segregants (1 replicate), denoted by F_1 – prefix that have been used to set up backcross lines (black columns). The colored columns represent the survival of hybrids from the F_1 x S crosses showing a decline in survival. The grey column represents the phenotype of a second backcross hybrid derived from a BCI individual. (B) Phenotypic distributions of backcross lines I, II, and III (BCI=red, BCII=turquoise, BCIII=green) and the F_1 (black) are plotted as a X-Y straight marked scatter plot, after phenotypes have been clustered by survival. Each data point represents the number of segregants that share this phenotypic class. Quantitative data from CFU assays of 200 F_1, 199 BCI, 197 BCII, and 86 BCIII segregants are represented here.

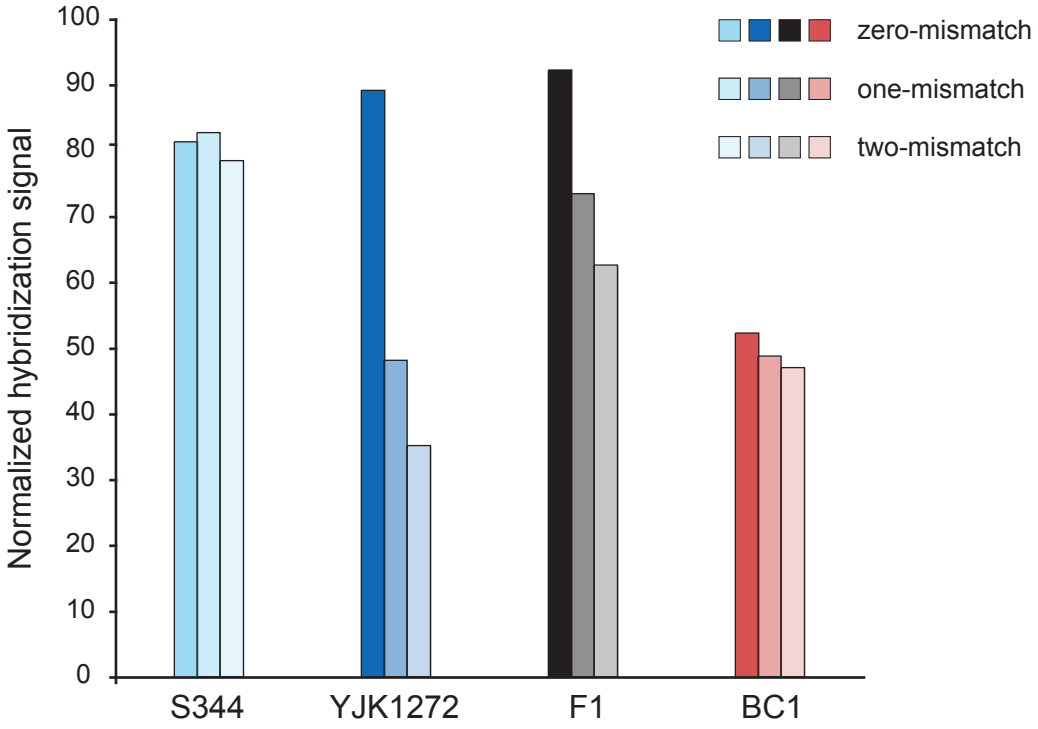

FIGURE 4.3**:** Shown are the hybridization signal values for the parental strains S344, YJK1272 and BSA hybridizations of the F_1 and BCI segregants. The signal has been normalized for GC-content and melting temperature. For each strain the zero-mismatch control and analyses A (one-mismatch) and B (two-mismatch) are represented in different shades of color.

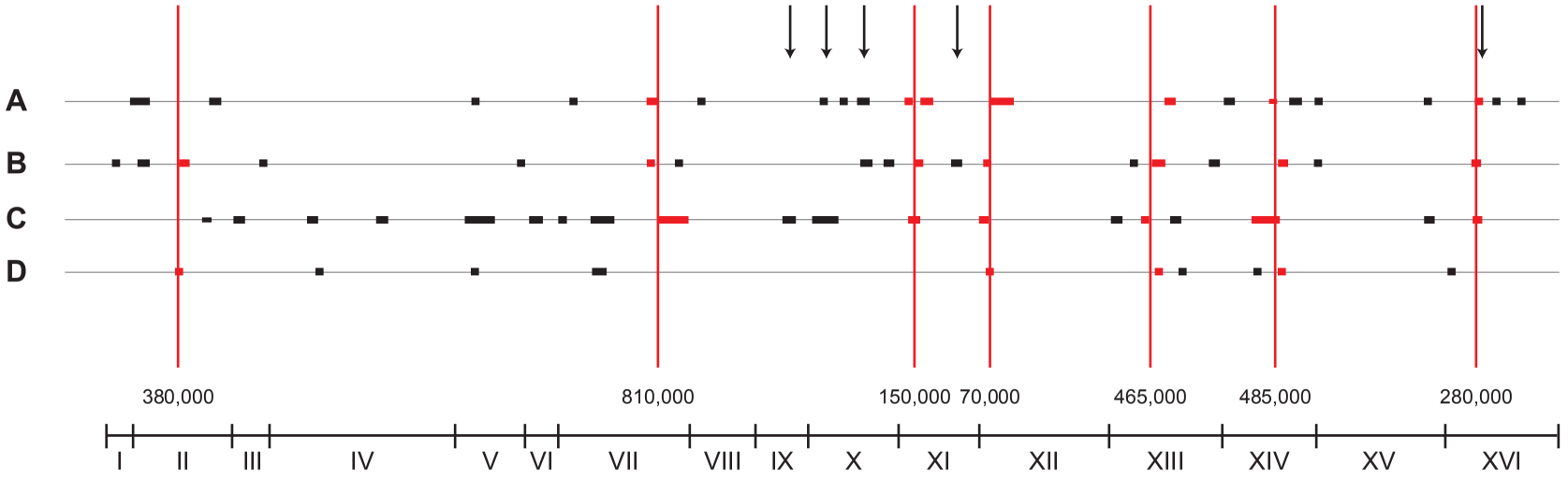

FIGURE 4.4: Shown is a combination of all four S98 BSA and 4x2k SSA genotyping analyses. (A) S98 one-mismatch SFPs, (B) S98 two-mismatch SFPs, (C) 4x2k SFPs with gaps, (D) 4x2k ≥ 3 consecutive SFPs. The black horizontal line at the bottom is the *S. cerevisiae* genome with its chromosomes indicated by roman numerals between the beginning (left) and end (right) end of each chromosome (short vertical bars). Chromosome lengths are drawn to scale. Candidate QTLs are marked by short horizontal bars. Red bars represents loci that were found in the most conservative analysis (B) and at least one other analysis. These regions are highlighted by red vertical lines and their approximate position on the chromosome is marked at the bottom. Black arrows point to candidate QTLs that have been tested with diagnostic RFLPs (Table 4.5).

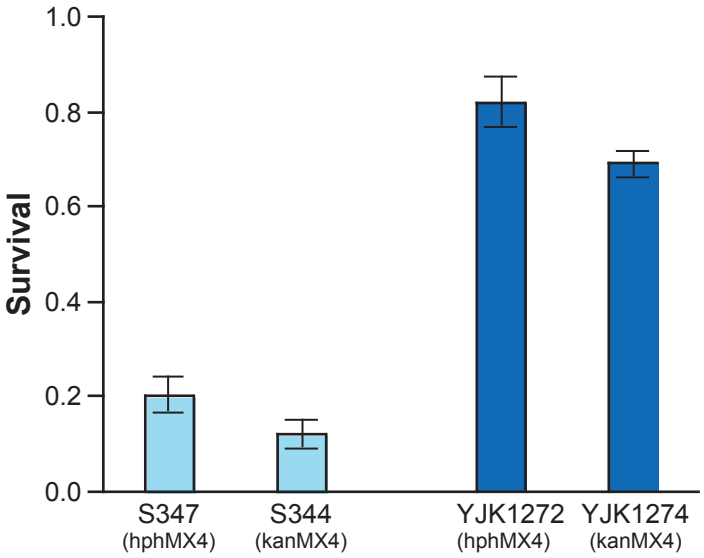

FIGURE 4.5**:** Both backgrounds carrying either hphMX4 or kanMX4 were tested three times for survival in 20 mM TBHP. Plotted is the mean ± SEM of each experiment and strains are color coded by background

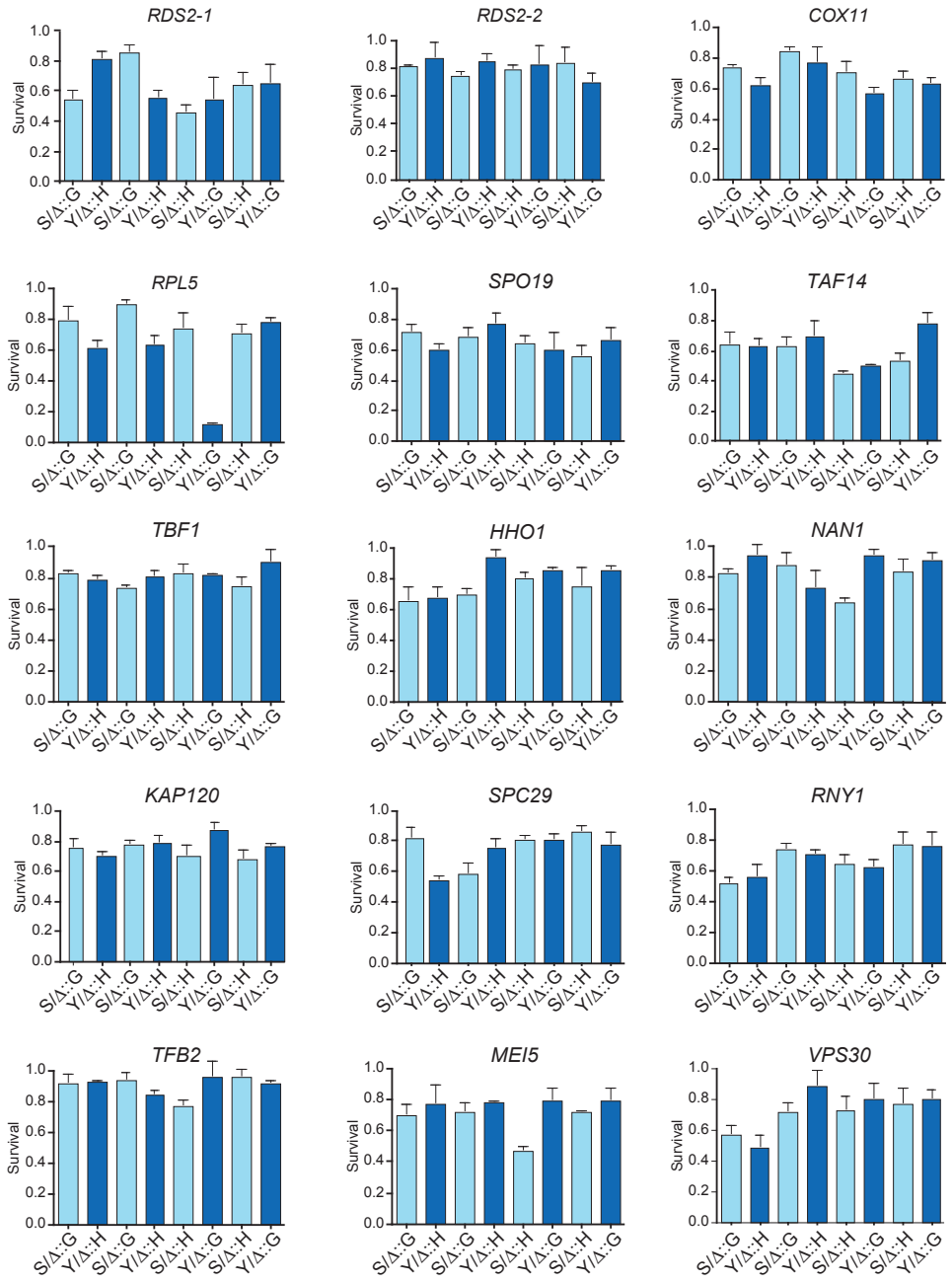

FIGURE 4.6: Each bar graph represents the four comparisons conducted for each gene and is labeled with the gene's name at the top. RHA has been conducted twice for *RDS2* on four different transformants. The different sets are indicated as *RDS2-1* and *RDS2-2*. Survival in 16 mM TBHP is compared directly between a hybrid strain having the wild type S allele but the Y allele replaced with a kanMX4 (G) drug resistance marker and a strain with the Y allele and the S allele replaced with the hphMX4 (H) drug resistance marker (first two columns). The same comparison was repeated on one more pair of transformants (columns three and four) and on strains with switched drug markers (columns five to eight). Shown are the mean ± SEM. Light and dark blue colors indicate which allele is present in the hybrid.

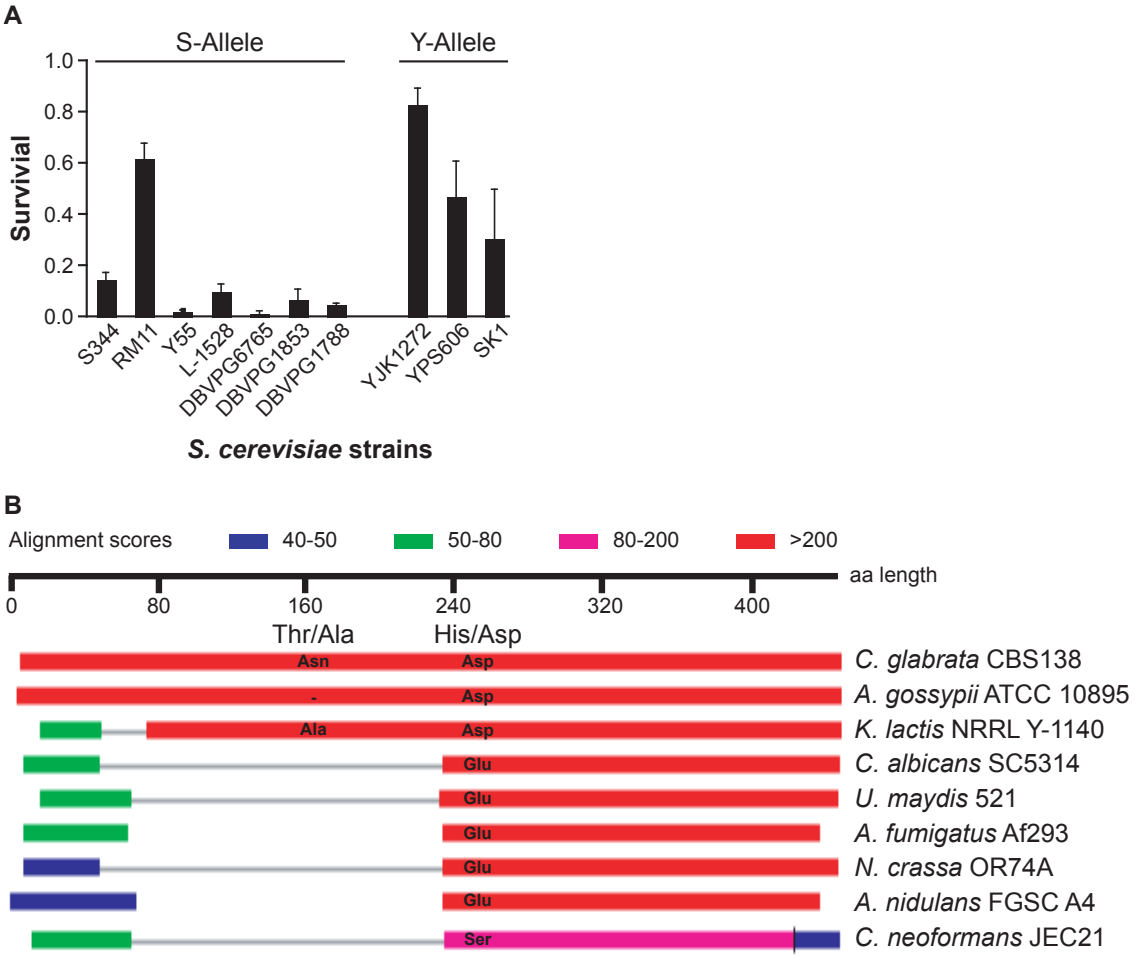

FIGURE 4.7: (A) *S. cerevisiae* strains carrying either the Thr/His S allele or the Ala/Asp Y allele were compared for peroxide survival in 20 mM TBHP. (B) Rds2 BLAST results for nine different fungal species. The alignment shows evolutionary conservation around amino acid position 251, but not for 169. Both positions are marked with the *S. cerevisiae* substitutions (Thr/Ala, His/Asp). All species, except *C. neoformans*, have either an aspartic acid or glutamic acid (Glu) residue on that position. The dash at amino acid residue 169 in *A. gossypii* denotes a gap in the alignment.

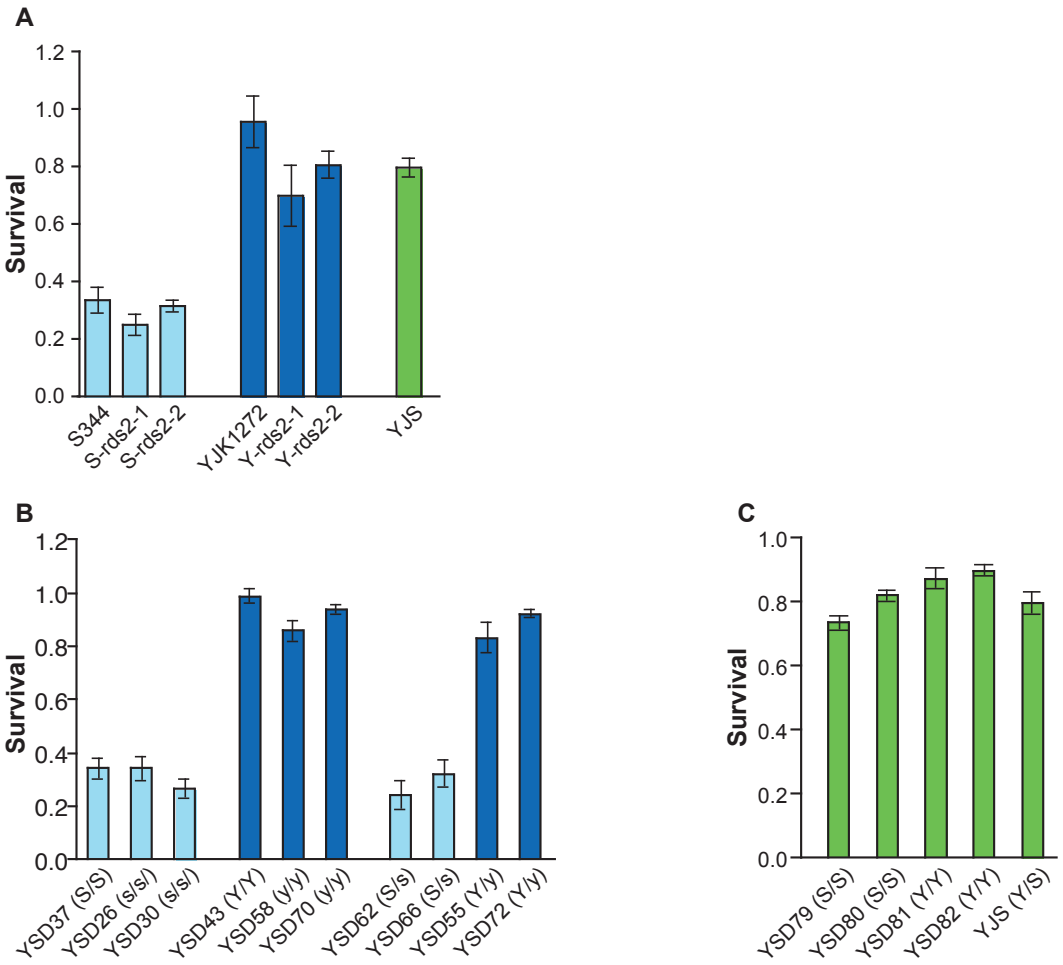

FIGURE 4.8**:** (A) Homozygous deletions of *RDS2* in the S and the Y backgrounds lead to decreased survival in the Y background. The bar graph presents the mean of three replicates and its standard error of survival in 16 mM TBHP. Wild type strains (S344, YJK1272) and deletion mutants are color-coded as before and the hybrid (YJS) is added to the chart in green. (B) The non-synonymous SNP on position 751 was exchanged between the S and the Y background. Plotted are the means and their errors for six (S) and eight (Y) replicates. Strains are color coded by background and for clarity allelic configurations on position 751 are indicated in brackets. (C) Testing survival of homozygous SNP configurations in the hybrid background. Shown is the mean of six replicates and its error.

5

Summary and Future Directions

5.1 Summary

The generation of ROS is a universal host defense mechanism and the ability of pathogens to respond to oxidative stress is correlated with bacterial virulence (257, 260). I showed that clinical isolates of *S. cerevisiae* survived peroxide treatment better than strains from other ecological backgrounds. This pattern is of interest for two reasons. First, *S. cerevisiae* is one of the most versatile genetic model systems. Major insights into the eukaryotic oxidative stress response, damage control and consequences have been gained from studies on this simple eukaryote. Second, until recently little was known about *S. cerevisiae* population biology and evolution. Others have shown that strains associated with fermentation differ from wild strains in the soil. Yet, little is known about the forces that shaped population structure. In addition to the previously recognized ecological niches of brewery, vineyard, spoiling fruit, and soils, *S. cerevisiae* has recently been isolated in clinical settings, where it causes infections similar to *C. albicans*. The origin and evolution of clinical strains and virulence-associated traits remain elusive.

Investigating the difference in peroxide survival observed in a clinical and a laboratory strain of *S. cerevisiae* provides knowledge about the eukaryotic oxidative stress response, the contribution that this phenotype has had on the origin of pathogenicity in *S. cerevisiae* and insights into how pathogens respond to mechanisms of host defense. I devised three sets of experiments for my thesis research to address: (i) population structure in *S. cerevisiae* and the evolutionary history of pathogenicity and peroxide survival, (ii) the biochemistry of peroxide survival and the effect of oxidative stress response candidates, and (iii) the genetic basis of peroxide survival in *S. cerevisiae*.

By applying population genetic methods of DNA sequence analysis and comparing a diverse set of 103 wild and clinical strains of *S. cerevisiae* for peroxide survival, I was able to identify three genetically diverse subgroups. In addition to the domesticated and soil strains, PCA analysis indicated a third group that included the majority of clinical isolates and some fruit and brewery strains. Interestingly, the soil isolates from the Eastern United States are genetically homogenous, while genetic exchange occurs between the major groups and populations. When tested for peroxide survival the clinical and soil strains survived better than any other group. This suggests, in combination with the population genetic data, that resistance to peroxide is a prerequisite for pathogenesis, and that it has potentially originated multiple times independently.

I conducted biochemical assays to determine killing efficiency and the effect that growth phase and catalase enzyme activities have on peroxide survival. Semi-quantitative expression profiles of the catalases, as well as OSR and GSR candidates, were recorded and compared between the clinical and the laboratory strain and their hybrid. The experiments demonstrated that TBHP kills cells immediately, that YJK1272 secretes a factor that improves the survival of S344 slightly and that lower survival of S344 compared to YJK1272 and the hybrid is restricted to the expo-

nential growth phase. Neither the catalase activities nor the expression profiles of the other oxidative stress response candidates differed consistently among strains. These results suggest that the phenotypic difference is not due to catalase activity or Oxidative or General Stress Response mechanisms but to a novel phentoype that requires the cells to be metabolically active.

Genetic and phenotypic analyses of the parental strains, their hybrid, and F_1 and backcross segregants by microarray-assisted QTL mapping, reciprocal hemizygosity analyses and homologous allele replacements showed that peroxide survival is a dominant quantitative trait that is affected by a recessive non-synonymous polymorphism in the zinc cluster protein encoding gene *RDS2*. This quantitative trait nucleotide reduces survival of YJK1272 by 15% but has no effect on S344, suggesting divergence in the downstream targets of this transcription factor. Evolutionary conservation of the acidic amino acid present in YJK1272 implies that the Y allele is ancestral and the S allele of recent origin.

5.2 Future Directions

5.2.1 Investigation of high-quality candidate QTLs and QTNs

In addition to the QTL on chromosome XVI that exhibited marker-trait association and eventually led to the identification of a novel QTN, the previous chapter presented data for five additional high-quality QTLs. These should be tested for marker-trait associations, using a similar RFLP approach. Furthermore, one of these loci contains genes containing QTNs that have previously been implicated in high-temperature growth and sporulation (82, 299). Strains carrying the D30G substitution in *MKT1* and S258N in *END3* should be tested for peroxide survival to determine if either gene might be involved in a multiple stress responses.

5.2.2 RDS2 allele frequency, natural selection and evolutionary history

DNA sequence data from the Sanger Center show that the C751G substitution occurs in multiple *S. cerevisiae* strains. Hence, it will be important to assess allele frequency of *RDS2*, determine the selective pressures that have shaped the patterns of polymorphism in the gene and linked loci to further understand its impact on *S. cerevisiae* pathogenicity. The same DNA sequence data and sequences from sibling species should be tested for positive selection along lineages using PAML (342). The evolutionary history and relative age of *RDS2* could be investigated by sequencing the entire locus and identification of haplotype blocks and linkage disequilibrium.

5.2.3 Biochemical characterization of the secreted factor

The physical nature of the short-lived factor secreted by YJK1272 that improves survival of S344 is unknown. Survival of S344 improves in co-culture experiments but only marginally in conditioned media, suggesting that activity declines over time due to unfavorable media conditions, i.e. TBHP, pH, salt content, and temperature. Conditioned media experiments should be repeated at different time points to determine the factor's activity profile. To determine if the factor is a protein, a sample of YJK1272 conditioned media should be digested with Proteinase K and tested on S344. Assuming that the factor is a protein, its size and thermostability could be identified by size exclusion chromatography with subsequent SDS-electrophoresis and heating to different temperatures.

Conditioned media from cells in stationary phase provided protection from H_2O_2 and superoxide in *C. albicans* and induces pseudohyphal and invasive growth in *S. cerevisiae* (50, 120, 265, 328). These phenotypic changes are elicited by the quorum sensing molecules farnesol, phenylethanol and tryptophol (50, 328). To assess the impact of quorum sensing molecules on peroxide survival in *S. cerevisiae*, (i) S344 cells should be treated with TBHP in YJK1272 media conditioned by cells

in stationary phase, (ii) YJK1272 media should be tested for the presence of quorum sensing molecules (50), and commercially available quorum sensing molecules, should be added to S344 survival assays.

5.2.4 Functional characterization of Rds2

As described in Chapter 1 the transcription factors Yap1 and Skn7 are intimately involved in the OSR and adaptation to oxidative stress in *S. cerevisiae*. Their genes are in the same epistasis group and co-activate transcription of oxidative stress response genes (173, 223). To determine if Rds2 acts in the same pathway, complementation analysis of double mutants could be carried out. To do so, *rds2*, *yap1* and *skn7* mutants in the Y background should be crossed to generate double mutants. A double mutant that exhibits lower survival than the wild type would suggest that Rds2 acts in the same pathway as the other two transcription factors.

rds2 deletion mutants are sensitive to ketoconazole and calcoflour white (4, 5). To assess the influence of C751G ketoconazole and calcoflour sensitivity, homozygous allele replacement and hybrids homozygous for either SNP should be assayed. If C751G affects resistance to ketozonazole and calcoflour white, their mode of inheritance should be investigated by quantitatively phenotyping the hybrid YJS and the F_1 segregants. Given the complex nature of drug resistance and cell wall architecture, both traits are likely to be quantitative and continuous variation in the F_1 segregants would be a likely result.

Rds2 is phosphorylated by the serine/threonine kinase Snf1 at an unknown site upon shifting cells to ethanol as the sole carbon source (294). Furthermore, Rds2 localization data show that the protein localizes to the cytoplasm and the nucleus (153), supporting a model in which Rds2 is phoshorylated in the cytoplasm and moves to the nucleus to activate transcription. To test the hypothesis that Rds2 and its aspartic acid residue (D251) are parts of a second phosphorelay signaling system

involved in oxidative stress response in *S. cerevisiae*, Rds2 phosphorylation patterns and consequences during oxidative stress need to be investigated. It needs to be demonstrated that the aspartic acid residue is indeed phosphorylated in oxidative conditions. If phosphorylation of D251 is critical, transcriptional activation should be detected upon phosphorylation. The kinase and phosphorelay intermediate that phosphorylate D251 need to be characterized. Phosphorylation of D251 by Snf1 can be tested by employing the β-galactosidase reporter system in a strain with aspartic acid, histidine, or alanine on position 251 in *RDS2*. If Snf1 does not phosphorylate D251, phophorylation by Ypd1, the phosphorelay between Sln1 and Skn7, should be tested using β-galactosidase reporter screens and phosphotransfer assays (192). If neither of these factors is involved, a synthetic genetic array analysis with *rds2* as query could be conducted to identify other Rds2 interactions (313). To rule out the possibility that H251 is oxidatively damaged and the protein rendered non-functional, His-tagged Rds2 should be extracted from S and Y strains treated with TBHP and investigated using mass-spectrometry.

The presence of both alleles in the *S. cerevisiae* population strongly suggests that both alleles are functional. It is conceivable that both alleles respond to different conditions, similar to the findings in Yap1, which activates different genes in response to diamide and H_2O_2 (324). Additionally, Rds2 appears to differentially activate gene transcription depending on the available carbon source and in response to stress (294). This raises the question for the environmental conditions that lead to transcriptional activation by Rds2 and the down stream targets of Rds2 in S288c and YJM128. Expression profiles recorded for wild type and allele replacement strains during different oxidative stresses and other stress conditions, such as high-temperature, osmolarity, and pH would identify different target genes during oxidative stress in S288c and YJM789 and demonstrate if Rds2 activates gene expression in response to other common stressors as well.

My thesis research has provided novel insights into the evolutionary history of one of the oldest domesticated organisms turned pathogen. By applying a population genetic framework in combination with QTL mapping in natural variants of *S. cerevisiae*, I was able to show that the ability to survive oxidative stress is indeed associated with the clinical origin of *S. cerevisiae* strains and that a single nucleotide in *RDS2* is responsible for parts of this dramatic association. By identifying a novel function for the zinc cluster protein Rds2 this research has contributed to understanding fungal oxidative stress response and opened the possibility of a novel drug target.

Appendix A

Comparison of Peroxide Survival in *Candida* Species and *S. cerevisiae*

Opportunistic ascomycetous yeasts vary in clinical frequency, affected patient populations and disease spectrum. For example, the commensal *C. albicans* is the most commonly isolated yeast in the hospital, causing a range of infections from thrush to systemic candidiasis in immunocompetent and immunocompromised individuals (217, 345). *C. glabrata* is the second most common cause of candidiasis and commonly associated with infections of oral cavities in HIV infected individuals (204, 251). *C. parapsilosis* is particularly often isolated from the blood of patients in neonatal intensive care units and from the hands of health care workers (315). *C. lusitaniae* and *S. cerevisiae* are much less frequently found in clinical settings and are currently classified as emerging pathogens (142). These differences in opportunistic lifestyles are likely to be due in part to inter-species variation in resistance to host defense mechanisms, such as oxidative stress.

To assess phenotypic variation in oxidative stress resistance between and within species, nine *C. parapsilosis* strains and ten isolates of *C. albicans*, *C. glabrata*, *C.*

lusitaniae, and *S. cerevisiae* were subjected to disc diffusion assays (see below) and the zone of clearing measured as an expression of resistance (Table A.1). Zones of clearing differ within and between species. The smallest zones of clearing were measured in *C. glabrata* and the largest in *S. cerevisiae* and *C. lusitaniae* (Figure A.1), suggesting a high degree of oxidative stress resistance in *C. glabrata* but not *S. cerevisiae* and *C. lusitaniae*. Differences were detected between almost all species ($P < 0.0001$), with two exceptions: *C. albicans* vs. *C. parapsilosis* and *C. lusitaniae* vs. *S. cerevisiae*. Intra-species comparisons showed that *S. cerevisiae* (16.1) and *C. parapsilosis* (14.4) had highest variance, *C. lusitaniae* (8.5) and *C. glabrata* (11.7) were intermediate and *C. albicans* (3.4) had the lowest levels of variance.

Three levels of oxidative stress resistance were observed in this set of ascomycetous yeasts: *C. glabrata* > *C. albicans* & *C. parapsilosis* > *C. lusitaniae* & *S. cerevisiae*. The clinically most prevalent yeasts were also most resistant to oxidative stress, providing one possible explanation as to why some species appear more often in clinical settings than others. Intra-species variation ranged from smallest in *C. albicans* to largest in *C. lusitaniae* and *S. cerevisiae*. Meiotic recombination, which is largely absent from *C. albicans* but present in *C. lusitaniae* and *S. cerevisiae* could be the cause for differences in variation. Note that the *S. cerevisiae* isolate YJM145, a derivative of the clinical isolate YJM789, was almost as resistant as *C. albicans*, whereas the laboratory strain S288c was the most sensitive *S. cerevisiae* strain. This is the initial observation that lead to the development of my thesis research.

Disc diffusion assay. Yeast cultures were grown over night in SD media (Chapter 2) at 30^{o}C while shaking (250rpm), diluted to a starting optical density of 0.1 in 50 ml SD media and incubated until OD_{600}=0.6 at 30^{o}C while shaking (250 rpm). Cells were washed twice with 5ml of 0.9% (w/v) NaCl and cell numbers adjusted to $1x10^7$ cells/ml in 10 ml of 1.25% (w/v) pre-heated (37^{o}C) top agar. Immediately after inoculation, the top agar was poured into dishes containing 20 ml SD agar

(Chapter 3). Upon polymerization of the top agar, a 10 mm paper disc was placed in the center of the dish and 10 μl 1xPBS containing 0.5 mM TBHP added. Plates were transferred to the incubator after 30 minutes, incubated for 48 hours at 37^{o}C and the zones of clearing measured. All experiments were done in triplicates and inter-species differences analyzed with one-way ANOVAs with Bonferroni correction and intra-species variances calculated.

Table A.1: Shown are the identification (ID) and origin of each yeast strain included in this study as well as its mean zone of clearing (mm) ± one standard deviation (SD). Strains with the largest and smallest zone of clearing are indicated by (+) and (-).

Species	Strain ID	Origin	Zone of clearing ± SD
C. glabrata			
	CBS138[1]	Faeces of man	16.7 ± 2.31
	MMRL 8[2]	Blood	23.0 ± 1.00 (-)
	MMRL 10	Urine	13.0 ± 1.00
	MMRL 11	CF tissue	12.0 ± 0.00
	MMRL 12	Bronchial brush	11.0 ± 1.00 (+)
	MMRL 21	Catheter	14.3 ± 0.58
	MMRL 31	Stool	12.7 ± 0.58
	MMRL 133	Vagina	14.7 ± 0.58
	MMRL 330	Oral, AIDS, Brasil	13.0 ± 0.00
	MMRL 1380	Blood culture	13.0 ± 1.00
C. albicans			
	SC5314	Patient	26.7 ± 1.53 (-)
	MMRL 18	DUMC[3], stool	25.7 ± 1.15
	MMRL 105	DUMC, skin	24.3 ± 0.58
	MMRL 725	Oral, AIDS patient, Italy	21.3 ± 0.58 (+)
	MMRL 761	Throat; neutropenic patient	21.7 ±
	MMRL 1133	Creek water	21.3 ± 0.58 (+)
	MMRL 1150	Local water sample	23.7 ± 0.58
	MMRL 2022	Mouth; volunteer	22.7 ± 0.58

Continued on next page

[1] The Centralbureau voor Schimmelcultures

[2] Medical Mycological Research Laboratory

[3] Duke University Medical Center

Species	Strain ID	Origin	Zone of clearing ± SD
	MMRL 1375	Blood culture	22.7 ± 0.58
	MMRL 1377	Blood culture	22.3 ± 0.58
C. parapsilosis			
	CBS 604	Case of sprue	22.7 ± 3.51
	MMRL 1598	Blood culture, DUMC patient	22.3 ± 1.53
	MMRL 1675	Glen Bulmer, The Philipines (33)	28.3 ± 2.52
	MMRL 1920	Glen Bulmer, The Philipines (33)	26.3 ± 6.66
	MMRL 2450	Bronchial wash, genotype I	22.3 ± 0.58
	MMRL 2452	Blood, genotype II	22.7 ± 4.73
	MMRL 2456	Hand, genotype III	28.7 ± 1.53 (-)
	MMRL 2500	Fingernail, volunteer	17.7 ± 1.53 (+)
	MMRL 2501	Fingernail, volunteer	28.7 ± 4.73
C. lusitaniae			
	ATCC[4] 42720	Blood, leukemia	37.0 ± 4.36
	ATCC 24009	Sputum, Norway	32.7 ± 1.15
	ATCC 38533	Citrus peel juice, Israel	35.0 ± 1.73
	DUMC 100.97	Clinical isolate, MATa	34.0 ± 1.00
	DUMC 110.92	Clinical isolate, MATα	31.0 ± 1.00
	DUMC 117.96	Clinical isolate, MATα	35.7 ± 1.15
	DUMC 124.00	Clinical isolate, MATa	33.0 ± 1.00
	DUMC 127.01	Clinical isolate, MATα	29.3 ± 1.53 (+)
	MMRL 2652	MAT a, MIC = 2 μg/ml[5]	37.7 ± 0.58 (-)
	MMRL 2658	Clinical isolate, MIC = 0.25μg/ml	29.7 ± 3.51

Continued on next page

[4] American Type Culture Collection

[5] Amphotericin B, minimum inhibitory concentration

Species	Strain ID	Origin	Zone of clearing ± SD
S. cerevisiae			
	S288c	Laboratory strain (224)	40.3 ± 2.08 (-)
	YJM 145	Lung, HIV patient (309)	28.3 ± 3.21
	RM11	Fermenting grape must, Italy (225)	31.0 ± 1.73
	MMRL 125	DUMC, stool	33.0 ± 3.61
	MMRL 2497	NC State, peritoneal dialysate	29.3 ± 2.31
	SM1	*Q. alba*, soil, Stone Mountain Park	28.7 ± 0.00
	SM12	*Acer* spp., soil, Stone Mountain Park	28.7 ± 0.58
	O2	*Q. prinus*, soil, Occoneechee Natural Area	29.3 ± 1.15
	Ysb1	Perenterol forte, this study	26.3 ± 1.15 (+)
	WLP570	Belgian Golden Ale	34 ± 2.00

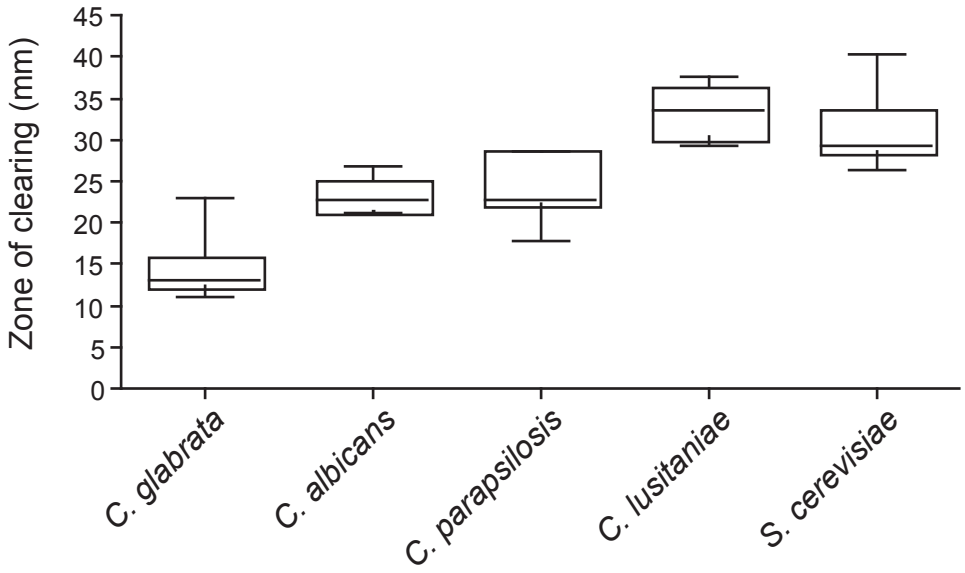

FIGURE A.1**:** Triplicates of each strain in each species are combined and the zones of clearing (mm) in response to 0.5 mM TBHP represented. The box marks the 25 to 75 percentile and the bar inside the box the mean. The whiskers on the top and the bottom of the box represent the most extreme outliers in each species (Table A.1). Species are ranked by resistance from most to least resistant.

Appendix B

Escaping from Concerted Evolution – Domestication and the Relaxation of Evolutionary Constraints on the rDNA Array

Concerted evolution ensures that the DNA sequences of all members of a gene family are more similar to each other than to orthologous repeats in related species (347). The fungal rDNA array is an example of a non-coding genomic region that evolves in a concerted fashion (107). The molecular mechanism by which sequence similarity between gene copies is maintained is known as homogenization but remains to be fully elucidated (87). To investigate the distribution of ITS sequence types among ecologically distinct *S. cerevisiae* isolates and to verify correct species identification, the ITS of 90 strains was amplified and sequenced using standard primers ITS1 and ITS 4 (Chapter 2) (329). ITS sequences from strains with multiple types were cloned using the TOPO TA Cloning Kit (Invitrogen).

62 different ITS types were identified and numbers of types per strain vary between *S. cerevisiae* isolates from different backgrounds. Four of 16 brewery strains have three or seven different ITS types. One clinical and one fruit isolate have four

types. All other isolates have one or two ITS types, consistent with allelic variation in diploids. The fruit strain with four ITS types has been isolated from pozol, a Mexican fermented beverage. This pattern of multiple ITS sequence types found almost exclusively in isolates employed in fermentation strongly suggest a role of domestication in release from concerted evolution. The ITS phylogram shows that isolates with multiple ITS types have been derived multiple times from brewery and fruit strains with only one type (Figure B.1), suggesting that with the discovery of fermentation and subsequent domestication of brewery strains concerted evolution of the rDNA relaxed.

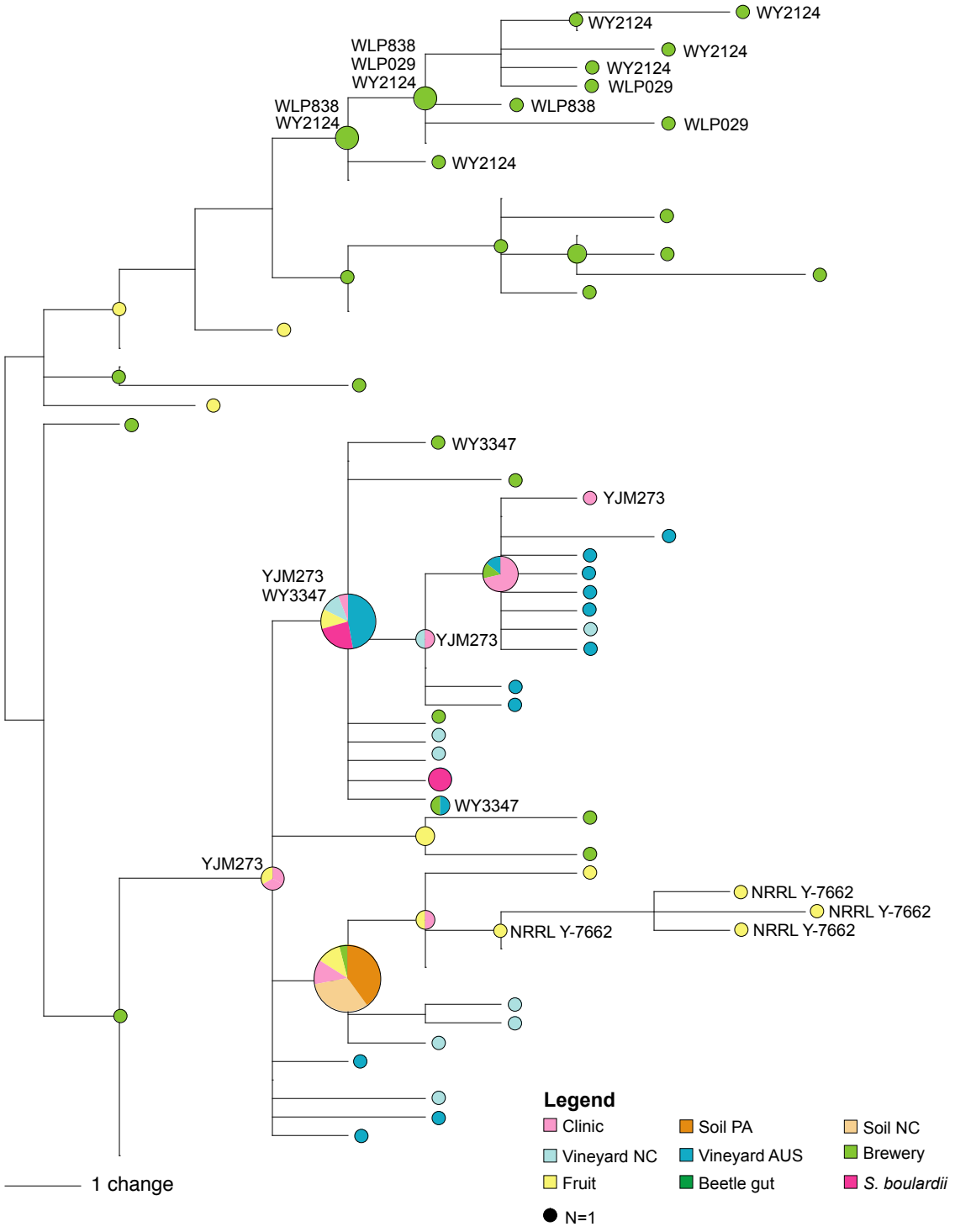

FIGURE B.1: 62 ITS sequence types from *S. cerevisiae* strains used in Chapter 2 were analyzed using the Maximum Parsimony criterion with gaps coded as fifth character state and the tree mid-point rooted. Strains are color -coded by origin and the size of each circle reflects the number of identical sequence types as indicated in the legend.

Appendix C

S. cerevisiae Soil Isolates from North Carolina Live in Sympatry with Sibling Species and Exhibit Very Little Genetic Variation

S. cerevisiae strains were isolated from soil at the base of oak and other trees at two locations in North Carolina using a modified version of a previously described enrichment protocol (292). Two approaches, species-specific multiplex PCR primers, amplifying parts of the coding regions of GDP-mannose pyrophosphorylase (*PSA1*) and chitin synthase I (*CHS1*) and ITS sequencing were used to identify *S. cerevisiae* and distinguish it from its sibling species *S. paradoxus*. From 30 samples collected at Occoneechee State Natural Area, twelve were culture positive and eight of those were identified as *S. cerevisiae*. In Stone Mountain 70 samples were collected 45 of which were culture positive and six *S. cerevisiae* (Figure C.1). Four of eight Occoneechee State Natural Area samples and five of six Stone Mountain State Park samples were collected in close proximity to oak tress. At the second location between two and six samples were collected from 23 different trees along the Widows Creek trail. *S. cerevisiae* was found under five trees (four oak, one maple) and in each case it was

found to co-habit with other yeast species, including *Zygosaccharomyces fermentatii*, *S. cariocanus*, *S. paradoxus*, and *Candida* spp. All North Carolina soil isolates are homothallic, MATa/α, have the same ITS type and are genetically identical at three of five nuclear coding loci (*ACT1*, *MLS1*, *RPB1*). Strains from North Carolina have a different *PHD1* allele than isolates from Pennsylvania and two Stone Mountain isolates differ at *ADP1* from all other soil isolates (Chapter 2).

Soil sampling and enrichment media. Soil samples from the base of oak and other trees were collected at two sites in North Carolina. In a preliminary study to test sampling procedure and enrichment protocol, a total of 30 samples, one per tree, was collected in February 2005 in Occoneechee State Natural Area in Hillsborough (OS) from 12 chestnut oaks (*Quercus prinus*), 8 oaks (*Quercus* spp.), 3 loblolly pines (*Pinus taeda*), 2 maples (*Acer* spp.), 1 tulip poplar (*Liriodendron tulipifera*), 2 decomposing tree trunks of unknown species, 1 wintergreen bush (*Gaultheria* spp.), 1 shrubbery. At the second site, Stone Mountain State Park in Roaring Gap (SM), 70 samples were collected in July 2006 from 23 trees. This time, 2-6 specimens per tree were collected from 10 chestnut oaks (*Q. prinus*), 9 white oaks (*Q. alba*), and one each from loblolly pine (*P. taeda*), maple (*Acer* spp.), tulip poplar (*L. tulipifera*) and *Quercus* spp.

Soil sampling and enrichment culturing was executed as follows. A 1.5 ml Eppendorf tube was filled 2/3 with soil from the tree base and refrigerated over night. All samples were processed using the two-step enrichment protocol described by Sniegowksi, Dombrowski, and Fingerman, with two modifications of the PIM2 media, (i) no antifoam was added and (ii) the YNB did not contain amino acids and $(NH_4)_2SO_4$ (292). Instead, 37.8 mM $(NH_4)_2SO_4$ were added to PIM2. After successful enrichment and isolation of yeast-like colonies, all isolates were microscopically inspected for yeast morphology. Positive samples were cultured on YPD plates for 2 days at 30^{o}C and DNA extracted using the CTAB-method (108).

Molecular species identification. Two approaches were taken to identify *S. cerevisiae* and distinguish it from *S. paradoxus*. In a primary screen, species-specific PCR primers for multiplex PCR were designed. Primers amplify parts of *PSA1* and *CHS1* from *S. cerevisiae* and *S. paradoxus* and produce differently large amplicons (Table C.1). The *PSA1* forward primers are species-specific because the 3' position is designed to fit only one or the other species. The *PSA1* reverse primers anneal to different position in the gene and generate differently sized amplicons. The *CHS1* primer pair amplifies DNA in a species-specific fashion because the primers anneal to unique regions in the coding regions of each species, generating amplicons of different size (Table C.1). Multiplex PCR was conducted by mixing 0.6 μM of each of the species-specific primers for one gene with the TaKaRa Ex Taq kit. The PCR routine consisted of 5 minutes denaturing at 95^{o}C, 35 cycles of 30 seconds at 95^{o}C, 30 seconds at 53^{o}C, 45 seconds at 72^{o}C, followed by a 10 minutes extension at 72^{o}C. The amplicons were separated in a 1.5% (w/v) agarose gel. To verify PCR results the ITS was amplified and sequenced for each sample collected at OS and SM using the previously described primers and protocol (Chapter 2). Each site was analyzed for how many soil specimens gave rise to yeast isolates, species composition, association of *S. cerevisiae* with a particular tree species sampled, and species richness and composition for each tree from the SM site (Figure C.1).

Table C.1: Species-specific primers that differentially amplify parts of *PSA1* and *CHS1* *S. cerevisiae* (SC) and *S. paradoxus* (SP) from soil samples.

Locus	Primer	Position	Primer sequence (3' → 5')	Fragment length (bp)
PSA1				
	PSA1-SCF	310-330	ATTTTTCGTCCTAAACTCCGAC	
	PSA1-SCR	888-907	AGGAGTGGTTCTTGATGGTG	597
	PSA1-SPF	309-330	CATTTTTCGTCTTGAACTCAGAT	
	PSA1-SPR	648-666	TTGACCAACGTCCATCCAA	357
CHS1				
	CHS1-SCF	51-72	GAATGAACCTTCCTATGAACTC	
	CHS1-SCR	551-570	CATAACCATCGCTACTAGAAG	519
	CHS1-SPF	69-90	GCTACAAAATTCCCATAGTGGA	
	CHS1-SPR	675-695	CTTTTCGCCTGTAAGCCATGA	626

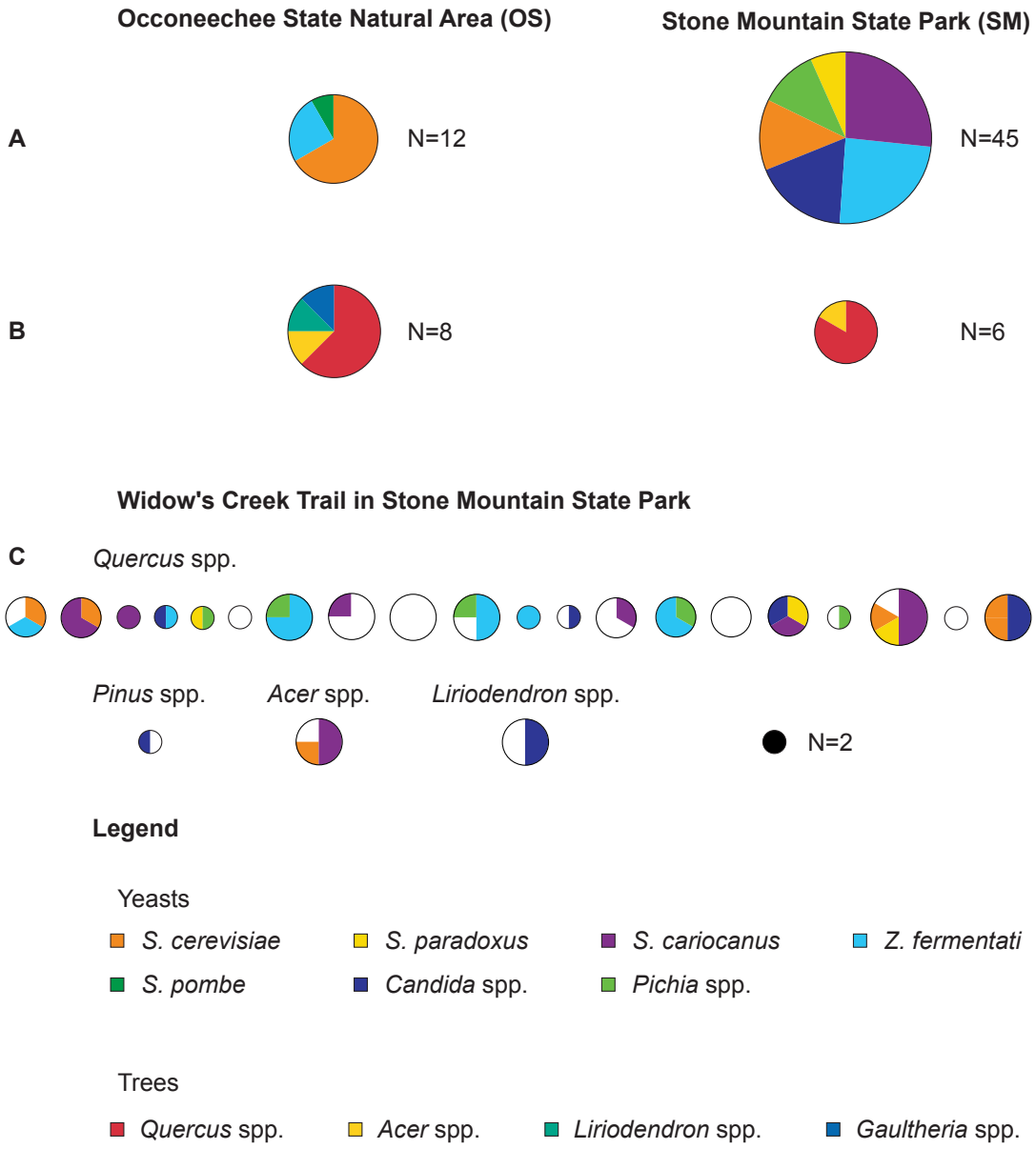

FIGURE C.1: (A) Species composition at OS and SM sites. Pie charts represent sampling success at OS and SM. The size of the pie charts indicates the number of samples, each piece of the pie chart represents a subset of data. (B) Species that were identified by ITS sequence identity in either place. (C) *S. cerevisiae* is preferentially associated with *Quercus* spp. tree.

Appendix D

Fertility Parameters of *S. cerevisiae* Strains Used in Chapter 2

In order for a *S. cerevisiae* strain to be amenable for genetic analyses it must sporulate sufficiently and give rise to viable spores. Since sporulation conditions can vary between strains, combinations of two different media, as liquid and solid preparations, and two temperatures were tested to determine which conditions promote sporulation. Spore viability was assessed as the percentage of colonies that grew from ten to twelve tetrads dissected for each strain. Up to four segregants per strain were subsequently tested for sporulation to identify homothallic and heterothallic strains. In addition to sporulation parameters, the mating type configuration was determined for each strain using allele-specific PCR primers (B. Nicholson, pers. comm.).

Sporulation frequency among 103 strains varied widely. As expected the *S. boulardii* isolates were sporulation negative and so were three brewery and one fruit isolate. Spore viability was zero in four brewery and one fruit isolate. All soil isolates and strains from North Carolinian vineyards are homothallic. In all other groups homothallic and heterothallic strains were found. All, but one clinical isolate, are

MATa/α. The clinical strain YJM308 is MATα, sporulated with low frequency and yielded spores with very low viability. Table D.1 summarizes sporulation conditions, frequency and spore viability for each strain.

Sporulation media. S. cerevisiae strains were tested for sporulation in liquid 0.5% (w/v) potassium acetate (KAc), on diet KAc plates (2% (w/v) KAc, 2% (w/v) agar) and on regular KAc plates (0.22% (w/v) yeast extract, 0.05% (w/v) dextrose, 2% (w/v) KAc, 2% (w/v) agar). Plates were incubated at 25^{o}C or 30^{o}C and liquid KAc at 30^{o}C (59) for up to seven days. Sporulation frequency was determined microscopically and rated +, ++, and +++. With + reflecting lowest sporulation efficiency and +++ highest.

Mating type PCR. Mating type PCR was carried using the TaKaRa Ex Taq kit with 0.6 μM of each primer in 25 μl total volume. Primers BN269 (GCACG-GAATATGGGACTACTTCG) BN270 (ACTCCACTTCAAGTAAGAGTTTG) are allele-specific forward primers, annealing to the MAT locus and the silent cassettes and BN271 (AGTCACATCAAGATCGTTTATGG) is a general reverse primer that anneals specifically to the MAT locus. The PCR regime encompassed 10 minutes of denaturation at 95^{o}C, 35 cycles of 20 seconds at 92^{o}C, 30 seconds at 53^{o}C, and 2 minutes 30 seconds at 72^{o}C, followed by final extension for 6 minutes at 72^{o}C. PCR products differed in length (MATa=492bp, MATα=369) and were electrophoretically separated in 1.2% (w/v) agarose.

Table D.1: Fertility parameters and mating type configuration of *Saccharomyces cerivisiae* isolates used in Chapter 2 and sporulation in their segregants.

Origin	Strain ID	Sporulation condition	Sporulation frequency	Spore viability (%)	Spore analysis A	B	C	D	MAT
Clinic									
	MMRL124	plate, 30^{o}C	++	70	HET[1]	HET			a/α
	MMRL125	liquid, 30^{o}C	+++	97	HO[2]	HET	HO	HET	a/α
	MMRL1620	plate*[3], 30^{o}C	++	100	HET				a/α
	MMRL2497	plate*, 30^{o}C	+	15	HET	HET			a/α
	YJM273	liquid, 30^{o}C	++	85	HO	HET	HET	HET	a/α
	YJM308	plate*, 30^{o}C	+	20	HET				α
	YJM309	liquid, 30^{o}C	+	22	HO	HO			a/α
	YJM310	liquid, 30^{o}C	+	87	HO	HO	HO	HO	a/α
	YJM311	liquid, 30^{o}C	+	27	HO	HO	HO		a/α
	YJM419	plate*, 30^{o}C	+	87	HET	HET	HET	HET	a/α
	YJM434	plate*, 30^{o}C	+	50	HO	HO			a/α
	YJM436	liquid, 30^{o}C	+	10		HO			a/α
	YJM440	liquid, 30^{o}C	+	95	HET	HET	HET	HET	a/α
	YJM454	liquid, 30^{o}C	+	80	HO	HET	HET	HET	a/α
Brewery									
	WY2124	negative							a/α
	WY3787	plate, 25^{o}C	+++	22	HO	HET			a/α
	WY 1026	plate, 25^{o}C	++	2					a/α
	WLP838	negative							a/α
	WLP029	negative							a/α
	WY3347	plate, 25^{o}C	+++	100	HO	HO	HO	HO	a/α
	WY1388	plate*, 30^{o}C	+	50	HET	HET	HET		a/α

Continued on next page

[1] Heterothallic-this spore does not sporulate

[2] Homothallic-this spore sporulates

[3] Asterisk indicates regular KAc plates

Origin	Strain ID	Sporulation condition	Sporulation frequency	Spore viability (%)	Spore analysis A	B	C	D	MAT
	WLP033	plate*, 25^{o}C	+	0					a/α
	WLP775	plate, 25^{o}C	+++	50	HO	HO			a/α
	WLP036	plate, 25^{o}C	+++	72	HET	HO	HET		a/α
	WLP570	plate, 25^{o}C	+	50	HET	HET			a/α
	WLP007	plate, 25^{o}C	+	10					a/α
	WLP099	plate, 25^{o}C	+	37	HET	HO			a/α
	WY3632	plate, 25^{o}C	+++	30	HET	HET			a/α
	WLP656	plate, 25^{o}C	+++	100	HO	HO	HO	HO	a/α
	WY3184	plate*, 25^{o}C	++	0					a/α
Fruit									
	NRRL Y-35	plate*, 30^{o}C	+	91	HET	HET	HET	HET	a/α
	NRRL Y-963	plate, 25^{o}C	+++	97	HO	HO	HO	HO	a/α
	NRRL Y-382	plate, 25^{o}C	+	31	ND				a/α
	NRRL Y-1537	plate, 25^{o}C	++	80	HO	HO	HO	HET	a/α
	NRRL Y-7568	plate, 25^{o}C	+++	100	HO	HO	HO	HO	a/α
	NRRL YB-210	plate, 25^{o}C	+++	10	ND				a/α
	NRRL YB-4081	plate, 25^{o}C	+++	100	HO	HO	HO	HO	a/α
	NRRL YB-4082	plate, 25^{o}C	++	100	HET	HET	HET	HET	a/α
	NRRL YB-432	plate, 25^{o}C	+++	2	HET				a/α
	NRRL YB-908	plate, 25^{o}C	+++	93	HO	HO	HO	HO	a/α
	NRRL Y-5511	plate, 25^{o}C	+	80	HET	HO	HO	HET	a/α
	NRRL Y-5997	plate, 25^{o}C	+	58	HET	HO	HET	HET	a/α
	NRRL Y-7662	negative							a/α
	NRRL Y-11857	plate, 25^{o}C	+	74	HET	HET	HO	HET	a/α
	NRRL Y-11878	plate, 25^{o}C	++	71	HO	HO	HO	HO	a/α
	NRRL Y-12769	plate, 25^{o}C	++	48	HET	HET			a/α
PA Soil									
	YP128	(292)	+++	98	HO	HO	HO	HO	a/α
	YP129	(292)	+++	77	HO	HO	HO	HO	a/α
	YP133	(292)	+++	64	HO	HO	HO	HO	a/α

Continued on next page

Origin	Strain ID	Sporulation condition	Sporulation frequency	Spore viability (%)	Spore analysis A	B	C	D	MAT
	YP134	(292)	+++	77	HO	HO	HO	HO	a/α
	YP139	(292)	+++	91	HO	HO	HO	HO	a/α
	YP141	(292)	+++	89	HO	HO	HO	HO	a/α
	YP142	(292)	+++	84	HO	HO	HO	HO	ND
	YP143	(292)	+++	98	HO	HO	HO	HO	a/α
	YP154	(292)	+++	44	HO	HO	HO	HO	a/α
	YP163	(292)	+++	98	HO	HO	HO	HO	ND
NC Soil									
	O1	liquid, 30^{o}C	+++	100	HO	HO	HO	HO	a/α
	O2	liquid, 30^{o}C	+++	90	HO	HO	HO	HO	a/α
	O3	liquid, 30^{o}C	+++	100	HO	HO	HO	HO	a/α
	O4	liquid, 30^{o}C	+++	100	HO	HO	HO	HO	a/α
	O6	liquid, 30^{o}C	+++	90	HO	HO	HO	HO	a/α
	O7	liquid, 30^{o}C	+++	95	HO	HO	HO	HO	a/α
	O8	liquid, 30^{o}C	+++	100	HO	HO	HO	HO	a/α
	O9	liquid, 30^{o}C	+++	90	HO	HO	HO	HO	a/α
	SM1	liquid, 30^{o}C	+++	90	HO	HO	HO	HO	a/α
	SM2	liquid, 30^{o}C	+++	90	HO	HO	HO	HO	a/α
	SM12	liquid, 30^{o}C	+++	90	HO	HO	HO	HO	a/α
	SM17	liquid, 30^{o}C	+++	90	HO	HO	HO	HO	a/α
	SM66	liquid, 30^{o}C	+++	90	HO	HO	HO	HO	a/α
	SM69	liquid, 30^{o}C	+++	90	HO	HO	HO	HO	a/α
Vineyard AU									
	ARC112a	plate, 25^{o}C	+++	96	HO	HO	HO	HO	a/α
	ARA194b	plate, 25^{o}C	++	72	HET	HET	HET	HET	a/α
	ARS216a	plate, 25^{o}C	+++	98	HO	HO	HO	HO	a/α
	ARS250b	plate, 25^{o}C	+	93	HET	HET	HET	HO	a/α
	ARS277b	plate, 25^{o}C	+++	100	HO	HO	HO	HO	a/α
	ARA297a	plate, 25^{o}C	++	50	HET	HET			a/α
	ARA299a	plate, 25^{o}C	++	100	HET	HET	HET	HET	a/α

Continued on next page

Origin	Strain ID	Sporulation condition	Sporulation frequency	Spore viability (%)	Spore analysis A	B	C	D	MAT
	ARA306a	plate, 25^{o}C	++	100	HET	HET	HET	HET	a/α
	ARA315a	plate, 25^{o}C	++	100	HO	HO	HET	HET	a/α
	ARA316a	plate, 25^{o}C	++	100	HET	HO	HET	HET	a/α
	ARC364a	plate, 25^{o}C	++	66	HO	HO	HO	HET	a/α
	ARA412a	plate, 25^{o}C	++	98	HET	HET	HO	HET	a/α
	ARA324a	plate, 25^{o}C	++	100	HET	HET	HO	HET	a/α
	ARA496a	plate, 25^{o}C	+++	94	HET	HET	HET	HET	a/α
Vineyard NC									
	ARN019a	plate, 25^{o}C	+++	40	HO	HET			a/α
	ARN020a	plate, 25^{o}C	++	75	HET	HO	HO	HET	a/α
	ARN022a	plate, 25^{o}C	++	81	HET	HO	HO	HO	a/α
	ARN056a	plate, 25^{o}C	++	100	HO	HO	HO	HO	a/α
	ARN179a	plate, 25^{o}C	+++	50	HO	HO			a/α
	ARN202b	plate, 25^{o}C	+++	100	HO	HO	HO	HO	a/α
	ARN231a	plate, 25^{o}C	+++	100	HO	HO	HO	HO	a/α
	ARN239a	plate, 25^{o}C	+++	98	HO	HO	HO	HO	a/α
	ARN244a	plate, 25^{o}C	+++	93	HO	HO	HO	HO	a/α
	ARN245a	plate, 25^{o}C	+++	91	HO	HO	HO	HO	a/α

Bibliography

[1] E. Aa, J. P. Townsend, R. I. Adams, K. M. Nielsen, and J. W. Taylor. Population structure and gene evolution in *Saccharomyces cerevisiae*. *FEMS Yeast Research*, 6(5):702–715, 2006.

[2] K. Z. Abshire and F. C. Neidhardt. Analysis of proteins synthesized by *Salmonella typhimurium* during growth within a host macrophage. *Journal of Bacteriology*, 175(12):3734–3743, 1993.

[3] P. Agapow and A. Burt. Indices of multilocus linkage disequilibrium. *Molecular Ecology Notes*, 1:101–102, 2001.

[4] B. Akache and B. Turcotte. New regulators of drug sensitivity in the family of yeast zinc cluster proteins. *Journal of Biological Chemistry*, 277(24):21254–21260, 2002.

[5] B. Akache, K. Wu, and B. Turcotte. Phenotypic analysis of genes encoding yeast zinc cluster proteins. *Nucleic Acids Research*, 29(10):2181–2190, 2001.

[6] E. Altenburg and H. J. Muller. The genetic basis of truncated wing, an inconstant and modifiable character in *Drosophila*. *Genetics*, 5:1–59, 1919.

[7] S. F. Altschul, W. Gish, W. Miller, E. W. Myers, and D. J. Lipman. Basic local alignment search tool. *Journal of Molecular Biology*, 215(3):403–410, 1990.

[8] K. Arai, K. Morishita, K. Shinmura, T. Kohno, S. R. Kim, T. Nohmi, M. Taniwaki, S. Ohwada, and J. Yokota. Cloning of a human homolog of the yeast *OGG1* gene that is involved in the repair of oxidative DNA damage. *Oncogene*, 14(23):2857–2861, 1997.

[9] H. Aref and W. V. Cruess. An investigation of the thermal death point of *Saccharomyces ellipsoideus*. *Journal of Bacteriology*, 27(5):443–452, 1934.

[10] N. Arnheim, C. Strange, and H. Erlich. Use of pooled DNA samples to detect linkage disequilibrium of polymorphic restriction fragments and human disease: studies of the HLA class II loci. *Proceedings of the National Academy of Sciences*, 82(20):6970–6974, 1985.

[11] J. N. Aucott, J. Fayen, H. Grossnicklas, A. Morrissey, M. M. Lederman, and R. A. Salata. Invasive infection with *Saccharomyces cerevisiae*: report of three cases and review. *Review of Infectious Diseases*, 12(3):406–411, 1990.

[12] A. M. Avery and S. V. Avery. *Saccharomyces cerevisiae* expresses three phospholipid hydroperoxide glutathione peroxidases. *Journal of Biological Chemistry*, 276(36):33730–33735, 2001.

[13] A. Baroja-Mazo, P. del Valle, J. Rua, S. de Cima, F. Busto, D. de Arriaga, and N. Smirnoff. Characterisation and biosynthesis of D-erythroascorbic acid in *Phycomyces blakesleeanus*. *Fungal Genetics and Biology*, 42(5):390–402, 2005.

[14] S. Bassetti, R. Frei, and W. Zimmerli. Fungemia with *Saccharomyces cerevisiae* after treatment with *Saccharomyces boulardii*. *American Journal of Medicine*, 105(1):71–72, 1998.

[15] M. Bayliak, H. Semchyshyn, and V. Lushchak. Effect of hydrogen peroxide on antioxidant enzyme activities in *Saccharomyces cerevisiae* is strain-specific. *Biochemistry (Mosc)*, 71(9):1013–1020, 2006.

[16] G. Ben-Ari, D. Zenvirth, A. Sherman, L. David, M. Klutstein, U. Lavi, J. Hillel, and G. Simchen. Four linked genes participate in controlling sporulation efficiency in budding yeast. *PLoS Genetics*, 2(11):e195, 2006.

[17] N. Benaroudj, D. H. Lee, and A. L. Goldberg. Trehalose accumulation during cellular stress protects cells and cellular proteins from damage by oxygen radicals. *Journal of Biological Chemistry*, 276(26):24261–24267, 2001.

[18] L. Bertram, C. Lange, K. Mullin, M. Parkinson, M. Hsiao, M. F. Hogan, B. M. M. Schjeide, B. Hooli, J. Divito, I. Ionita, H. Jiang, N. Laird, T. Moscarillo, K. L. Ohlsen, K. Elliott, X. Wang, D. Hu-Lince, M. Ryder, A. Murphy, S. L. Wagner, D. Blacker, K. D. Becker, and R. E. Tanzi. Genome-wide association analysis reveals putative Alzheimer's disease susceptibility loci in addition to APOE. *American Journal of Human Genetics*, 83(5):623–632, 2008.

[19] G. P. Bienert, A. L. B. Moller, K. A. Kristiansen, A. Schulz, I. M. Moller, J. K. Schjoerring, and T. P. Jahn. Specific aquaporins facilitate the diffusion of hydrogen peroxide across membranes. *Journal of Biological Chemistry*, 282(2):1183–1192, 2007.

[20] G. W. Birrell, J. A. Brown, H. I. Wu, G. Giaever, A. M. Chu, R. W. Davis, and J. M. Brown. Transcriptional response of *Saccharomyces cerevisiae* to DNA-damaging agents does not identify the genes that protect against these agents. *Proceedings of the National Academy of Sciences*, 99(13):8778–8783, 2002.

[21] P. H. Bissinger, R. Wieser, B. Hamilton, and H. Ruis. Control of *Saccharomyces cerevisiae* catalase T gene (*CTT1*) expression by nutrient supply via the RAS-cyclic AMP pathway. *Molecular and Cellular Biology*, 9(3):1309–1315, 1989.

[22] S. Bjelland and E. Seeberg. Mutagenicity, toxicity and repair of DNA base damage induced by oxidation. *Mutatation Research*, 531(1-2):37–80, 2003.

[23] W. F. Bodmer. Human genetics: the molecular challenge. *Cold Spring Harbor Symposia on Quantitative Biology*, 51 Pt 1:1–13, 1986.

[24] P. N. Borer, B. Dengler, I. Jr. Tinoco, and O. C. Uhlenbeck. Stability of ribonucleic acid double-stranded helices. *Journal of Molecular Biology*, 86(4):843–853, 1974.

[25] K. A. Borkovich, F. W. Farrelly, D. B. Finkelstein, J. Taulien, and S. Lindquist. Hsp82 is an essential protein that is required in higher concentrations for growth of cells at higher temperatures. *Molecular and Cellular Biology*, 9(9):3919–3930, 1989.

[26] H. C. Box, E. E. Budzinski, J. B. Dawidzik, J. S. Gobey, and H. G. Freund. Free radical-induced tandem base damage in DNA oligomers. *Free Radical Biology and Medicine*, 23(7):1021–1030, 1997.

[27] M. M. Bradford. A rapid and sensitive method for the quantitation of microgram quantities of protein utilizing the principle of protein-dye binding. *Analytical Biochemistry*, 72:248–254, 1976.

[28] M. R. Branco, H. S. Marinho, L. Cyrne, and F. Antunes. Decrease of H_2O_2 plasma membrane permeability during adaptation to H_2O_2 in *Saccharomyces cerevisiae*. *Journal of Biological Chemistry*, 279(8):6501–6506, 2004.

[29] M. J. Brauer, C. M. Christianson, D. A. Pai, and M. J. Dunham. Mapping novel traits by array-assisted bulk segregant analysis in *Saccharomyces cerevisiae*. *Genetics*, 173(3):1813–1816, 2006.

[30] R. B. Brem, G. Yvert, R. Clinton, and L. Kruglyak. Genetic dissection of transcriptional regulation in budding yeast. *Science*, 296(5568):752–755, 2002.

[31] K. J. Breslauer, R. Frank, H. Blocker, and L. A. Marky. Predicting DNA duplex stability from the base sequence. *Proceedings of the National Academy of Sciences*, 83(11):3746–3750, 1986.

[32] J. Bryan, K. McLean, E. Bradshaw, S. De Jong, M. Phillips, L. Castelli, and R. Waugh. Mapping QTLs for resistance to the cyst nematode *Globodera pallida* derived from the wild potato species *Solanum vernei*. *Theoretical and Applied Genetics*, 105(1):68–77, 2002.

[33] G. S. Bulmer, M. L. Marquez, L. Co-Barcelona, and R. A. Fromtling. Yeasts and fluconazole susceptibility in the Philippines. *Mycopathologia*, 146(3):117–120, 1999.

[34] D. Burke, D. Dawson, and T. Stearns. *Methods in yeast genetics: a cold spring harbor laboratory course manual*. Cold Spring Harbor Laboratory Press, 2000.

[35] E. Cabiscol, G. Belli, J. Tamarit, P. Echave, E. Herrero, and J. Ros. Mitochondrial Hsp60, resistance to oxidative stress, and the labile iron pool are closely connected in *Saccharomyces cerevisiae*. *Journal of Biological Chemistry*, 277(46):44531–44538, 2002.

[36] Z. P. Cakar, U. O. S. Seker, C. Tamerler, M. Sonderegger, and U. Sauer. Evolutionary engineering of multiple-stress resistant *Saccharomyces cerevisiae*. *FEMS Yeast Research*, 5(6-7):569–578, 2005.

[37] J. A. Calera, S. Paris, M. Monod, A. J. Hamilton, J. P. Debeaupuis, M. Diaquin, R. López-Medrano, F. Leal, and J. P. Latgé. Cloning and disruption of the antigenic catalase gene of *Aspergillus fumigatus*. *Infection and Immunity*, 65(11):4718–4724, 1997.

[38] A. Capriotti. Studies on wine yeasts in Italy with a note on must yeasts of Frankenthaler grapes cultivated in greenhouse. *Antonie Van Leeuwenhoek*, 20(4):374–384, 1954.

[39] A. Capriotti. Yeasts from U.S.A. soils. *Archiv für Mikrobiologie*, 57(4):406–413, 1967.

[40] H. C. Causton, B. Ren, S. S. Koh, C. T. Harbison, E. Kanin, E. G. Jennings, T. I. Lee, H. L. True, E. S. Lander, and R. A. Young. Remodeling of yeast genome expression in response to environmental changes. *Molecular Biology of the Cell*, 12(2):323–337, 2001.

[41] D. Cavalieri, P. E. McGovern, D. L. Hartl, R. Mortimer, and M. Polsinelli. Evidence for *S. cerevisiae* fermentation in ancient wine. *Journal of Molecular Evolution*, 57 Suppl 1:S226–32, 2003.

[42] S. Cesaro, P. Chinello, L. Rossi, and L. Zanesco. *Saccharomyces cerevisiae* fungemia in a neutropenic patient treated with *Saccharomyces boulardii*. *Support Care Cancer*, 8(6):504–505, 2000.

[43] H. Z. Chae, S. J. Chung, and S. G. Rhee. Thioredoxin-dependent peroxide reductase from yeast. *Journal of Biological Chemistry*, 269(44):27670–27678, 1994.

[44] S. Chander, Y. Q. Guo, X. H. Yang, J. Zhang, X. Q. Lu, J. B. Yan, T. M. Song, T. R. Rocheford, and J. S. Li. Using molecular markers to identify two major loci controlling carotenoid contents in maize grain. *Theoretical and Applied Genetics*, 116(2):223–233, 2008.

[45] C. Charizanis, H. Juhnke, B. Krems, and K. D. Entian. The mitochondrial cytochrome c peroxidase Ccp1 of *Saccharomyces cerevisiae* is involved in conveying an oxidative stress signal to the transcription factor Pos9 (Skn7). *Molecular and General Genetics*, 262(3):437–447, 1999.

[46] C. Charizanis, H. Juhnke, B. Krems, and K. D. Entian. The oxidative stress response mediated via Pos9/Skn7 is negatively regulated by the Ras/Pka pathway in *Saccharomyces cerevisiae*. *Molecular and General Genetics*, 261(4-5):740–752, 1999.

[47] V. Chaturvedi, B. Wong, and S. L. Newman. Oxidative killing of *Cryptococcus neoformans* by human neutrophils. Evidence that fungal mannitol protects by scavenging reactive oxygen intermediates. *Journal of Immunology*, 156(10):3836–3840, 1996.

[48] N. Chauhan and R. Calderone. Two-component signal transduction proteins as potential drug targets in medically important fungi. *Infection and Immunity*, 76(11):4795–4803, 2008.

[49] M. Chayakulkeeree and J. R. Perfect. Cryptococcosis. *Infectious Disease Clinics of North America*, 20(3):507–544, 2006.

[50] H. Chen and G. R. Fink. Feedback control of morphogenesis in fungi by aromatic alcohols. *Genes and Development*, 20(9):1150–1161, 2006.

[51] J. W. Chen, C. Dodia, S. I. Feinstein, M. K. Jain, and A. B. Fisher. 1-Cys peroxiredoxin, a bifunctional enzyme with glutathione peroxidase and phospholipase A2 activities. *Journal of Biological Chemistry*, 275(37):28421–28427, 2000.

[52] Q. Chen, J. Thorpe, Q. Ding, I. S. El-Amouri, and J. N. Keller. Proteasome synthesis and assembly are required for survival during stationary phase. *Free Radical Biology and Medicine*, 37(6):859–868, 2004.

[53] G. M. Chertow, E. R. Marcantonio, and R. G. Wells. *Saccharomyces cerevisiae* empyema in a patient with esophago-pleural fistula complicating variceal sclerotherapy. *Chest*, 99(6):1518–1519, 1991.

[54] J. K. Chia, S. M. Chan, and H. Goldstein. Baker's yeast as adjunctive therapy for relapses of *Clostridium difficile* diarrhea. *Clinical Infectious Diseases*, 20(6):1581, 1995.

[55] J. H. Choi, W. Lou, and A. Vancura. A novel membrane-bound glutathione S-transferase functions in the stationary phase of the yeast *Saccharomyces cerevisiae*. *Journal of Biological Chemistry*, 273(45):29915–29922, 1998.

[56] N. Cimolai, M. J. Gill, and D. Church. *Saccharomyces cerevisiae* fungemia: case report and review of the literature. *Diagnostic Microbiology and Infectious Disease*, 8(2):113–117, 1987.

[57] K. V. Clemons, L. C. Hanson, and D. A. Stevens. Colony phenotype switching in clinical and non-clinical isolates of *Saccharomyces cerevisiae*. *Journal of Medical and Veterinary Mycology*, 34(4):259–264, 1996.

[58] K. V. Clemons, J. H. McCusker, R. W. Davis, and D. A. Stevens. Comparative pathogenesis of clinical and nonclinical isolates of *Saccharomyces cerevisiae*. *Journal of Infectious Diseases*, 169(4):859–867, 1994.

[59] A. C. Codon, J. M. Gasent-Ramirez, and T. Benitez. Factors which affect the frequency of sporulation and tetrad formation in *Saccharomyces cerevisiae* baker's yeasts. *Applied and Environmental Microbiology*, 61(2):630–638, 1995.

[60] G. Cohen, F. Fessl, A. Traczyk, J. Rytka, and H. Ruis. Isolation of the catalase A gene of *Saccharomyces cerevisiae* by complementation of the *cta1* mutation. *Molecular and General Genetics*, 200(1):74–79, 1985.

[61] D. C. Coleman, D. J. Sullivan, D. E. Bennett, G. P. Moran, H. J. Barry, and D. B. Shanley. Candidiasis: the emergence of a novel species, *Candida dubliniensis*. *AIDS*, 11(5):557–567, 1997.

[62] E. J. Collinson, G. L. Wheeler, E. O. Garrido, A. M. Avery, S. V. Avery, and C. M. Grant. The yeast glutaredoxins are active as glutathione peroxidases. *Journal of Biological Chemistry*, 277(19):16712–16717, 2002.

[63] L. P. Collinson and I. W. Dawes. Inducibility of the response of yeast cells to peroxide stress. *Journal of General Microbiology*, 138(2):329–335, 1992.

[64] L. P. Collinson and I. W. Dawes. Isolation, characterization and overexpression of the yeast gene, *GLR1*, encoding glutathione reductase. *Gene*, 156(1):123–127, 1995.

[65] V. Costa, M. A. Amorim, E. Reis, A. Quintanilha, and P. Moradas-Ferreira. Mitochondrial superoxide dismutase is essential for ethanol tolerance of *Saccharomyces cerevisiae* in the post-diauxic phase. *Microbiology*, 143 (Pt 5):1649–1656, 1997.

[66] V. Costa and P. Moradas-Ferreira. Oxidative stress and signal transduction in *Saccharomyces cerevisiae*: insights into ageing, apoptosis and diseases. *Molecular Aspects of Medicine*, 22(4-5):217–246, 2001.

[67] V. M. V. Costa, M. A. Amorim, A. Quintanilha, and P. Moradas-Ferreira. Hydrogen peroxide-induced carbonylation of key metabolic enzymes in *Saccharomyces cerevisiae*: the involvement of the oxidative stress response regulators Yap1 and Skn7. *Free Radical Biology and Medicine*, 33(11):1507–1515, 2002.

[68] L. E. Cowen and W. J. Steinbach. Stress, drugs, and evolution: the role of cellular signaling in fungal drug resistance. *Eukaryotic Cell*, 7(5):747–764, 2008.

[69] G. M. Cox, T. S. Harrison, H. C. McDade, C. P. Taborda, G. Heinrich, A. Casadevall, and J. R. Perfect. Superoxide dismutase influences the virulence of *Cryptococcus neoformans* by affecting growth within macrophages. *Infection and Immunity*, 71(1):173–180, 2003.

[70] J. P. Crow, J. S. Beckman, and J. M. McCord. Sensitivity of the essential zinc-thiolate moiety of yeast alcohol dehydrogenase to hypochlorite and peroxynitrite. *Biochemistry*, 34(11):3544–3552, 1995.

[71] M. Cuéllar-Cruz, M. Briones-Martin-del Campo, I. Cañas Villamar, J. Montalvo-Arredondo, L. Riego-Ruiz, I. Castaño, and A. De Las Peñas. High resistance to oxidative stress in the fungal pathogen *Candida glabrata* is mediated by a single catalase, Cta1p, and is controlled by the transcription factors Yap1p, Skn7p, Msn2p, and Msn4p. *Eukaryotic Cell*, 7(5):814–825, 2008.

[72] G. Daum, P. C. Bohni, and G. Schatz. Import of proteins into mitochondria. cytochrome b2 and cytochrome-c peroxidase are located in the intermembrane space of yeast mitochondria. *Journal of Biological Chemistry*, 257(21):13028–13033, 1982.

[73] L. David, W. Huber, M. Granovskaia, J. Toedling, C. J. Palm, L. Bofkin, T. Jones, R. W. Davis, and L. M. Steinmetz. A high-resolution map of transcription in the yeast genome. *Proceedings of the National Academy of Sciences*, 103(14):5320–5325, 2006.

[74] J. M. Davies, C. V. Lowry, and K. J. Davies. Transient adaptation to oxidative stress in yeast. *Archives of Biochemistry and Biophysics*, 317(1):1–6, 1995.

[75] K. J. Davies. Protein damage and degradation by oxygen radicals. I. general aspects. *Journal of Biological Chemistry*, 262(20):9895–9901, 1987.

[76] K. J. Davies and M. E. Delsignore. Protein damage and degradation by oxygen radicals. III. modification of secondary and tertiary structure. *Journal of Biological Chemistry*, 262(20):9908–9913, 1987.

[77] K. J. Davies, M. E. Delsignore, and S. W. Lin. Protein damage and degradation by oxygen radicals. II. modification of amino acids. *Journal of Biological Chemistry*, 262(20):9902–9907, 1987.

[78] N. P. Degtyareva, L. Chen, P. Mieczkowski, T. D. Petes, and P. W. Doetsch. Chronic oxidative DNA damage due to DNA repair defects causes chromosomal instability in *Saccharomyces cerevisiae*. *Molecular and Cellular Biology*, 28(17):5432–5445, 2008.

[79] A. Delaunay, A. D. Isnard, and M. B. Toledano. H_2O_2 sensing through oxidation of the Yap1 transcription factor. *EMBO Journal*, 19(19):5157–5166, 2000.

[80] A. Delaunay, D. Pflieger, M. B. Barrault, J. Vinh, and M. B. Toledano. A thiol peroxidase is an H_2O_2 receptor and redox-transducer in gene activation. *Cell*, 111(4):471–481, 2002.

[81] A. Demogines, E. Smith, L. Kruglyak, and E. Alani. Identification and dissection of a complex DNA repair sensitivity phenotype in Baker's yeast. *PLoS Genetics*, 4(7):e1000123, 2008.

[82] A. M. Deutschbauer and R. W. Davis. Quantitative trait loci mapped to single-nucleotide resolution in yeast. *Nature Genetics*, 37(12):1333–1340, 2005.

[83] S. Diezmann, C. J. Cox, G. Schönian, R. J. Vilgalys, and T. G. Mitchell. Phylogeny and evolution of medical species of *Candida* and related taxa: a multigenic analysis. *Journal of Clinical Microbiology*, 42(12):5624–5635, 2004.

[84] S. W. Doniger, H. S. Kim, D. Swain, D. Corcuera, M. Williams, S.-P. Yang, and J. C. Fay. A catalog of neutral and deleterious polymorphism in yeast. *PLoS Genetics*, 4(8):e1000183, 2008.

[85] N. A. Doudican, B. Song, G. S. Shadel, and P. W. Doetsch. Oxidative DNA damage causes mitochondrial genomic instability in *Saccharomyces cerevisiae*. *Molecular and Cellular Biology*, 25(12):5196–5204, 2005.

[86] T. Douki, T. Delatour, F. Paganon, and J. Cadet. Measurement of oxidative damage at pyrimidine bases in gamma-irradiated DNA. *Chemical Research in Toxicology*, 9(7):1145–1151, 1996.

[87] G. Dover. Molecular drive: a cohesive mode of species evolution. *Nature*, 299(5879):111–117, 1982.

[88] T. Draculic, I. W. Dawes, and C. M. Grant. A single glutaredoxin or thioredoxin gene is essential for viability in the yeast *Saccharomyces cerevisiae*. *Molecular Microbiology*, 36(5):1167–1174, 2000.

[89] V. A. Dumbrava and M. L. Pall. Control of nucleotide and erythroascorbic acid pools by cyclic AMP in *Neurospora crassa*. *Biochimica et Biophysica Acta*, 926(3):331–338, 1987.

[90] D. F. Easton, K. A. Pooley, A. M. Dunning, P. D. P. Pharoah, D. Thompson, D. G. Ballinger, J. P. Struewing, J. Morrison, H. Field, R. Luben, N. Wareham, S. Ahmed, C. S. Healey, R. Bowman, K. B. Meyer, C. A. Haiman, L. K. Kolonel, B. E. Henderson, L. Le Marchand, P. Brennan, S. Sangrajrang, V. Gaborieau, F. Odefrey, C.-Y. Shen, P.-E. Wu, H.-C. Wang, D. Eccles, D. G. Evans, J. Peto, O. Fletcher, N. Johnson, S. Seal, M. R. Stratton, N. Rahman, G. Chenevix-Trench, S. E. Bojesen, B. G. Nordestgaard, C. K. Axelsson, M. Garcia-Closas, L. Brinton, S. Chanock, J. Lissowska, B. Peplonska, H. Nevanlinna, R. Fagerholm, H. Eerola, D. Kang, K.-Y. Yoo, D.-Y. Noh, S.-H. Ahn, D. J. Hunter, S. E. Hankinson, D. G. Cox, P. Hall, S. Wedren, J. Liu, Y.-L. Low, N. Bogdanova, P. Schurmann, T. Dork, R. A. E. M. Tollenaar, C. E. Jacobi, P. Devilee, J. G. M. Klijn, A. J. Sigurdson, M. M. Doody, B. H. Alexander, J. Zhang, A. Cox, I. W. Brock, G. MacPherson, M. W. R. Reed, F. J. Couch, E. L. Goode, J. E. Olson, H. Meijers-Heijboer, A. van den Ouweland, A. Uitterlinden, F. Rivadeneira, R. L. Milne, G. Ribas, A. Gonzalez-Neira, J. Benitez, J. L. Hopper, M. McCredie, M. Southey, G. G. Giles, C. Schroen, C. Justenhoven, H. Brauch, U. Hamann, Y.-D. Ko, A. B. Spurdle, J. Beesley, X. Chen, A. Mannermaa, V.-M. Kosma, V. Kataja, J. Hartikainen, N. E. Day, D. R. Cox, and B. A. J. Ponder. Genome-wide association study identifies novel breast cancer susceptibility loci. *Nature*, 447(7148):1087–1093, 2007.

[91] A. Enache-Angoulvant and C. Hennequin. Invasive *Saccharomyces* infection: a comprehensive review. *Clinical Infectious Diseases*, 41(11):1559–1568, 2005.

[92] B. Enjalbert, A. Nantel, and M. Whiteway. Stress-induced gene expression in *Candida albicans*: absence of a general stress response. *Molecular Biology of the Cell*, 14(4):1460–1467, 2003.

[93] F. Estruch and M. Carlson. Two homologous zinc finger genes identified by

multicopy suppression in a *SNF1* protein kinase mutant of *Saccharomyces cerevisiae*. *Molecular and Cellular Biology*, 13(7):3872–3881, 1993.

[94] B. A. Evert, T. B. Salmon, B. Song, L. Jingjing, W. Siede, and P. W. Doetsch. Spontaneous DNA damage in *Saccharomyces cerevisiae* elicits phenotypic properties similar to cancer cells. *Journal of Biological Chemistry*, 279(21):22585–22594, 2004.

[95] R. C. Fahey, G. L. Newton, B. Arrick, T. Overdank-Bogart, and S. B. Aley. *Entamoeba histolytica*: a eukaryote without glutathione metabolism. *Science*, 224(4644):70–72, 1984.

[96] M. E. Farah and D. C. Amberg. Conserved actin cysteine residues are oxidative stress sensors that can regulate cell death in yeast. *Molecular Biology of the Cell*, 18(4):1359–1365, 2007.

[97] J. C. Fay and J. A. Benavides. Evidence for domesticated and wild populations of *Saccharomyces cerevisiae*. *PLoS Genetics*, 1(1):66–71, 2005.

[98] J. Felsenstein. Phylip - phylogeny inference package. *Cladistics*, 5:164–166, 1989.

[99] J. A. Flattery-O'Brien and I. W. Dawes. Hydrogen peroxide causes *RAD9*-dependent cell cycle arrest in G2 in *Saccharomyces cerevisiae* whereas menadione causes G1 arrest independent of *RAD9* function. *Journal of Biological Chemistry*, 273(15):8564–8571, 1998.

[100] C. Fleury, M. Pampin, A. Tarze, and B. Mignotte. Yeast as a model to study apoptosis? *Bioscience Reports*, 22(1):59–79, 2002.

[101] D. H. Flint, J. F. Tuminello, and M. H. Emptage. The inactivation of Fe-S cluster containing hydro-lyases by superoxide. *Journal of Biological Chemistry*, 268(30):22369–22376, 1993.

[102] T. R. Flower, L. S. Chesnokova, C. A. Froelich, C. Dixon, and S. N. Witt. Heat shock prevents alpha-synuclein-induced apoptosis in a yeast model of Parkinson's disease. *Journal of Molecular Biology*, 351(5):1081–1100, 2005.

[103] M. R. Foolad, P. Subbiah, and L. Zhang. Common QTL affect the rate of tomato seed germination under different stress and nonstress conditions. *International Journal of Plant Genomics*, 2007:97386, 2007.

[104] A. Forche, K. Alby, D. Schaefer, A. D. Johnson, J. Berman, and R. J. Bennett. The parasexual cycle in *Candida albicans* provides an alternative pathway to meiosis for the formation of recombinant strains. *PLoS Biology*, 6(5):e110, 2008.

[105] D. Fradin, S. Heath, J. Lepercq, M. Lathrop, and P. Bougneres. Identification of distinct quantitative trait loci affecting length or weight variability at birth in humans. *Journal of Clinical Endocrinology & Metabolism*, 91(10):4164–4170, 2006.

[106] A. Frary, T. C. Nesbitt, S. Grandillo, E. Knaap, B. Cong, J. Liu, J. Meller, R. Elber, K. B. Alpert, and S. D. Tanksley. fw2.2: a quantitative trait locus key to the evolution of tomato fruit size. *Science*, 289(5476):85–88, 2000.

[107] A. R. D. Ganley and T. Kobayashi. Highly efficient concerted evolution in the ribosomal DNA repeats: total rDNA repeat variation revealed by whole-genome shotgun sequence data. *Genome Research*, 17(2):184–191, 2007.

[108] M. Gardes and T. D. Bruns. ITS primers with enhanced specificity for basidiomycetes–application to the identification of mycorrhizae and rusts. *Molecular Ecology*, 2(2):113–118, 1993.

[109] H. W. Gardner. Oxygen radical chemistry of polyunsaturated fatty acids. *Free Radical Biology and Medicine*, 7:65–86, 1989.

[110] E. O. Garrido and C. M. Grant. Role of thioredoxins in the response of *Saccharomyces cerevisiae* to oxidative stress induced by hydroperoxides. *Molecular Microbiology*, 43(4):993–1003, 2002.

[111] S. Garza, J. A. Teixido, V. Sanchis, I. Vinas, and S. Condon. Heat resistance of *Saccharomyces cerevisiae* strains isolated from spoiled peach puree. *International Journal of Food Microbiology*, 23(2):209–213, 1994.

[112] A. P. Gasch, P. T. Spellman, C. M. Kao, O. Carmel-Harel, M. B. Eisen, G. Storz, D. Botstein, and P. O. Brown. Genomic expression programs in

the response of yeast cells to environmental changes. *Molecular Biology of the Cell*, 11(12):4241–4257, 2000.

[113] H. Geldermann. Investigations on inheritance of quantitative characters in animals by gene marker. I. methods. *Theoretical and Applied Genetics*, 46:319–330, 1975.

[114] L. Gellon, R. Barbey, P. Auffret van der Kemp, D. Thomas, and S. Boiteux. Synergism between base excision repair, mediated by the DNA glycosylases Ntg1 and Ntg2, and nucleotide excision repair in the removal of oxidatively damaged DNA bases in *Saccharomyces cerevisiae*. *Molecular Genetics and Genomics*, 265(6):1087–1096, 2001.

[115] M. Georges, D. Nielsen, M. Mackinnon, A. Mishra, R. Okimoto, A. T. Pasquino, L. S. Sargeant, A. Sorensen, M. R. Steele, and X. Zhao. Mapping quantitative trait loci controlling milk production in dairy cattle by exploiting progeny testing. *Genetics*, 139(2):907–920, 1995.

[116] M. A. Ghannoum. Potential role of phospholipases in virulence and fungal pathogenesis. *Clinical Microbiology Reviews*, 13(1):122–143, 2000.

[117] R. D. Gietz and R. H. Schiestl. Applications of high efficiency lithium acetate transformation of intact yeast cells using single-stranded nucleic acids as carrier. *Yeast*, 7(3):253–263, 1991.

[118] S. S. Giles, J. R. Perfect, and G. M. Cox. Cytochrome-c peroxidase contributes to the antioxidant defense of *Cryptococcus neoformans*. *Fungal Genetics and Biology*, 42(1):20–29, 2005.

[119] S. S. Giles, J. E. Stajich, C. Nichols, Q. D. Gerrald, J. A. Alspaugh, F. Dietrich, and J. R. Perfect. The *Cryptococcus neoformans* catalase gene family and its role in antioxidant defense. *Eukaryot Cell*, 5(9):1447–1459, 2006.

[120] C. J. Gimeno, P. O. Ljungdahl, C. A. Styles, and G. R. Fink. Unipolar cell divisions in the yeast *S. cerevisiae* lead to filamentous growth: regulation by starvation and RAS. *Cell*, 68(6):1077–1090, 1992.

[121] M. R. Goddard and A. Burt. Recurrent invasion and extinction of a selfish gene. *Proceedings of the National Academy of Sciences*, 96(24):13880–13885, 1999.

[122] C. Godon, G. Lagniel, J. Lee, J. M. Buhler, S. Kieffer, M. Perrot, H. Boucherie, M. B. Toledano, and J. Labarre. The H_2O_2 stimulon in *Saccharomyces cerevisiae*. *Journal of Biological Chemistry*, 273(35):22480–22489, 1998.

[123] A. Goffeau, B. G. Barrell, H. Bussey, R. W. Davis, B. Dujon, H. Feldmann, F. Galibert, J. D. Hoheisel, C. Jacq, M. Johnston, E. J. Louis, H. W. Mewes, Y. Murakami, P. Philippsen, H. Tettelin, and S. G. Oliver. Life with 6000 genes. *Science*, 274(5287):546, 563–7, 1996.

[124] D. Goldblatt and A. J. Thrasher. Chronic granulomatous disease. *Clinical and Experimental Immunology*, 122(1):1–9, 2000.

[125] A. L. Goldstein and J. H. McCusker. Three new dominant drug resistance cassettes for gene disruption in *Saccharomyces cerevisiae*. *Yeast*, 15(14):1541–1553, 1999.

[126] S. Goltz, J. Kaput, and G. Blobel. Isolation of the yeast nuclear gene encoding the mitochondrial protein, cytochrome-c peroxidase. *Journal of Biological Chemistry*, 257(18):11186–11190, 1982.

[127] P. González-Parraga, J. A. Hernández, and J. C. Arguelles. Role of antioxidant enzymatic defences against oxidative stress H_2O_2 and the acquisition of oxidative tolerance in *Candida albicans*. *Yeast*, 20(14):1161–1169, 2003.

[128] W. Görner, E. Durchschlag, M. T. Martinez-Pastor, F. Estruch, G. Ammerer, B. Hamilton, H. Ruis, and C. Schüller. Nuclear localization of the C_2H_2 zinc finger protein Msn2p is regulated by stress and protein kinase A activity. *Genes and Development*, 12(4):586–597, 1998.

[129] C. M. Grant. Role of the glutathione/glutaredoxin and thioredoxin systems in yeast growth and response to stress conditions. *Molecular Microbiology*, 39(3):533–541, 2001.

[130] C. M. Grant, L. P. Collinson, J. H. Roe, and I. W. Dawes. Yeast glutathione reductase is required for protection against oxidative stress and is a target gene for yAP-1 transcriptional regulation. *Molecular Microbiology*, 21(1):171–179, 1996.

[131] C. M. Grant and I. W. Dawes. Synthesis and role of glutathione in protection against oxidative stress in yeast. *Redox Report*, 2:223–229, 1996.

[132] C. M. Grant, F. H. MacIver, and I. W. Dawes. Glutathione is an essential metabolite required for resistance to oxidative stress in the yeast *Saccharomyces cerevisiae*. *Current Genetics*, 29(6):511–515, 1996.

[133] C. M. Grant, F. H. MacIver, and I. W. Dawes. Glutathione synthetase is dispensable for growth under both normal and oxidative stress conditions in the yeast *Saccharomyces cerevisiae* due to an accumulation of the dipeptide gamma-glutamylcysteine. *Molecular Biology of the Cell*, 8(9):1699–1707, 1997.

[134] C. M. Grant, G. Perrone, and I. W. Dawes. Glutathione and catalase provide overlapping defenses for protection against hydrogen peroxide in the yeast *Saccharomyces cerevisiae*. *Biochemical and Biophysical Research Communications*, 253(3):893–898, 1998.

[135] S. W. Griffiths and C. L. Cooney. Relationship between protein structure and methionine oxidation in recombinant human alpha 1-antitrypsin. *Biochemistry*, 41(20):6245–6252, 2002.

[136] J. M. Gutteridge. The role of superoxide and hydroxyl radicals in phospholipid peroxidation catalysed by iron salts. *FEBS Letters*, 150(2):454–458, 1982.

[137] B. Halliwell and J. M. C. Gutteridge. *Free radicals in biology and medicine*. Oxford University Press, 2007.

[138] A. J. Hamilton and M. D. Holdom. Antioxidant systems in the pathogenic fungi of man and their role in virulence. *Medical Mycology*, 37(6):375–389, 1999.

[139] D. Harman. Role of free radicals in mutation, cancer, aging, and the maintenance of life. *Radiation Research*, 16:753–763, 1962.

[140] K. D. Harshman, W. S. Moye-Rowley, and C. S. Parker. Transcriptional activation by the SV40 AP-1 recognition element in yeast is mediated by a factor similar to AP-1 that is distinct from *GCN4*. *Cell*, 53(2):321–330, 1988.

[141] R. Hasan, C. Leroy, A. D. Isnard, J. Labarre, E. Boy-Marcotte, and M. B Toledano. The control of the yeast H_2O_2 response by the Msn2/4 transcription factors. *Molecular Microbiology*, 45(1):233–241, 2002.

[142] K. C. Hazen. New and emerging yeast pathogens. *Clinical Microbiology Reviews*, 8(4):462–478, 1995.

[143] R. S. Herdeiro, M. D. Pereira, A. D. Panek, and E. C. A. Eleutherio. Trehalose protects *Saccharomyces cerevisiae* from lipid peroxidation during oxidative stress. *Biochimica et Biophysica Acta*, 1760(3):340–346, 2006.

[144] E. Herrero, J. Ros, J. Tamarit, and G. Belli. Glutaredoxins in fungi. *Photosynthesis Research*, 89(2-3):127–140, 2006.

[145] V. J. Higgins, N. Alic, G. W. Thorpe, M. Breitenbach, V. Larsson, and I. W. Dawes. Phenotypic analysis of gene deletant strains for sensitivity to oxidative stress. *Yeast*, 19(3):203–214, 2002.

[146] J. A. Hoch. Two-component and phosphorelay signal transduction. *Current Opinion in Microbiology*, 3(2):165–170, 2000.

[147] C. S. Hoffman and F. Winston. A ten-minute DNA preparation from yeast efficiently releases autonomous plasmids for transformation of *Escherichia coli*. *Gene*, 57(2-3):267–272, 1987.

[148] H. P. Hoffmann, A. Szabo, and C. J. Avers. Cytochemical localization of catalase activity in yeast peroxisomes. *Journal of Bacteriology*, 104(1):581–584, 1970.

[149] H. Hortner, G. Ammerer, E. Hartter, B. Hamilton, J. Rytka, T. Bilinski, and H. Ruis. Regulation of synthesis of catalases and iso-1-cytochrome c in *Saccharomyces cerevisiae* by glucose, oxygen and heme. *European Journal of Biochemistry*, 128(1):179–184, 1982.

[150] R. S. Houlston, E. Webb, P. Broderick, A. M. Pittman, M. C. Di Bernardo, S. Lubbe, I. Chandler, J. Vijayakrishnan, K. Sullivan, S. Penegar, L. Carvajal-Carmona, K. Howarth, E. Jaeger, S. L. Spain, A. Walther, E. Barclay, L. Martin, M. Gorman, E. Domingo, A. S. Teixeira, D. Kerr, J.-B. Cazier, I. Niittymaki, S. Tuupanen, A. Karhu, L. A. Aaltonen, I. P. M. Tomlinson, S. M. Farrington, A. Tenesa, J. G. D. Prendergast, R. A. Barnetson, R. Cetnarskyj, M. E. Porteous, P. D. P. Pharoah, T. Koessler, J. Hampe, S. Buch, C. Schafmayer, J. Tepel, S. Schreiber, H. Volzke, J. Chang-Claude, M. Hoffmeister, H. Brenner, B. W. Zanke, A. Montpetit, T. J. Hudson, S. Gallinger, H. Campbell, and M. G. Dunlop. Meta-analysis of genome-wide association data

identifies four new susceptibility loci for colorectal cancer. *Nature Genetics*, 40(12):1426–1435, 2008.

[151] X. H. Hu, M. H. Wang, T. Tan, J. R. Li, H. Yang, L. Leach, R. M. Zhang, and Z. W. Luo. Genetic dissection of ethanol tolerance in the budding yeast *Saccharomyces cerevisiae*. *Genetics*, 175(3):1479–1487, 2007.

[152] H. L. Huang and M. C. Brandriss. The regulator of the yeast proline utilization pathway is differentially phosphorylated in response to the quality of the nitrogen source. *Molecular and Cellular Biology*, 20(3):892–899, 2000.

[153] W. Huh, J. V. Falvo, L. C. Gerke, A. S. Carroll, R. W. Howson, J. S. Weissman, and E. K. O'Shea. Global analysis of protein localization in budding yeast. *Nature*, 425(6959):686–691, 2003.

[154] W. K. Huh, S. T. Kim, H. Kim, G. Jeong, and S. O. Kang. Deficiency of D-erythroascorbic acid attenuates hyphal growth and virulence of *Candida albicans*. *Infection and Immunity*, 69(6):3939–3946, 2001.

[155] W. K. Huh, S. T. Kim, K. S. Yang, Y. J. Seok, Y. C. Hah, and S. O. Kang. Characterisation of D-arabinono-1,4-lactone oxidase from *Candida albicans* ATCC 10231. *European Journal of Biochemistry*, 225(3):1073–1079, 1994.

[156] W. K. Huh, B. H. Lee, S. T. Kim, Y. R. Kim, G. E. Rhie, Y. W. Baek, C. S. Hwang, J. S. Lee, and S. O. Kang. D-Erythroascorbic acid is an important antioxidant molecule in *Saccharomyces cerevisiae*. *Molecular Microbiology*, 30(4):895–903, 1998.

[157] Y. Inoue, T. Matsuda, K. Sugiyama, S. Izawa, and A. Kimura. Genetic analysis of glutathione peroxidase in oxidative stress response of *Saccharomyces cerevisiae*. *Journal of Biological Chemistry*, 274(38):27002–27009, 1999.

[158] S. Ito-Harashima and J. H. McCusker. Positive and negative selection LYS5MX gene replacement cassettes for use in *Saccharomyces cerevisiae*. *Yeast*, 21(1):53–61, 2004.

[159] G. Y. N. Iyer, M. F. Islam, and J. H. Quastel. Biochemical aspects of phagocytosis. *Nature*, 192:535–541, 1961.

[160] S. Izawa, Y. Inoue, and A. Kimura. Importance of catalase in the adaptive response to hydrogen peroxide: analysis of acatalasaemic *Saccharomyces cerevisiae*. *Biochemical Journal*, 320 (Pt 1):61–67, 1996.

[161] S. Izawa, K. Maeda, T. Miki, J. Mano, Y. Inoue, and A. Kimura. Importance of glucose-6-phosphate dehydrogenase in the adaptive response to hydrogen peroxide in *Saccharomyces cerevisiae*. *Biochemical Journal*, 330 (Pt 2):811–817, 1998.

[162] T. Y. James, F. Kauff, C. L. Schoch, P. B. Matheny, V. Hofstetter, C. J. Cox, G. Celio, C. Gueidan, E. Fraker, J. Miadlikowska, H. T. Lumbsch, A. Rauhut, V. Reeb, A. E. Arnold, A. Amtoft, J. E. Stajich, K. Hosaka, G. Sung, D. Johnson, B. O'Rourke, M. Crockett, M. Binder, J. M. Curtis, J. C. Slot, Z. Wang, A. W. Wilson, A. Schussler, J. E. Longcore, K. O'Donnell, S. Mozley-Standridge, D. Porter, P. M. Letcher, M. J. Powell, J. W. Taylor, M. M. White, G. W. Griffith, D. R. Davies, R. A. Humber, J. B. Morton, J. Sugiyama, A. Y. Rossman, J. D. Rogers, D. H. Pfister, D. Hewitt, K. Hansen, S. Hambleton, R. A. Shoemaker, J. Kohlmeyer, B. Volkmann-Kohlmeyer, R. A. Spotts, M. Serdani, P. W. Crous, K. W. Hughes, K. Matsuura, E. Langer, G. Langer, W. A. Untereiner, R. Lucking, B. Budel, D. M. Geiser, A. Aptroot, P. Diederich, I. Schmitt, M. Schultz, R. Yahr, D. S. Hibbett, F. Lutzoni, D. J. McLaughlin, J. W. Spatafora, and R. Vilgalys. Reconstructing the early evolution of fungi using a six-gene phylogeny. *Nature*, 443(7113):818–822, 2006.

[163] D. J. Jamieson. *Saccharomyces cerevisiae* has distinct adaptive responses to both hydrogen peroxide and menadione. *Journal of Bacteriology*, 174(20):6678–6681, 1992.

[164] D. J. Jamieson, D. W. Stephen, and E. C. Terriere. Analysis of the adaptive oxidative stress response of *Candida albicans*. *FEMS Microbiology Letters*, 138(1):83–88, 1996.

[165] S. M. Jazwinski. Molecular mechanisms of yeast longevity. *Trends in Microbiology*, 7(6):247–252, 1999.

[166] R. Jensen, G. F. Sprague Jr., and I. Herskowitz. Regulation of yeast mating-type interconversion: feedback control of HO gene expression by the mating-type locus. *Proceedings of the National Academy of Sciences*, 80(10):3035–3039, 1983.

[167] J. S. Jeong, S. J. Kwon, S. W. Kang, S. G. Rhee, and K. Kim. Purification and characterization of a second type thioredoxin peroxidase (type II TPx) from *Saccharomyces cerevisiae*. *Biochemistry*, 38(2):776–783, 1999.

[168] J. E. Kammenga, A. Doroszuk, J. A. G. Riksen, E. Hazendonk, L. Spiridon, A.-J. Petrescu, M. Tijsterman, R. H. A. Plasterk, and J. Bakker. A *Caenorhabditis elegans* wild type defies the temperature-size rule owing to a single nucleotide polymorphism in *tra-3*. *PLoS Genetics*, 3(3):e34, 2007.

[169] S. E. Kane, I. Pastan, and M. M. Gottesman. Genetic basis of multidrug resistance of tumor cells. *Journal of Bioenergetics and Biomembranes*, 22(4):593–618, 1990.

[170] J. E. Klaunig and L. M. Kamendulis. The role of oxidative stress in carcinogenesis. *Annual Review of Pharmacology and Toxicology*, 44:239–267, 2004.

[171] P. Konecny, F. M. Drummond, K. N. Tish, and J. W. Tapsall. *Saccharomyces cerevisiae* oesophagitis in an HIV-infected patient. *International Journal of STD and AIDS*, 10(12):821–822, 1999.

[172] N. S. Kosower and E. M. Kosower. Formation of disulfides with diamide. *Methods in Enzymology*, 143:264–271, 1987.

[173] B. Krems, C. Charizanis, and K. D. Entian. Mutants of saccharomyces cerevisiae sensitive to oxidative and osmotic stress. *Current Genetics*, 27(5):427–434, 1995.

[174] B. Krems, C. Charizanis, and K. D. Entian. The response regulator-like protein Pos9/Skn7 of *Saccharomyces cerevisiae* is involved in oxidative stress resistance. *Current Genetics*, 29(4):327–334, 1996.

[175] A. Kren, Y. M. Mamnun, B. E. Bauer, C. Schuller, H. Wolfger, K. Hatzixanthis, M. Mollapour, C. Gregori, P. Piper, and K. Kuchler. War1p, a novel transcription factor controlling weak acid stress response in yeast. *Molecular and Cellular Biology*, 23(5):1775–1785, 2003.

[176] S. Kuge, M. Arita, A. Murayama, K. Maeta, S. Izawa, Y. Inoue, and A. Nomoto. Regulation of the yeast Yap1p nuclear export signal is mediated by redox signal-induced reversible disulfide bond formation. *Molecular and Cellular Biology*, 21(18):6139–6150, 2001.

[177] S. Kuge and N. Jones. *YAP1* dependent activation of *TRX2* is essential for the response of *Saccharomyces cerevisiae* to oxidative stress by hydroperoxides. *EMBO Journal*, 13(3):655–664, 1994.

[178] S. Kuge, N. Jones, and A. Nomoto. Regulation of yAP-1 nuclear localization in response to oxidative stress. *EMBO Journal*, 16(7):1710–1720, 1997.

[179] H. Kusch, S. Engelmann, D. Albrecht, J. Morschhauser, and M. Hecker. Proteomic analysis of the oxidative stress response in *Candida albicans*. *Proteomics*, 7(5):686–697, 2007.

[180] D. J. Kvitek, J. L. Will, and A. P. Gasch. Variations in stress sensitivity and genomic expression in diverse *S. cerevisiae* isolates. *PLoS Genetics*, 4(10):e1000223, 2008.

[181] M. Kwon, S. Chong, S. Han, and K. Kim. Oxidative stresses elevate the expression of cytochrome-c peroxidase in *Saccharomyces cerevisiae*. *Biochimica et Biophysica Acta*, 1623(1):1–5, 2003.

[182] K. J. Kwon-Chung, I. Polacheck, and T. J. Popkin. Melanin-lacking mutants of *Cryptococcus neoformans* and their virulence for mice. *Journal of Bacteriology*, 150(3):1414–1421, 1982.

[183] K. J. Kwon-Chung and J. C. Rhodes. Encapsulation and melanin formation as indicators of virulence in *Cryptococcus neoformans*. *Infection and Immunity*, 51(1):218–223, 1986.

[184] C. Lamarre, O. Ibrahim-Granet, C. Du, R. Calderone, and J. P. Latgé. Characterization of the *SKN7* ortholog of *Aspergillus fumigatus*. *Fungal Genetics and Biology*, 44(7):682–690, 2007.

[185] E. S. Lander and D. Botstein. Mapping mendelian factors underlying quantitative traits using RFLP linkage maps. *Genetics*, 121(1):185–199, 1989.

[186] P. Laun, A Pichovä, F. Madeo, J. Fuchs, A. Ellinger, S. Kohlwein, I. Dawes, K. U. Fröhlich, and M. Breitenbach. Aged mother cells of *Saccharomyces cerevisiae* show markers of oxidative stress and apoptosis. *Molecular Microbiology*, 39(5):1166–1173, 2001.

[187] J. Lee, C. Godon, G. Lagniel, D. Spector, J. Garin, J. Labarre, and M. B. Toledano. Yap1 and Skn7 control two specialized oxidative stress response regulons in yeast. *Journal of Biological Chemistry*, 274(23):16040–16046, 1999.

[188] J. Lee, D. Spector, C. Godon, J. Labarre, and M. B. Toledano. A new antioxidant with alkyl hydroperoxide defense properties in yeast. *Journal of Biological Chemistry*, 274(8):4537–4544, 1999.

[189] J. Legras, D. Merdinoglu, J.-M. Cornuet, and F. Karst. Bread, beer and wine: *Saccharomyces cerevisiae* diversity reflects human history. *Molecular Ecology*, 16(10):2091–2102, 2007.

[190] C. Leonards-Schippers, W. Gieffers, F. Salamini, and C. Gebhardt. The R1 gene conferring race-specific resistance to *Phytophthora infestans* in potato is located on potato chromosome V. *Molecular and General Genetics*, 233(1-2):278–283, 1992.

[191] L. Letavayova, E. Markova, K. Hermanska, V. Vlckova, D. Vlasakova, M. Chovanec, and J. Brozmanova. Relative contribution of homologous recombination and non-homologous end-joining to DNA double-strand break repair after oxidative stress in *Saccharomyces cerevisiae*. *DNA Repair (Amst)*, 5(5):602–610, 2006.

[192] S. Li, A. Ault, C. L. Malone, D. Raitt, S. Dean, L. H. Johnston, R. J. Deschenes, and J. S. Fassler. The yeast histidine protein kinase, Sln1p, mediates phosphotransfer to two response regulators, Ssk1p and Skn7p. *EMBO Journal*, 17(23):6952–6962, 1998.

[193] T. Lindahl and D. E. Barnes. Repair of endogenous DNA damage. *Cold Spring Harbor Symposia on Quantitative Biology*, 65:127–133, 2000.

[194] H. Liu, C. A. Styles, and G. R. Fink. *Saccharomyces cerevisiae* S288c has a mutation in *FLO8*, a gene required for filamentous growth. *Genetics*, 144(3):967–978, 1996.

[195] L. Liu, R. P. Tewari, and P. R. Williamson. Laccase protects *Cryptococcus neoformans* from antifungal activity of alveolar macrophages. *Infection and Immunity*, 67(11):6034–6039, 1999.

[196] F. A. Loewus, K. Saito, R. K. Suto, and E. Maring. Conversion of D-arabinose to D-erythroascorbic acid and oxalic acid in *Sclerotinia sclerotiorum*. *Biochemical and Biophysical Research Communications*, 212(1):196–203, 1995.

[197] F. Lu, D. Wang, D. Bai, and L. Du. Adaptive response of *Saccharomyces cerevisiae* to hyperosmotic and oxidative stress. *Process Biochemistry*, 40:3614–3618, 2005.

[198] S. Luikenhuis, G. Perrone, I. W. Dawes, and C. M. Grant. The yeast *Saccharomyces cerevisiae* contains two glutaredoxin genes that are required for protection against reactive oxygen species. *Molecular Biology of the Cell*, 9(5):1081–1091, 1998.

[199] V. I. Lushchak and D. V. Gospodaryov. Catalases protect cellular proteins from oxidative modification in *Saccharomyces cerevisiae*. *Cell Biology International*, 29(3):187–192, 2005.

[200] M. Lynch and B. Walsh. *Genetics and analysis of quantitative traits*. Sinauer Associates, Inc., 1998.

[201] F. Madeo, E. Fröhlich, and K. U. Fröhlich. A yeast mutant showing diagnostic markers of early and late apoptosis. *Journal of Cell Biology*, 139(3):729–734, 1997.

[202] F. Madeo, E. Fröhlich, M. Ligr, M. Grey, S. J. Sigrist, D. H. Wolf, and K. U. Fröhlich. Oxygen stress: a regulator of apoptosis in yeast. *Journal of Cell Biology*, 145(4):757–767, 1999.

[203] F. Madeo, E. Herker, C. Maldener, S. Wissing, S. Lachelt, M. Herlan, M. Fehr, K. Lauber, S. J. Sigrist, S. Wesselborg, and K. U. Fröhlich. A caspase-related protease regulates apoptosis in yeast. *Molecular Cell*, 9(4):911–917, 2002.

[204] J. R. Maenza, W. G. Merz, M. J. Romagnoli, J. C. Keruly, R. D. Moore, and J. E. Gallant. Infection due to fluconazole-resistant *Candida* in patients with AIDS: prevalence and microbiology. *Clinical Infectious Diseases*, 24(1):28–34, 1997.

[205] G. Marchler, C. Schüller, G. Adam, and H. Ruis. A *Saccharomyces cerevisiae* UAS element controlled by protein kinase A activates transcription in response to a variety of stress conditions. *EMBO Journal*, 12(5):1997–2003, 1993.

[206] M. Marques, D. Mojzita, M. A. Amorim, T. Almeida, S. Hohmann, P. Moradas-Ferreira, and V. Costa. The Pep4p vacuolar proteinase contributes to the turnover of oxidized proteins but *PEP4* overexpression is not sufficient to increase chronological lifespan in *Saccharomyces cerevisiae*. *Microbiology*, 152(Pt 12):3595–3605, 2006.

[207] K. A. Marr, R. A. Carter, F. Crippa, A. Wald, and L. Corey. Epidemiology and outcome of mould infections in hematopoietic stem cell transplant recipients. *Clinical Infectious Diseases*, 34(7):909–917, 2002.

[208] M. T. Martinez-Pastor, G. Marchler, C. Schüller, A. Marchler-Bauer, H. Ruis, and F. Estruch. The *Saccharomyces cerevisiae* zinc finger proteins Msn2p and Msn4p are required for transcriptional induction through the stress response element (STRE). *EMBO Journal*, 15(9):2227–2235, 1996.

[209] P. B. Matheny, Z. Wang, M. Binder, J. M. Curtis, Y. W. Lim, R. H. Nilsson, K. W. Hughes, V. Hofstetter, J. F. Ammirati, C. L. Schoch, E. Langer, G. Langer, D. J. McLaughlin, A. W. Wilson, T. Froslev, Z. Ge, R. W. Kerrigan, J. C. Slot, Z. Yang, T. J. Baroni, M. Fischer, K. Hosaka, K. Matsuura, M. T. Seidl, J. Vauras, and D. S. Hibbett. Contributions of *RPB2* and *TEF1* to the phylogeny of mushrooms and allies (basidiomycota, fungi). *Molecular Phylogenetics and Evolution*, 43(2):430–451, 2007.

[210] M. J. McCullough, K. V. Clemons, C. Farina, J. H. McCusker, and D. A. Stevens. Epidemiological investigation of vaginal *Saccharomyces cerevisiae* isolates by a genotypic method. *Journal of Clinical Microbiology*, 36(2):557–562, 1998.

[211] M. J. McCullough, K. V. Clemons, J. H. McCusker, and D. A. Stevens. Species identification and virulence attributes of *Saccharomyces boulardii* (nom. inval.). *Journal of Clinical Microbiology*, 36(9):2613–2617, 1998.

[212] J. H. McCusker. *Saccharomyces cerevisiae* - an emerging and model pathogenic fungus. ASM Press, 2006.

[213] J. H. McCusker, K. V. Clemons, D. A. Stevens, and R. W. Davis. Genetic characterization of pathogenic *Saccharomyces cerevisiae* isolates. *Genetics*, 136(4):1261–1269, 1994.

[214] J. H. McCusker, K. V. Clemons, D. A. Stevens, and R. W. Davis. *Saccharomyces cerevisiae* virulence phenotype as determined with CD-1 mice is associated with the ability to grow at 42^{o}C and form pseudohyphae. *Infection and Immunity*, 62(12):5447–5455, 1994.

[215] L. V. McFarland. *Saccharomyces boulardii* is not *Saccharomyces cerevisiae*. *Clinical Infectious Diseases*, 22:200–201, 1996.

[216] P. E. McGovern, J. Zhang, J. Tang, Z. Zhang, G. R. Hall, R. A. Moreau, A. Nunez, E. D. Butrym, M. P. Richards, C. Wang, G. Cheng, Z. Zhao, and C. Wang. Fermented beverages of pre- and proto-historic China. *Proceedings of the National Academy of Sciences*, 101(51):17593–17598, 2004.

[217] M. M. McNeil, S. L. Nash, R. A. Hajjeh, M. A. Phelan, L. A. Conn, B. D. Plikaytis, and D. W. Warnock. Trends in mortality due to invasive mycotic diseases in the United States, 1980-1997. *Clinical Infectious Diseases*, 33(5):641–647, 2001.

[218] H. Meiron, E. Nahon, and D. Raveh. Identification of the heterothallic mutation in HO-endonuclease of *S. cerevisiae* using HO/ho chimeric genes. *Current Genetics*, 28(4):367–373, 1995.

[219] R. W. Michelmore, I. Paran, and R. V. Kesseli. Identification of markers linked to disease-resistance genes by bulked segregant analysis: a rapid method to detect markers in specific genomic regions by using segregating populations. *Proceedings of the National Academy of Sciences*, 88(21):9828–9832, 1991.

[220] K. I. Minard and L. McAlister-Henn. Antioxidant function of cytosolic sources of NADPH in yeast. *Free Radical Biology and Medicine*, 31(6):832–843, 2001.

[221] H. Mirzaei and F. Regnier. Identification and quantification of protein carbonylation using light and heavy isotope labeled Girard's P reagent. *Journal of Chromatography A*, 1134(1-2):122–133, 2006.

[222] I. Moreno, N. Tutrone, R. Sentandreu, and E. Valentin. *Saccharomyces cerevisiae* Rds2 transcription factor involvement in cell wall composition and architecture. *International Microbiology*, 11(1):57–63, 2008.

[223] B. A. Morgan, G. R. Banks, W. M. Toone, D. Raitt, S. Kuge, and L. H. Johnston. The Skn7 response regulator controls gene expression in the oxidative

stress response of the budding yeast *Saccharomyces cerevisiae*. *EMBO Journal*, 16(5):1035–1044, 1997.

[224] R. K. Mortimer and J. R. Johnston. Genealogy of principal strains of the yeast genetic stock center. *Genetics*, 113(1):35–43, 1986.

[225] R. K. Mortimer, P. Romano, G. Suzzi, and M. Polsinelli. Genome renewal: a new phenomenon revealed from a genetic study of 43 strains of *Saccharomyces cerevisiae* derived from natural fermentation of grape musts. *Yeast*, 10(12):1543–1552, 1994.

[226] R. K. Mortimer, D. Schild, C. R. Contopoulou, and J. A. Kans. Genetic map of *Saccharomyces cerevisiae*, edition 10. *Yeast*, 5(5):321–403, 1989.

[227] W. S. Moye-Rowley. Transcriptional control of multidrug resistance in the yeast *Saccharomyces*. *Progress in Nucleic Research and Molecular Biology*, 73:251–279, 2003.

[228] W. S. Moye-Rowley, K. D. Harshman, and C. S. Parker. Yeast *YAP1* encodes a novel form of the jun family of transcriptional activator proteins. *Genes and Development*, 3(3):283–292, 1989.

[229] E. G. Muller. A glutathione reductase mutant of yeast accumulates high levels of oxidized glutathione and requires thioredoxin for growth. *Molecular Biology of the Cell*, 7(11):1805–1813, 1996.

[230] L. A. H. Muller and J. H. McCusker. A multispecies-based taxonomic microarray reveals interspecies hybridization and introgression in *Saccharomyces cerevisiae*. *FEMS Yeast Research*, 9(1):143–152, 2009.

[231] Y. Nakagawa, K. Koide, K. Watanabe, Y. Morita, I. Mizuguchi, and T. Akashi. The expression of the pathogenic yeast *Candida albicans* catalase gene in response to hydrogen peroxide. *Microbiology and Immunology*, 43(7):645–651, 1999.

[232] D. F. Nathan, M. H. Vos, and S. Lindquist. In vivo functions of the *Saccharomyces cerevisiae* Hsp90 chaperone. *Proceedings of the National Academy of Sciences*, 94(24):12949–12956, 1997.

[233] G. Naumov, E. Naumova, and M. Korhola. Genetic identification of natural *Saccharomyces sensu stricto* yeasts from Finland, Holland and Slovakia. *Antonie Van Leeuwenhoek*, 61(3):237–243, 1992.

[234] G. I. Naumov, E. S. Naumova, and P. D. Sniegowski. *Saccharomyces paradoxus* and *Saccharomyces cerevisiae* are associated with exudates of North American oaks. *Canadian Journal of Microbiology*, 44(11):1045–1050, 1998.

[235] R. Nestelbacher, P. Laun, D. Vondrakova, A. Pichova, C. Schüller, and M. Breitenbach. The influence of oxygen toxicity on yeast mother cell-specific aging. *Experimental Gerontology*, 35(1):63–70, 2000.

[236] J. A. Nick, C. T. Leung, and F. A. Loewus. Isolation and identification of erythroascorbic acid in *Saccharomyces cerevisiae* and *Lipomyces starkeyi*. *Plant Science*, 46:181–187, 1986.

[237] C. R. Nishida, E. B. Gralla, and J. S. Valentine. Characterization of three yeast copper-zinc superoxide dismutase mutants analogous to those coded for in familial amyotrophic lateral sclerosis. *Proceedings of the National Academy of Sciences*, 91(21):9906–9910, 1994.

[238] A. Nourani, D. Papajova, A. Delahodde, C. Jacq, and J. Subik. Clustered amino acid substitutions in the yeast transcription regulator Pdr3p increase pleiotropic drug resistance and identify a new central regulatory domain. *Molecular and General Genetics*, 256(4):397–405, 1997.

[239] C. M. O'Gorman, H. T. Fuller, and P. S. Dyer. Discovery of a sexual cycle in the opportunistic fungal pathogen *Aspergillus fumigatus*. *Nature*, 457(7228):471–474, 2009.

[240] I. M. Ota and A. Varshavsky. A yeast protein similar to bacterial two-component regulators. *Science*, 262(5133):566–569, 1993.

[241] S. Paris, D. Wysong, J.-P. Debeaupuis, K. Shibuya, B. Philippe, R. D. Diamond, and J. P. Latgé. Catalases of *Aspergillus fumigatus*. *Infection and Immunity*, 71(6):3551–3562, 2003.

[242] E. G. Pasyukova, C. Vieira, and T. F. Mackay. Deficiency mapping of quantitative trait loci affecting longevity in *Drosophila melanogaster*. *Genetics*, 156(3):1129–1146, 2000.

[243] A. H. Paterson, E. S. Lander, J. D. Hewitt, S. Peterson, S. E. Lincoln, and S. D. Tanksley. Resolution of quantitative traits into mendelian factors by using a complete linkage map of restriction fragment length polymorphisms. *Nature*, 335(6192):721–726, 1988.

[244] R. Peakall and P. E. Smouse. Genalex 6: genetic analysis in excel. population genetic software for teaching and research. *Molecular Ecology Notes*, 6:288–295, 2006.

[245] J. R. Pedrajas, E. Kosmidou, A. Miranda-Vizuete, J. A. Gustafsson, A. P. Wright, and G. Spyrou. Identification and functional characterization of a novel mitochondrial thioredoxin system in *Saccharomyces cerevisiae*. *Journal of Biological Chemistry*, 274(10):6366–6373, 1999.

[246] H. Pelletier and J. Kraut. Crystal structure of a complex between electron transfer partners, cytochrome-c peroxidase and cytochrome c. *Science*, 258(5089):1748–1755, 1992.

[247] M. Penninckx. A short review on the role of glutathione in the response of yeasts to nutritional, environmental, and oxidative stresses. *Enzyme and Microbial Technology*, 26(9-10):737–742, 2000.

[248] M. J. Penninckx. An overview on glutathione in *Saccharomyces* versus non-conventional yeasts. *FEMS Yeast Research*, 2(3):295–305, 2002.

[249] E. O. Perlstein, D. M. Ruderfer, G. Ramachandran, S. J. Haggarty, L. Kruglyak, and S. L. Schreiber. Revealing complex traits with small molecules and naturally recombinant yeast strains. *Chemical Biology*, 13(3):319–327, 2006.

[250] M. A. Pfaller and D. J. Diekema. Rare and emerging opportunistic fungal pathogens: concern for resistance beyond *Candida albicans* and *Aspergillus fumigatus*. *Journal of Clinical Microbiology*, 42(10):4419–4431, 2004.

[251] M. A. Pfaller and D. J. Diekema. Epidemiology of invasive candidiasis: a persistent public health problem. *Clinical Microbiology Reviews*, 20(1):133–163, 2007.

[252] A. Poljak, I. W. Dawes, B. A. Ingelse, M. W. Duncan, G. A. Smythe, and C. M. Grant. Oxidative damage to proteins in yeast cells exposed to adaptive levels of H_2O_2. *Redox Report*, 8(6):371–377, 2003.

[253] S. C. Popoff, A. I. Spira, A. W. Johnson, and B. Demple. Yeast structural gene (*APN1*) for the major apurinic endonuclease: homology to *Escherichia coli* endonuclease IV. *Proceedings of the National Academy of Sciences*, 87(11):4193–4197, 1990.

[254] S. Quarrie, V. Lazic-Jancic, D. Kovacevic, A. Steed, and S. Pekic. Bulk segregant analysis with molecular markers and its use for improving drought resistance in maize. *Journal of Experimental Botany*, 50:1299–1306, 1999.

[255] D. C. Raitt, A. L. Johnson, A. M. Erkine, K. Makino, B. Morgan, D. S. Gross, and L. H. Johnston. The Skn7 response regulator of *Saccharomyces cerevisiae* interacts with Hsf1 in vivo and is required for the induction of heat shock genes by oxidative stress. *Molecular Biology of the Cell*, 11(7):2335–2347, 2000.

[256] P. Raspor, S. Plesnicar, Z. Gazdag, M. Pesti, M. Miklavcic, B. Lah, R. Logar-Marinsek, and B. Poljsak. Prevention of intracellular oxidation in yeast: the role of vitamin E analogue, Trolox (6-hydroxy-2,5,7,8-tetramethylkroman-2-carboxyl acid). *Cell Biology International*, 29(1):57–63, 2005.

[257] R. B. Rea, C. G. M. Gahan, and C. Hill. Disruption of putative regulatory loci in *Listeria monocytogenes* demonstrates a significant role for Fur and PerR in virulence. *Infection and Immunity*, 72(2):717–727, 2004.

[258] T. Replansky, V. Koufopanou, D. Greig, and G. Bell. *Saccharomyces sensu stricto* as a model system for evolution and ecology. *Trends in Ecology and Evolution*, 23(9):494–501, 2008.

[259] M. Reth. Hydrogen peroxide as second messenger in lymphocyte activation. *Nature Immunology*, 3(12):1129–1134, 2002.

[260] E. Riboulet, N. Verneuil, S. La Carbona, N. Sauvageot, Y. Auffray, A. Hartke, and J. Giard. Relationships between oxidative stress response and virulence in *Enterococcus faecalis*. *Journal of Molecular Microbiology and Biotechnology*, 13(1-3):140–146, 2007.

[261] S. Ricci, R. Janulczyk, and L. Bjorck. The regulator PerR is involved in oxidative stress response and iron homeostasis and is necessary for full virulence of *Streptococcus pyogenes*. *Infection and Immunity*, 70(9):4968–4976, 2002.

[262] P. Rice, I. Longden, and A. Bleasby. EMBOSS: the european molecular biology open software suite. *Trends in Genetics*, 16(6):276–277, 2000.

[263] C. Richter. Biophysical consequences of lipid peroxidation in membranes. *Chemistry and Physics of Lipids*, 44(2-4):175–189, 1987.

[264] K. J. Rieger, M. El-Alama, G. Stein, C. Bradshaw, P. P. Slonimski, and K. Maundrell. Chemotyping of yeast mutants using robotics. *Yeast*, 15(10B):973–986, 1999.

[265] R. L. Roberts and G. R. Fink. Elements of a single MAP kinase cascade in *Saccharomyces cerevisiae* mediate two developmental programs in the same cell type: mating and invasive growth. *Genes and Development*, 8(24):2974–2985, 1994.

[266] M. T. Rodriguez-Manzaneque, J. Ros, E. Cabiscol, A. Sorribas, and E. Herrero. Grx5 glutaredoxin plays a central role in protection against protein oxidative damage in *Saccharomyces cerevisiae*. *Molecular and Cellular Biology*, 19(12):8180–8190, 1999.

[267] D. R. Rosen, T. Siddique, D. Patterson, D. A. Figlewicz, P. Sapp, A. Hentati, D. Donaldson, J. Goto, J. P. O'Regan, and H. X. Deng. Mutations in Cu/Zn superoxide dismutase gene are associated with familial amyotrophic lateral sclerosis. *Nature*, 362(6415):59–62, 1993.

[268] A. L. Rouse. *Evolution of a yeast transcriptional egulatory network: genetic phenotypic and fitness variation*. PhD thesis, Duke University, 2007.

[269] J. Rozas, J. C. Sanchez-DelBarrio, X. Messeguer, and R. Rozas. DnaSP, DNA polymorphism analyses by the coalescent and other methods. *Bioinformatics*, 19(18):2496–2497, 2003.

[270] H. Ruis and C. Schüller. Stress signaling in yeast. *Bioessays*, 17(11):959–965, 1995.

[271] B. Ruscic, A. F. Wagner, L. B. Harding, R. L. Asher, D. Feller, D. A. Dixon, K. A. Peterson, Y. Song, X. Qian, C. Ng, J. Liu, W. Chen, and D. Schwenke. On the enthalpy of formation of hydroxyl radical and gas-phase bond dissociation energies of water and hydroxyl. *The Journal of Physical Chemistry*, 106(11):2727–2747, 2002.

[272] W. Rychlik, W. J. Spencer, and R. E. Rhoads. Optimization of the annealing temperature for DNA amplification in vitro. *Nucleic Acids Research*, 18(21):6409–6412, 1990.

[273] I. Sadowski, C. Costa, and R. Dhanawansa. Phosphorylation of Ga14p at a single C-terminal residue is necessary for galactose-inducible transcription. *Molecular and Cellular Biology*, 16(9):4879–4887, 1996.

[274] K. Sakamoto, Y. Tominaga, K. Yamauchi, Y. Nakatsu, K. Sakumi, K. Yoshiyama, A. Egashira, S. Kura, T. Yao, M. Tsuneyoshi, H. Maki, Y. Nakabeppu, and T. Tsuzuki. MUTYH-null mice are susceptible to spontaneous and oxidative stress induced intestinal tumorigenesis. *Cancer Research*, 67(14):6599–6604, 2007.

[275] Y. Sanchez, J. Taulien, K. A. Borkovich, and S. Lindquist. Hsp104 is required for tolerance to many forms of stress. *EMBO Journal*, 11(6):2357–2364, 1992.

[276] A. J. Sbarra and M. L. Karnovsky. The biochemical basis of phagocytosis. I. metabolic changes during the ingestion of particles by polymorphonuclear leukocytes. *Journal of Biological Chemistry*, 234(6):1355–1362, 1959.

[277] A. P. Schmitt and K. McEntee. Msn2p, a zinc finger DNA-binding protein, is the transcriptional activator of the multistress response in *Saccharomyces cerevisiae*. *Proceedings of the National Academy of Sciences*, 93(12):5777–5782, 1996.

[278] N. Schnell and K. D. Entian. Identification and characterization of a *Saccharomyces cerevisiae* gene (*PAR1*) conferring resistance to iron chelators. *European Journal of Biochemistry*, 200(2):487–493, 1991.

[279] N. Schnell, B. Krems, and K. D. Entian. The *PAR1* (*YAP1/SNQ3*) gene of *Saccharomyces cerevisiae*, a c-jun homologue, is involved in oxygen metabolism. *Current Genetics*, 21(4-5):269–273, 1992.

[280] J. W. Schopf. Microfossils of the Early Archean Apex chert: new evidence of the antiquity of life. *Science*, 260:640–646, 1993.

[281] A. V. Segre, A. W. Murray, and J.-Y. Leu. High-resolution mutation mapping reveals parallel experimental evolution in yeast. *PLoS Biology*, 4(8):e256, 2006.

[282] A. Shartava, C. A. Monteiro, F. A. Bencsath, K. Schneider, B. T. Chait, R. Gussio, L. A. Casoria-Scott, A. K. Shah, C. A. Heuerman, and S. R. Goodman. A posttranslational modification of beta-actin contributes to the slow dissociation of the spectrin-protein 4.1-actin complex of irreversibly sickled cells. *Journal of Cell Biology*, 128(5):805–818, 1995.

[283] M. K. Shigenaga, T. M. Hagen, and B. N. Ames. Oxidative damage and mitochondrial decay in aging. *Proceedings of the National Academy of Sciences*, 91(23):10771–10778, 1994.

[284] J. M. Simmie, G. Black, H. J. Curran, and J. P. Hinde. Enthalpies of formation and bond dissociation energies of lower alkyl hydroperoxides and related hydroperoxy and alkoxy radicals. *Journal of Physical Chemistry A*, 112(22):5010–5016, 2008.

[285] K. Singh, P. J. Kang, and H. Park. The Rho5 GTPase is necessary for oxidant-induced cell death in budding yeast. *Proceedings of the National Academy of Sciences*, 105(5):1522–1527, 2008.

[286] P. Singh, N. Chauhan, A. Ghosh, F. Dixon, and R. Calderone. *SKN7* of *Candida albicans*: mutant construction and phenotype analysis. *Infection and Immunity*, 72(4):2390–2394, 2004.

[287] H. Sinha, L. David, R. C. Pascon, S. Clauder-Munster, S. Krishnakumar, M. Nguyen, G. Shi, J. Dean, R. W. Davis, P. J. Oefner, J. H. McCusker, and L. M. Steinmetz. Sequential elimination of major-effect contributors identifies additional quantitative trait loci conditioning high-temperature growth in yeast. *Genetics*, 180(3):1661–1670, 2008.

[288] H. Sinha, B. P. Nicholson, L. M. Steinmetz, and J. H. McCusker. Complex genetic interactions in a quantitative trait locus. *PLoS Genetics*, 2(2):e13, 2006.

[289] M. Skoneczny, A. Chelstowska, and J. Rytka. Study of the coinduction by fatty acids of catalase A and acyl-CoA oxidase in standard and mutant *Saccharomyces cerevisiae* strains. *European Journal of Biochemistry*, 174(2):297–302, 1988.

[290] N. Skovgaard. New trends in emerging pathogens. *International Journal of Food Microbiology*, 120(3):217–224, 2007.

[291] D. Smith, D. Metzgar, C. Wills, and J. Fierer. Fatal *Saccharomyces cerevisiae* aortic graft infection. *Journal of Clinical Microbiology*, 40(7):2691–2692, 2002.

[292] P. D. Sniegowski, P. G. Dombrowski, and E. Fingerman. *Saccharomyces cerevisiae* and *Saccharomyces paradoxus* coexist in a natural woodland site in North America and display different levels of reproductive isolation from European conspecifics. *FEMS Yeast Research*, 1(4):299–306, 2002.

[293] J. D. Sobel, J. Vazquez, M. Lynch, C. Meriwether, and M. J. Zervos. Vaginitis due to *Saccharomyces cerevisiae*: epidemiology, clinical aspects, and therapy. *Clinical Infectious Diseases*, 16(1):93–99, 1993.

[294] N. Soontorngun, M. Larochelle, S. Drouin, F. Robert, and B. Turcotte. Regulation of gluconeogenesis in *Saccharomyces cerevisiae* is mediated by activator and repressor functions of Rds2. *Molecular and Cellular Biology*, 27(22):7895–7905, 2007.

[295] A. Sousa-Lopes, F. Antunes, L. Cyrne, and H. S. Marinho. Decreased cellular permeability to H_2O_2 protects *Saccharomyces cerevisiae* cells in stationary phase against oxidative stress. *FEBS Letters*, 578(1-2):152–156, 2004.

[296] W. Spevak, F. Fessl, J. Rytka, A. Traczyk, M. Skoneczny, and H. Ruis. Isolation of the catalase T structural gene of *Saccharomyces cerevisiae* by functional complementation. *Molecular and Cellular Biology*, 3(9):1545–1551, 1983.

[297] C. Srinivasan, A. Liba, J. A. Imlay, J. S. Valentine, and E. B. Gralla. Yeast lacking superoxide dismutase(s) show elevated levels of "free iron" as measured by whole cell electron paramagnetic resonance. *Journal of Biological Chemistry*, 275(38):29187–29192, 2000.

[298] T. M. Stearns, J. E. Beever, B. R. Southey, M. Ellis, F. K. McKeith, and S. L. Rodriguez-Zas. Evaluation of approaches to detect quantitative trait loci for

growth, carcass, and meat quality on swine chromosomes 2, 6, 13, and 18. II. multivariate and principal component analyses. *Journal of Animal Science*, 83(11):2471–2481, 2005.

[299] L. M. Steinmetz, H. Sinha, D. R. Richards, J. I. Spiegelman, P. J. Oefner, J. H. McCusker, and R. W. Davis. Dissecting the architecture of a quantitative trait locus in yeast. *Nature*, 416(6878):326–330, 2002.

[300] M. Stephens and P. Donnelly. A comparison of bayesian methods for haplotype reconstruction from population genotype data. *American Journal of Human Genetics*, 73(5):1162–1169, 2003.

[301] M. Stephens, N. J. Smith, and P. Donnelly. A new statistical method for haplotype reconstruction from population data. *American Journal of Human Genetics*, 68(4):978–989, 2001.

[302] A. Sturtevant. The linear arrangement of six sex-linked factors in *Drosophila*, as shown by their mode of association. *Journal of Experimental Zoology*, 14:43–59, 1913.

[303] S. Suh, J. V. McHugh, D. D. Pollock, and M. Blackwell. The beetle gut: a hyperdiverse source of novel yeasts. *Mycological Research*, 109(Pt 3):261–265, 2005.

[304] D. J. Sullivan, T. J. Westerneng, K. A. Haynes, D. E. Bennett, and D. C. Coleman. *Candida dubliniensis* sp. nov.: phenotypic and molecular characterization of a novel species associated with oral candidosis in HIV-infected individuals. *Microbiology*, 141 (Pt 7):1507–1521, 1995.

[305] T. Tadauchi, T. Inada, K. Matsumoto, and K. Irie. Posttranscriptional regulation of *HO* expression by the mkt1-pbp1 complex. *Molecular and Cellular Biology*, 24(9):3670–3681, 2004.

[306] T. Taira, Y. Saito, T. Niki, S. M. M. Iguchi-Ariga, K. Takahashi, and H. Ariga. DJ-1 has a role in antioxidative stress to prevent cell death. *EMBO Reports*, 5(2):213–218, 2004.

[307] A. L. Tappel and H. Zalkin. Lipide peroxidation in isolated mitochondria. *Archives of Biochemistry and Biophysics*, 80:326–332, 1959.

[308] T. Tatsuta, S. Augustin, M. Nolden, B. Friedrichs, and T. Langer. m-AAA protease-driven membrane dislocation allows intramembrane cleavage by rhomboid in mitochondria. *EMBO Journal*, 26(2):325–335, 2007.

[309] O. W. Tawfik, C. J. Papasian, A. Y. Dixon, and L. M. Potter. *Saccharomyces cerevisiae* pneumonia in a patient with acquired immune deficiency syndrome. *Journal of Clinical Microbiology*, 27(7):1689–1691, 1989.

[310] J. Thacker. Inactivation and mutation of yeast cells by hydrogen peroxide. *Mutation Research*, 33(2-3):147–156, 1975.

[311] B. Thomas and M. F. Beal. Parkinson's disease. *Human Molecular Genetics*, 16 Spec No. 2:R183–94, 2007.

[312] G. W. Thorpe, C. S. Fong, N. Alic, V. J. Higgins, and I. W. Dawes. Cells have distinct mechanisms to maintain protection against different reactive oxygen species: oxidative-stress-response genes. *Proceedings of the National Academy of Sciences*, 101(17):6564–6569, 2004.

[313] A. H. Tong, M. Evangelista, A. B. Parsons, H. Xu, G. D. Bader, N. Page, M. Robinson, S. Raghibizadeh, C. W. Hogue, H. Bussey, B. Andrews, M. Tyers, and C. Boone. Systematic genetic analysis with ordered arrays of yeast deletion mutants. *Science*, 294(5550):2364–2368, 2001.

[314] M. E. Tosello, M. S. Biasoli, A. G. Luque, H. M. Magaro, and A. R. Krapp. Oxidative stress response involving induction of protective enzymes in *Candida dubliniensis*. *Medical Mycology*, 45(6):535–540, 2007.

[315] E. C. van Asbeck, Y. Huang, A. N. Markham, K. V. Clemons, and D. A. Stevens. *Candida parapsilosis* fungemia in neonates: genotyping results suggest healthcare workers hands as source, and review of published studies. *Mycopathologia*, 164(6):287–293, 2007.

[316] P. A. van der Kemp, D. Thomas, R. Barbey, R. de Oliveira, and S. Boiteux. Cloning and expression in *Escherichia coli* of the *OGG1* gene of *Saccharomyces cerevisiae*, which codes for a DNA glycosylase that excises 7,8-dihydro-8-oxoguanine and 2,6-diamino-4-hydroxy-5-N-methylformamidopyrimidine. *Proceedings of the National Academy of Sciences*, 93(11):5197–5202, 1996.

[317] F. J. G. M. van Kuijk, A. Sevanian, G. J. Handelman, and E. A. Dratz. A new role for phospholipase A2: protection of membranes from lipid peroxidation damage. *Trends in Biochemical Sciences*, 12:31–34, 1987.

[318] A. Vaughan-Martini and A. Martini. Facts, myths and legends on the prime industrial microorganism. *Journal of Industrial Microbiology*, 14(6):514–522, 1995.

[319] M. J. Volles and P. T. Lansbury Jr. Relationships between the sequence of alpha-synuclein and its membrane affinity, fibrillization propensity, and yeast toxicity. *Journal of Molecular Biology*, 366(5):1510–1522, 2007.

[320] A. Wach, A. Brachat, R. Pohlmann, and P. Philippsen. New heterologous modules for classical or PCR-based gene disruptions in *Saccharomyces cerevisiae*. *Yeast*, 10(13):1793–1808, 1994.

[321] S. S. Wallace. Biological consequences of free radical-damaged DNA bases. *Free Radical Biology and Medicine*, 33(1):1–14, 2002.

[322] S. D. Weger, A. Ganji, K. V. Clemons, J. K. Byron, Y. Minn, and D. A. Stevens. Correlation of the frequency of petite formation by isolates of *Saccharomyces cerevisiae* with virulence. *Medical Mycology*, 40(2):161–168, 2002.

[323] W. Wei, J. H. McCusker, R. W. Hyman, T. Jones, Y. Ning, Z. Cao, Z. Gu, D. Bruno, M. Miranda, M. Nguyen, J. Wilhelmy, C. Komp, R. Tamse, X. Wang, P. Jia, P. Luedi, P. J. Oefner, L. David, F. S. Dietrich, Y. Li, R. W. Davis, and L. M. Steinmetz. Genome sequencing and comparative analysis of *Saccharomyces cerevisiae* strain YJM789. *Proceedings of the National Academy of Sciences*, 104(31):12825–12830, 2007.

[324] J. A. Wemmie, S. M. Steggerda, and W. S. Moye-Rowley. The *Saccharomyces cerevisiae* AP-1 protein discriminates between oxidative stress elicited by the oxidants H_2O_2 and diamide. *Journal of Biological Chemistry*, 272(12):7908–7914, 1997.

[325] J. A. Wemmie, A. L. Wu, K. D. Harshman, C. S. Parker, and W. S. Moye-Rowley. Transcriptional activation mediated by the yeast AP-1 protein is required for normal cadmium tolerance. *Journal of Biological Chemistry*, 269(20):14690–14697, 1994.

[326] E. Werle, C. Schneider, M. Renner, M. Volker, and W. Fiehn. Convenient single-step, one tube purification of PCR products for direct sequencing. *Nucleic Acids Research*, 22(20):4354–4355, 1994.

[327] M. Werner-Washburne, E. Braun, G. C. Johnston, and R. A. Singer. Stationary phase in the yeast *Saccharomyces cerevisiae*. *Microbiological Reviews*, 57(2):383–401, 1993.

[328] C. Westwater, E. Balish, and D. A. Schofield. *Candida albicans*-conditioned medium protects yeast cells from oxidative stress: a possible link between quorum sensing and oxidative stress resistance. *Eukaryotic Cell*, 4(10):1654–1661, 2005.

[329] T. J. White, T. Bruns, S. Lee, and J. W. Taylor. PCR protocols: a guide to methods and applications, 1990.

[330] R. B. Wickner. *MKT1*, a nonessential *Saccharomyces cerevisiae* gene with a temperature-dependent effect on replication of M2 double-stranded RNA. *Journal of Bacteriology*, 169(11):4941–4945, 1987.

[331] J. S. Williams, G. J. Mufti, S. Powell, J. R. Salisbury, and E. M. Higgins. *Saccharomyces cerevisiae* emboli in an immunocompromised patient with relapsed acute myeloid leukaemia. *Clinical and Experimental Dermatology*, 32(4):395–397, 2007.

[332] C. C. Winterbourn and D. Metodiewa. Reactivity of biologically important thiol compounds with superoxide and hydrogen peroxide. *Free Radical Biology and Medicine*, 27(3-4):322–328, 1999.

[333] E. A. Winzeler and R. W. Davis. Functional analysis of the yeast genome. *Current Opinion in Genetics & Development*, 7(6):771–776, 1997.

[334] E. A. Winzeler, D. R. Richards, A. R. Conway, A. L. Goldstein, S. Kalman, M. J. McCullough, J. H. McCusker, D. A. Stevens, L. Wodicka, D. J. Lockhart, and R. W. Davis. Direct allelic variation scanning of the yeast genome. *Science*, 281(5380):1194–1197, 1998.

[335] E. A. Winzeler, D. D. Shoemaker, A. Astromoff, H. Liang, K. Anderson, B. Andre, R. Bangham, R. Benito, J. D. Boeke, H. Bussey, A. M. Chu, C. Connelly, K. Davis, F. Dietrich, S. W. Dow, M. El Bakkoury, F. Foury, S. H.

Friend, E. Gentalen, G. Giaever, J. H. Hegemann, T. Jones, M. Laub, H. Liao, N. Liebundguth, D. J. Lockhart, A. Lucau-Danila, M. Lussier, N. M'Rabet, P. Menard, M. Mittmann, C. Pai, C. Rebischung, J. L. Revuelta, L. Riles, C. J. Roberts, P. Ross-MacDonald, B. Scherens, M. Snyder, S. Sookhai-Mahadeo, R. K. Storms, S. Veronneau, M. Voet, G. Volckaert, T. R. Ward, R. Wysocki, G. S. Yen, K. Yu, K. Zimmermann, P. Philippsen, M. Johnston, and R. W. Davis. Functional characterization of the *S. cerevisiae* genome by gene deletion and parallel analysis. *Science*, 285(5429):901–906, 1999.

[336] J. Wisniak. Louis-Jacques Thenard. *Revista CENIC Ciencias Quimicas*, 33:141–149, 2002.

[337] H. Wisplinghoff, T. Bischoff, S. M. Tallent, H. Seifert, R. P. Wenzel, and M. B. Edmond. Nosocomial bloodstream infections in US hospitals: analysis of 24,179 cases from a prospective nationwide surveillance study. *Clinical Infectious Diseases*, 39(3):309–317, 2004.

[338] J. T. Witten, C. T. L. Chen, and B. A. Cohen. Complex genetic changes in strains of *Saccharomyces cerevisiae* derived by selection in the laboratory. *Genetics*, 177(1):449–456, 2007.

[339] F. L. Wormley Jr., G. Heinrich, J. L. Miller, J. R. Perfect, and G. M. Cox. Identification and characterization of an *SKN7* homologue in *Cryptococcus neoformans*. *Infection and Immunity*, 73(8):5022–5030, 2005.

[340] A. L. Wu and W. S. Moye-Rowley. *GSH1*, which encodes gamma-glutamylcysteine synthetase, is a target gene for yAP-1 transcriptional regulation. *Molecular and Cellular Biology*, 14(9):5832–5839, 1994.

[341] D. R. Wysong, L. Christin, A. M. Sugar, P. W. Robbins, and R. D. Diamond. Cloning and sequencing of a *Candida albicans* catalase gene and effects of disruption of this gene. *Infection and Immunity*, 66(5):1953–1961, 1998.

[342] Z. Yang. Paml: a program package for phylogenetic analysis by maximum likelihood. *Computer Applications in the Biosciences*, 13(5):555–556, 1997.

[343] H. J. You, R. L. Swanson, and P. W. Doetsch. *Saccharomyces cerevisiae* possesses two functional homologues of *Escherichia coli* endonuclease III. *Biochemistry*, 37(17):6033–6040, 1998.

[344] S. Youngchim, R. Morris-Jones, R. J. Hay, and A. J. Hamilton. Production of melanin by *Aspergillus fumigatus*. *Journal of Medical Microbiology*, 53(Pt 3):175–181, 2004.

[345] T. E. Zaoutis, J. Argon, J. Chu, J. A. Berlin, T. J. Walsh, and C. Feudtner. The epidemiology and attributable outcomes of candidemia in adults and children hospitalized in the United States: a propensity analysis. *Clinical Infectious Diseases*, 41(9):1232–1239, 2005.

[346] K. S. Zaret and F. Sherman. alpha-aminoadipate as a primary nitrogen source for *Saccharomyces cerevisiae* mutants. *Journal of Bacteriology*, 162(2):579–583, 1985.

[347] E. A. Zimmer, S. L. Martin, S. M. Beverley, Y. W. Kan, and A. C. Wilson. Rapid duplication and loss of genes coding for the alpha chains of hemoglobin. *Proceedings of the National Academy of Sciences*, 77(4):2158–2162, 1980.

Biography

Stephanie Diezmann

Born on March 19, 1975 in Berlin, Germany

Education

2002-2008	Ph.D., University Program in Genetics & Genomics, Duke University, Durham, NC, USA
1997-2002	Biology Diploma, Humboldt Universität, Berlin, Germany
1994-1997	Laboratory Technician Professional Training, Charité, Universitätsmedizin, Berlin, Germany

Honors and Awards

2008	Yeast Genetics and Molecular Biology Meeting, Travel Grant, Genetics Society of America, Toronto, ON, Canada
2007	XXIIIrd International Conference on Yeast Genetics and Molecular Biology, Travel Grant, Duke University Mycology Research Unit, Melbourne, Victoria, Australia
2006	Yeast Genetics and Molecular Biology Meeting, Travel Grant, Genetics Society of America, Princeton, New Jersey, USA
2005	FEBS Advanced Lecture Course Human Fungal Pathogens, Tuition Scholarship, La Colle-sur-loup, France
2002-2004	NIH Training Grant, University Program in Genetics & Genomics, Duke University, Durham, NC, USA
2001	Diploma Scholarship, German Academic Exchange Service, Duke University, Durham, NC, USA

Publications

1. Diezmann S and Dietrich, FS. 2009. *Saccharomyces cerevisiae*: population divergence and resistance to oxidative stress in clinical, domesticated and wild

isolates. *PLoS ONE* accepted in principle pending revisions

2. Al-Jawabreh, A, Diezmann S, Müller, M, Wirth, T, Schnur, LF, Strelkova, MV, Kovalenko, DA, Razakov, SA, Schwenkenbecher, J, Kuhls, K, Schönian, G. 2008. Identification of geographically distributed sub-populations of *Leishmania (Leishmania) major* by microsatellite analysis. *BMC Evolutionary Biology* 8:183-194

3. Fraser, JA, Lim SMC, Diezmann S, Wenink EC, Arndt CG, Cox GM, Dietrich FS, Heitman J. 2006. Yeast diversity sampling on the San Juan Islands reveals no evidence for the spread of the Vancouver Island *Cryptococcus gattii* outbreak to this locale. *FEMS Yeast Reseach* 6:620-624

4. Fraser JA, Giles SS, Wenink EC, Geunes-Boyer SG, Wright JR, Diezmann S, Allen A, Stajich JE, Dietrich FS, Perfect JR, Heitman J. 2005. Same-sex mating and the origin of the Vancouver Island *Cryptococcus gattii* outbreak. *Nature* 437:1360-1364

5. Diezmann S, Cox CJ, Schönian G, Vilgalys RJ, Mitchell TG. 2004. Phylogeny and evolution of medical species of *Candida* and related taxa: a multigenic analysis. *Journal of Clinical Microbiology* 42:5624-5635

6. Fraser JA, Diezmann S, Subaran RL, Allen A, Lengeler KB, Dietrich FS, Heitman J. 2004. Convergent evolution of chromosomal sex-determining regions in the animal and fungal kingdoms. *PLoS Biology* 2:2243-2255